

**CHARACTERIZATION AND MODELING OF SHRINKAGE CRACKING OF  
CEMENTITIOUSLY STABILIZED LAYERS IN PAVEMENT**

By

JINGAN WANG

A dissertation submitted in partial fulfillment of  
the requirements for the degree of

Doctor of Philosophy

WASHINGTON STATE UNIVERSITY  
Department of Civil and Environmental Engineering

JULY 2013

© Copyright by JINGAN WANG, 2013  
All Rights Reserved

UMI Number: 3598136

All rights reserved

INFORMATION TO ALL USERS

The quality of this reproduction is dependent upon the quality of the copy submitted.

In the unlikely event that the author did not send a complete manuscript and there are missing pages, these will be noted. Also, if material had to be removed, a note will indicate the deletion.



UMI 3598136

Published by ProQuest LLC (2013). Copyright in the Dissertation held by the Author.

Microform Edition © ProQuest LLC.

All rights reserved. This work is protected against unauthorized copying under Title 17, United States Code



ProQuest LLC.  
789 East Eisenhower Parkway  
P.O. Box 1346  
Ann Arbor, MI 48106 - 1346

© Copyright by JINGAN WANG, 2013  
All Rights Reserved

To the Faculty of Washington State University:

The members of the Committee appointed to examine the dissertation of JINGAN WANG find it satisfactory and recommend it to be accepted.

---

Haifang Wen, Ph.D., Chair

---

Balasingam Muhunthan, Ph.D.

---

David McLean, Ph.D.

---

William Cofer, Ph.D.

## **ACKNOWLEDGEMENTS**

Four-year life at Pullman, what I have harvested is not only this dissertation, but also wonderful memories. The support, care, patience and encouragement from my advisor, committee members, my family and all my friends accompanied my whole time here. Herein, I want to express my deep appreciation to all of you.

First I would like to thank my advisor, Dr. Haifang Wen. Your trust makes me brave to try this big national project. Your patience and encouragement make me learn something day by day. Your advices from theory to practice deepen my understanding in pavement engineering. Your excellent guidance makes this dissertation possible. As a friend, your care and support make me feel warm during my graduate study, and give us a comfortable research atmosphere.

I appreciate Dr. David McLean, Dr. Balasingam Muhunthan, and Dr. William Cofer, who are willing to provide advises and serve as my committee members. Also special thanks Dr. Balasingam Muhunthan for your advises on the project and your instructions on constitutive modeling, which always illuminate me on the research road. Also your kindness and enthusiasm help me a lot in my life. Also thanks Dr. David McLean for training me on using the mixer and hydraulic machine. Thanks Dr. William Cofer, your finite element class note is my key to the world of computer programming. Thanks Dr. Shihui Shen from several aspects. Your class of highway materials makes me understand more and further about the pavement materials. Your suggestions help me a lot when I met difficulties in life. Also thanks Dr. Tuncer Edil, Dr. James Tinjum, and other fellows at University of Wisconsin at Madison for the cooperation on this research.

Thanks the technicians in machine shop, Miles Pepper, Robert "Kurt" Hutchinson, Gary Held. You guys always give me a lot of suggestions on my weird ideas, and make them from numbers and drawings on a sheet of paper to awe-inspiring devices. Also you are eager to teach me how to use the complicated machines, "strolling and chatting" in your shop was even one of my best periods during my study. Also thanks Robert Lentz for helping and teaching me set up electronic equipments.

I would like to thank all the undergraduate students for helping the laboratory tests, Justin Hammond, Clay Peterman, Melaku Dubie, Aliz Logman, Samuel Yemane, Alexander Gebremeskel, and Aron Sturko. Also thanks Dr. Fangliang Chen and Dr. Wei Fan for helping set up the non-damaged test device.

Special thanks go to my good friend Xiaojun Li who has provided a lot of ideas and work on this research, also helped me a lot in life. I have spent four years in a friendly and wonderful group. I enjoy this wonderful period with all these following buddies, Bhusal Sushanta, Huanan Yu, Xin Lu, Kalehiwot Manahiloh, Sutharsan Thiyagarajah, Shenghua Wu, Weiguang Zhang, Kun Zhang, Mengqi Wu, Nathan Bower, Junyan Yi, Mark Rose, Noel Vijayaruban. Because of all your guys, research is not boring, you create this relaxing and joyful environment.

I would like to acknowledge the funding support by National Cooperative Highway Research Program for this research and the academic and technical support from the faculty and staff of the Department of Civil Engineering of Washington State University.

I would never have been able to finish my dissertation without the support from my family. I owe the gratitude from the bottom of my heart to my family members, my father Chenglin Wang, my mother Yongzhi Shao, my father-in-law Xichun Zhao, my mother-in-law

Xiaoru Bian. At last I am so thankful for having my wife Jing Zhao in my life, your love is my motivation for everything. You are my most significant decision in my life.

CHARACTERIZATION AND MODELING OF SHRINKAGE CRACKING OF  
CEMENTITIOUSLY STABILIZED LAYERS IN PAVEMENT

ABSTRACT

By Jingan Wang, Ph.D.  
Washington State University  
July 2013

Chair: Haifang Wen

This research identifies the properties of cementitious stabilized materials that significantly affect shrinkage cracking in pavements with cementitious stabilized layers. Methods for measuring these properties are recommended. The research approach consists of literature review, test procedure evaluation, and model development and calibration.

Based on the test procedure evaluation, unconfined compressive strength, and indirect tensile strength and modulus tests are recommended. A suite of shrinkage-related tests is used to develop shrinkage cracking models; these tests include free drying shrinkage (including ultimate drying shrinkage), coefficient of thermal expansion, coefficient of friction, and restrained shrinkage cracking tests.

Performance-related models are developed based on laboratory experiments, including strength and modulus growth models, and shrinkage cracking models. The strength growth models are developed based on extended testing at different curing times up to 360 days under standard curing conditions. Temperature and relative humidity are included in the growth models to assess indirect tensile strength and modulus values, which are critical to early-age shrinkage cracking and are sensitive to early-age curing conditions. Restrained shrinkage cracking tests are

conducted on laboratory-scale beams. These results considering the effect of moisture gradient and drying shrinkage gradient along the depth of CSL are used to develop new mechanistic based shrinkage crack spacing and width models.

It is found that neither the existing models nor the developed mechanistic based models can predict crack spacing and width in the field. Empirical shrinkage crack spacing and width models are developed based on dimensional analysis using field data.

The developed shrinkage cracking models are recommended for incorporation into the Mechanistic-Empirical Pavement Design Guide, thus allowing for rational analysis and design procedures for pavements with cementitiously stabilized layers. The performance properties and their test procedures also are recommended. Three levels of material property characterization are provided. For those properties that do not have AASHTO or ASTM test methods, test procedures are drafted.

## TABLE OF CONTENTS

ACKNOWLEDGEMENTS .....	iii
ABSTRACT .....	vi
TABLE OF CONTENTS .....	viii
LIST OF TABLES .....	xii
LIST OF FIGURES .....	xiv
CHAPTER 1: INTRODUCTION .....	1
1.1 PROBLEM STATEMENT .....	1
1.2 OBJECTIVES .....	2
1.3 ORGANIZATION OF DISSERTATION .....	2
CHAPTER 2: LITERATURE REVIEW FINDINGS .....	3
2.1 PERFORMANCE ISSUES OF PAVEMENT DUE TO SHRINKAGE OF CSL .....	3
2.1.1 Hot Mix Asphalt Pavement .....	3
2.1.2 Concrete Pavement .....	6
2.2 PROPERTIES OF CSM LINKED TO SHRINKAGE CRACKING .....	7
2.2.1 Shrinkage of CSL .....	7
2.2.2 Strength and Stiffness of CSM .....	11
2.2.3 Interface Bond .....	15
2.2.4 Techniques to Mitigate Shrinkage Cracking .....	15
2.3 SHRINKAGE CRACKING MODELS .....	17
2.3.1 Drying Shrinkage Strain Model .....	17
2.3.2 Shrinkage Cracking Models .....	19
2.4 TEST PROCEDURES FOR CSM PROPERTIES .....	21

2.4.1 Strength and Modulus Tests .....	21
2.4.2 Shrinkage Tests .....	28
2.5 SUMMARY .....	32
CHAPTER 3: SOIL PROPERTIES AND MIX DESIGN.....	33
3.1 BASIC SOIL PROPERTIES.....	33
3.2 MIX DESIGN .....	34
3.2.1 Soil-Cement.....	34
3.2.2 Soil-Fly Ash (Class C).....	35
3.2.3 Soil-Lime.....	36
3.3 SUMMARY .....	39
CHAPTER 4: TEST PROCEDURE EVALUATION.....	40
4.1 APPRAISAL OF TEST PROCEDURES .....	40
4.1.1 Strength and Modulus Tests .....	41
4.1.2 Shrinkage Tests .....	44
4.1.3 Friction/Bond.....	45
4.2 LABORATORY TEST PROCEDURE EVALUATION .....	48
4.2.1 IDT Test.....	50
4.2.2 Shrinkage and Cracking .....	56
4.3 SUMMARY .....	75
CHAPTER 5: EXPERIMENTAL RESULTS .....	77
5.1 STRENGTH AND MODULUS GROWTH TESTS .....	77
5.1.1 UCS and IDT Strength at 68°F and 100% RH .....	78
5.1.2 IDT Strength and Modulus at Various RH and Temperatures .....	80

5.2 SHRINKAGE AND CRACKING TESTS .....	85
5.2.1 Coefficient of Thermal Expansion (COTE) .....	86
5.2.2 Ultimate Drying Shrinkage.....	87
5.2.3 Gradient Drying Shrinkage.....	88
5.2.4 Restrained Shrinkage Cracking .....	89
5.2.5 Coefficient of Friction .....	92
5.3 SUMMARY .....	94
CHAPTER 6: MODEL DEVELOPMENT .....	96
6.1 STRENGTH AND MODULUS GROWTH MODELS.....	96
6.1.1 Correlations between UCS and IDT Tests .....	96
6.1.2 Strength Growth Model.....	98
6.1.3 IDT Strength and Modulus Growth Model Considering Temperature and RH Effect	99
6.2 SHRINKAGE STRAIN MODELS .....	101
6.2.1 Ultimate Drying Shrinkage Strain Model.....	101
6.2.2 Gradient Drying Shrinkage Strain Model.....	102
6.2.3 Thermal Shrinkage Strain Model .....	104
6.3 SHRINKAGE CRACKING MODELS .....	105
6.4 SUMMARY .....	110
CHAPTER 7: MODEL CALIBRATION WITH FIELD DATA .....	112
7.1 DATA COLLECTION.....	112
7.2 CALIBRATION PROCEDURES.....	116
7.3 CALIBRATION RESULTS .....	116
7.4 APPRAISAL OF SHRINKAGE CRACKING MODELS.....	121

7.5 SUMMARY .....	123
CHAPTER 8: CONCLUSIONS AND RECOMMENDATIONS .....	125
8.1 CONCLUSIONS .....	125
8.1.1 Models Recommended for the MEPGD.....	127
8.1.2 Material Inputs.....	127
8.2 RECOMMENDATIONS .....	131
8.2.1 Further Validation of Models .....	131
8.2.2 Reflective Cracking Model.....	131
REFERENCES .....	132
APPENDIX A. FINDINGS OF SURVEY AND REVIEW OF SPECIFICATIONS .....	139
APPENDIX B. MATLAB PROGRAM FOR IDT MODULUS PARAMETERS.....	180
APPENDIX C. MATLAB PROGRAM FOR SHRINKAGE CRACKING MODEL .....	185
APPENDIX D. DRAFT OF TEST PROTOCOLS.....	193

## LIST OF TABLES

Table 3-1. Characteristics of Host Soils .....	34
Table 3-2. Final Mix Design of Stabilized Mixtures .....	39
Table 3-3. Maximum Dry Density and Optimum Moisture Content.....	39
Table 4-1. Appraisal of Material Strength/Modulus Tests .....	43
Table 4-2. Appraisal of Test Methods for Shrinkage and Swelling .....	47
Table 4-3. Test Procedures Selected for Evaluation.....	48
Table 4-4. Parameters for IDT Modulus Test.....	55
Table 4-5. Summary of IDT Strength Test Results .....	56
Table 4-6. Summary of IDT Modulus Test Results.....	56
Table 4-7. Results of Bond Strength Tests .....	73
Table 5-1. Material Properties and Performance Tests.....	77
Table 5-2. Strength of Mixtures.....	78
Table 5-3. IDT Strength and Modulus of Mixtures .....	81
Table 5-4. Laboratory Test Plan for Shrinkage Model .....	86
Table 5-5. COTE Test Results .....	87
Table 5-6. Measured Ultimate Shrinkage Strain.....	88
Table 5-7. Laboratory Restrained Cracking Summary .....	91
Table 6-1. Parameters for IDT Strength/Modulus Model.....	100
Table 6-2. Parameters for Drying Shrinkage Strain Gradient Model .....	103
Table 7-1. Summary of Literature Data Related to CSL .....	113
Table 7-2. Typical Coefficient of Friction Values (Zhang and Li 2001).....	114

Table 7-3. Field-Calibrated Parameters of CSL Shrinkage Crack Spacing Model for Fine and Coarse Host Materials.....	121
Table 7-4. Field-Calibrated Parameters of CSL Shrinkage Crack Width Model for Fine and Coarse Host Materials.....	121
Table 7-5. Input for Simulation of Shrinkage Cracking Model.....	122
Table 8-1: Models Recommended for MEPDG .....	128
Table 8-2. Three Levels of Input for MEPDG.....	129
Table 8-3. Level 3 Input of UCS (psi) .....	130
Table 8-4. Level 3 Input of IDT Strength (psi).....	130
Table 8-5. Level 3 Input of IDT Modulus (ksi).....	130

## LIST OF FIGURES

Figure 2-1. Block Cracking in HMA with Stabilized Base (Scullion 2002) .....	4
Figure 2-2. Transverse Cracking due to Shrinkage Cracking of CSL (Freeman and Little 2002) .	5
Figure 2-3. Cracking of Concrete Pavement.....	7
Figure 2-4. Shrinkage Cracking of CSL (George 2001).....	8
Figure 2-5. Relationship between UCS and IDT Strength (Kennedy and Hudson 1973) .....	13
Figure 2-6. Modified Tensile Strength Test (Chakrabarti and Kodikara 2007) .....	22
Figure 2-7. IDT Test Setup (Yeo 2008).....	24
Figure 2-8. Unconfined Compressive Strength Test Setup .....	26
Figure 2-9. Free Drying Shrinkage Test .....	29
Figure 2-10. Restrained Slab at Base and Ends (Weiss et al. 1998).....	30
Figure 2-11. Test Setup of Coefficient of Thermal Expansion (Naik et al. 2006) .....	31
Figure 3-1. Gradation of Host Soils.....	33
Figure 3-2. Results for UCS after 7-day Curing for Cement-Stabilized Soils.....	35
Figure 3-3. Results for UCS after 7-day Curing for Class C Fly Ash-Stabilized Soils .....	36
Figure 3-4. pH Value vs. Lime Content.....	37
Figure 3-5. Results for UCS after 7-day Curing for Clay-Lime Mix .....	37
Figure 3-6. Results for UCS after 7-day Curing for Silt-Lime-Class F Fly Ash .....	38
Figure 4-1. Indirect Tensile (IDT) Strength Test Setup.....	51
Figure 4-2. IDT Modulus Test Setup.....	52
Figure 4-3. Aligning Jig for Gluing LVDT Mounts on the Specimen.....	53
Figure 4-4. Drill Press and Aligning Jig for Fastening LVDT Mounts with Screws .....	53

Figure 4-5. COTE Test Setup (Left: Gravel-Cement; Right: Clay-Lime).....	58
Figure 4-6. COTE Test of Clay-Lime between 77°F and 86°F .....	58
Figure 4-7. COTE Development of Clay-Lime Specimens.....	59
Figure 4-8. COTE Development of Gravel-Cement Specimens .....	59
Figure 4-9. Plaster Mold .....	60
Figure 4-10. Autogenous Shrinkage Test Setup .....	61
Figure 4-11. Autogenous Shrinkage Results of Clay-Lime and Gravel-Cement Specimens .....	61
Figure 4-12. Compaction Mold for Free Shrinkage Test.....	63
Figure 4-13. Test Setup to Evaluate the Effects of Specimen Dimension and Bottom Surface... ..	63
Figure 4-14. Effects of Specimen Dimension and Bottom Surface.....	64
Figure 4-15. Drying Shrinkage Test .....	64
Figure 4-16. Test Results for Drying Shrinkage Evaluation.....	65
Figure 4-17. Free Drying and Autogenous Shrinkage Results for Clay-Lime Specimens .....	66
Figure 4-18. Free Drying and Autogenous Shrinkage Results for Gravel-Cement Specimens....	66
Figure 4-19. Restrained Shrinkage Test for Clay-Lime when Epoxy is used as Bonding Agent (48 in. Long) .....	67
Figure 4-20. Restrained Shrinkage Test for Clay-Lime when Cement Mortar is used as Bonding Agent (48 in. Long).....	68
Figure 4-21. Crack Width Increase over Time for Clay-Lime Specimen when Epoxy is used as Bonding Agent.....	68
Figure 4-22. Crack Width Increase over Time for Clay-Lime Specimen when Cement Mortar is used as Bonding Agent .....	69

Figure 4-23. Restrained Shrinkage for Gravel-Cement when Epoxy is used as Bonding Agent (92 in. Long).....	69
Figure 4-24. Coefficient of Friction Test Setup.....	71
Figure 4-25. Bond Strength under Constant Loading Rate for Cement-Gravel (71.6 psi/min)....	72
Figure 4-26. Bond Strength under Constant Deformation Rate for Cement-Gravel (0.065 in./min) .....	72
Figure 4-27. Bond Strength Test when Cement Mortar is used as Bonding Agent.....	74
Figure 4-28. Bond Strength Test when Epoxy is used as Bonding Agent.....	74
Figure 4-29. Failure Surfaces after Bond Strength Tests.....	75
Figure 5-1. UCS Growth with Curing Age.....	79
Figure 5-2. IDT Strength Growth with Curing Age .....	80
Figure 5-3. IDT Strength Values at Various RH and Temperatures with Curing Age.....	83
Figure 5-4. IDT Modulus Values at Various RH and Temperatures with Curing Age .....	85
Figure 5-5. Free Drying Shrinkage with Moisture Gradation Test Setup.....	89
Figure 5-6. Restrained Shrinkage Test Setup with Sides Sealed.....	90
Figure 5-7. Transverse Crack in Lime-Clay Specimen (View from Top).....	90
Figure 5-8. Measured Crack Width .....	92
Figure 5-9. Relationship between IDT Strength of CSM and Coefficient of Friction when Epoxy is used as Bonding Agent.....	93
Figure 5-10. Relationship between IDT Strength and Coefficient of Friction in a Direct Shear Test.....	94
Figure 6-1. Correlation between IDT Strength and UCS .....	97
Figure 6-2. Correlation between IDT Strength and IDT Modulus .....	97

Figure 6-3. Comparison of Predicted and Measured Strength Values at Different Ages.....	99
Figure 6-4. Comparison of Measured and Predicted IDT Strength/Modulus Values.....	101
Figure 6-5 Measured and Predicted Ultimate Drying Shrinkage Results.....	102
Figure 6-6. Comparison of Measured and Predicted Gradient Drying Shrinkage Strain Values at Various Depths.....	104
Figure 6-7. Schematic Diagram of Slab Drying from Top Surface Only .....	106
Figure 6-8. Mechanism of Shrinkage Cracking.....	108
Figure 6-9. Comparison of Measured and Predicted Crack Spacing and Width from Lab Tests	109
Figure 7-1. Comparison of Predicted and Measured CSL Shrinkage Crack Spacing for Stabilized Fine Materials .....	119
Figure 7-2. Comparison of Predicted and Measured CSL Shrinkage Crack Spacing for Stabilized Coarse Materials .....	119
Figure 7-3. Comparison of Predicted and Measured CSL Shrinkage Crack Widths for Stabilized Fine Materials .....	120
Figure 7-4. Comparison of Predicted and Measured CSL Shrinkage Crack Widths for Stabilized Coarse Materials .....	120
Figure 7-5. Predicted Crack Spacing of Three Materials .....	123
Figure 7-6. Predicted Crack Widths of Three Materials.....	123

## **Dedication**

This dissertation is dedicated to my father Chenglin Wang, my mother Yongzhi Shao, my father-in-law Xichun Zhao, my mother-in-law Xiaoru Bian, and my wife Jing Zhao. This dissertation is the fruit of your unlimited support.

# **CHAPTER ONE**

## **INTRODUCTION**

### **1.1 PROBLEM STATEMENT**

The use of cementitiously stabilized materials (CSM), such as lean concrete, cement-stabilized aggregate, and soil stabilized with cement, lime, fly ash, or combinations thereof in the subgrade, subbase, and base layers of flexible and rigid pavement structures, is a widely accepted practice by many state highway agencies. Survey results, presented in Appendix A, indicate that state agencies consider transverse and block cracking to be the most severe distresses for pavements with CSL.

Transverse and block cracking, identified as the most severe distresses for pavements with cementitiously stabilized layers (CSL), are due to the shrinkage of CSL. Although a substantial amount of research has been undertaken to study the properties of these materials, very little research has been conducted that relates the properties (e.g., shrinkage) of such materials to the performance of the pavements in which they are used. The AASHTO *Interim Mechanistic-Empirical Pavement Design Guide Manual of Practice* (referred to as the MEPDG) (ARA 2004), developed under NCHRP Project 01-37A, provides a methodology for the analysis and performance prediction of pavements that incorporate such layers. However, the short- and long-term properties of these materials differ substantially depending on the type and quantity of the stabilizing agent, pavement structure, and environmental conditions during and after construction, etc. The characterization of such materials, the changes of their properties over time, and their cracking models have not been addressed adequately in the MEPDG. Also, few material properties

have been considered; other properties may have a significant effect on long-term performance and need to be considered.

Thus, research is needed to identify the properties of CSM that significantly affect shrinkage cracking of highway pavements and to recommend methods for measuring these properties. This information can be incorporated into the MEPDG, thus allowing for the rational analysis and development of design procedures for pavements constructed with stabilized layers.

## **1.2 OBJECTIVES**

The objective of this research is to recommend performance-related procedures for characterizing shrinkage cracking of CSL for use in pavement design and analysis and incorporation into the MEPDG. This research addresses material properties and related test methods that can be used to predict shrinkage cracking of CSL. It is concerned with subgrade, subbase, and/or base materials that have been stabilized with hydraulic cement, fly ash, lime, or combinations thereof and used in pavements.

## **1.3 ORGANIZATION OF DISSERTATION**

This dissertation consists of eight chapters. Chapter 1 introduces the background of this research problem. Chapter 2 presents the findings from the literature review. Chapter 3 describes the soil properties and mix design. Chapter 4 identifies and evaluates the test procedures. Chapter 5 summarizes the laboratory experiments. Chapter 6 presents model development from laboratory results. Chapter 7 discusses the results of the model calibration based on the collected field data. Chapter 8 provides conclusions and recommendations.

## **CHAPTER TWO**

### **LITERATURE REVIEW FINDINGS**

This chapter presents a comprehensive literature review on shrinkage cracking of CSL. It contains the pavement performance due to the shrinkage of CSL, properties of CSL linked to shrinkage cracking, the existing shrinkage and cracking models, and test procedures for CSL properties linked to shrinkage cracking.

#### **2.1 PERFORMANCE ISSUES OF PAVEMENT DUE TO SHRINKAGE OF CSL**

This summary of findings from the literature review covers the critical performance issues of pavements with CSL due to the shrinkage of CSL and properties of CSM that can be linked to these pavement performances. The performance issues of asphalt and concrete pavements with CSL are described as follows:

##### **2.1.1 Hot Mix Asphalt Pavement**

The performance of hot mix asphalt (HMA) pavement is significantly affected by CSL, especially when CSL are located directly underneath HMA layers. Stabilized subbase and base layers can reduce the rutting of HMA pavement as a result of minimal rutting in the subgrade, subbase, and base (Von Quintus et al. 2005). The bottom-up fatigue cracking of HMA also can be reduced. However, the shrinkage of CSL causes the most severe distresses for pavements with CSL, such as block cracking and transverse cracking, mostly when they are used as the base course.

###### *2.1.1.1 Block Cracking in HMA*

Block cracking often is reported in the HMA surface when the pavement has a stabilized base. Block cracking is caused by shrinkage of the underlying stabilized base and often occurs when the HMA layer is thin, as for local roads (Scullion 2002) (Figure 2-1). Block cracking appears at the surface, because vertical cracking develops through all pavement layers after extensive debonding occurs between the CSLs (Atkinson 1990). Highways in many parts of the world that use stiff bases and thin HMA layers also have encountered this problem (Yue and Yang 2004, Zube et al 1969). The shrinkage, caused by a loss of moisture and temperature variation, typically initiates shortly after construction and continues thereafter. According to Zube et al (1969), high unconfined compressive strength (UCS) causes block cracking and is likely due to the high shrinkage of CSL with high cement content and high strength. Block cracking can be mitigated by extending the CSL at least 1 ft into the shoulder due to the additional lateral support in the outer wheelpath (Zube et al 1969). In short, block cracking can be attributed to the shrinkage of CSL.



**Figure 2-1. Block Cracking in HMA with Stabilized Base (Scullion 2002)**

#### *2.1.1.2 Transverse Cracking Induced by Shrinkage of CSL*

Transverse cracking is the cracking perpendicular to pavement centerline, as shown in Figure 2-2, Transverse cracking in the surface layer, which results from shrinkage of the

stabilized base (Atkinson 1990, Chen 2007), starts from the bottom of the surface layer and propagates through the surface layers. The cracking is due to the bond between the surface layer and stabilized base (George 2002). Transverse cracking is also a concern for pavements with a stabilized subbase and granular base, but at a much later stage (Ramsey and Lund 1959). The shrinkage cracking of the subbase causes stress concentrations at the locations of the cracks and eventually affects the stress distribution in the surface layer.



**Figure 2-2. Transverse Cracking due to Shrinkage Cracking of CSL (Freeman and Little 2002)**

Atkinson (1990) reports that shrinkage cracking in CSL causes transverse cracking in HMA and is prominent in thin HMA pavement. Chen (2007) reports that lack of mellowing for lime slurry stabilized base layers causes shrinkage cracking and then transverse cracking in the HMA surface. Little et al. (1995) found that a high modulus value causes wide shrinkage cracks and low load transfers across the crack.

George (2002) found that high-strength CSL are prone to shrinkage cracking, based on Long-Term Pavement Performance (LTPP) and other pavements. When the 7-day in-service

strength is 300 psi or lower, no shrinkage cracking occurs. Increasing the fines content increases the cracking intensity. Bituminous curing of the CSL before the placement of the surface layers corresponds to 65% relative humidity (RH) for most specifications. In the laboratory, moist curing corresponds to 95% RH. Crack width is significantly affected by drying shrinkage. Crack spacing decreases with an increase in friction between the CSL and underlying layer. For wide shrinkage cracks, load transfer efficiency is between 35% and 55%, and 80% for fine cracks for coarse-grained aggregate. Cracks wider than 0.1 inch (measured on HMA surface) affect the pavement performance significantly. For fine-grained soil, the critical crack width is claimed to be 0.06 inch. Decreasing the strength of the CSL decreases the tensile stress in the CSL. There is an optimum shrinkage strain level: 525 microstrain for fine-grained soil and 310 microstrain for coarse-grained soils, respectively.

### **2.1.2 Concrete Pavement**

For concrete pavement with stabilized base layers, most of the reports indicate positive effects, such as reduced faulting, pumping, and cracking (Neal and Woodstrom 1977, ARA 2004, Selezneva et al. 2000, Ruiz et al. 2005, Hall and Crovetti 2007). Nussbaum and Childs (1975) report that using CSL greatly increases the load-carrying capacity of concrete slabs. However, a study by Mallela et al. (2007) shows that the bond between the concrete layer and stabilized base might contribute to early-stage cracking in concrete pavement. The use of a bond breaker is recommended in such cases (Mallela et al. 2007, Ruiz et al. 2005). The erosion of CSL, especially weakly stabilized materials, also may cause pumping and resultant faulting and cracking, as shown in Figure 2-3 (ARA 2004, Jung et al. 2009).



**Figure 2-3. Cracking of Concrete Pavement**

## **2.2 PROPERTIES OF CSM LINKED TO SHRINKAGE CRACKING**

Based on the previous discussion outlined in Section 2.1, the properties of CSL that are related to shrinkage cracking are identified and described in detail in the following sections.

### **2.2.1 Shrinkage of CSL**

Shrinkage cracking of CSL as base layers, as shown in Figure 2-4, can cause the cracking of the surface layer due to the bond between the surface layer and the CSL. Shrinkage of CSL includes autogenous shrinkage due to hydration, drying shrinkage due to loss of moisture and thermal shrinkage due to low temperature contraction (ACI 2008). Drying shrinkage is the major reason of shrinkage cracking (George 1968a; and Bofinger et al 1978). Shrinkage of CSL, when restrained (e.g., bonding from underlying layer), causes the development of tensile stress in the CSL. When the tensile stress exceeds the tensile strength of the stabilized materials, shrinkage cracking occurs (George 1990). Shrinkage cracking can occur within a few days or over a couple of years, depending on the curing, shrinkage strain, tensile strength and modulus, and other

factors. Shrinkage of CSL is affected by many factors, such as moisture, curing after compaction, additive content, raw material characteristics, and temperature variation.



**Figure 2-4. Shrinkage Cracking of CSL (George 2001)**

#### *2.2.1.1 Moisture and Curing*

Kodikara and Chakrabarti (2001) report that shrinkage results from moisture loss, which leads to matric suction (capillary forces), osmotic suction, and thermal cooling. George (1968a, 1990, 2001) reports that moisture content that is higher than the optimum moisture content (OMC) causes excessive shrinkage cracking. George (1990) also reports that shrinkage can be reduced by reducing molding moisture, increasing compaction density, avoiding montorillonite clay, and limiting the degree of saturation to 70 percent.

The moisture content in CSL is affected by the curing method. Sebesta (2005b) reports that bituminous curing is minimally effective in reducing cracking problems. Bituminous curing and dry curing provide little difference in shrinkage cracking for 4% cement sections. Shrinkage cracking occurs within the first two days. However, moist curing works better in mitigating shrinkage cracking than dry curing and prime curing for 8% cement sections. Norling (1973)

suggests curing the CSL as soon as possible to mitigate the early rapid moisture loss. George (1968a) notes that prolonged curing can decrease overall shrinkage, though it increases the shrinkage due to higher proportion of gel. And George (2002) indicates that unsurfacing the base layer can cause shrinkage cracks.

Pretorius and Monismith (1971) use the theory of viscoelasticity to analyze shrinkage cracking. Increasing the RH reduces the creep and shrinkage strain but increases the relaxation modulus. With an increase in curing time, the tensile strength continues to increase at 100% RH during curing. However, for other RH values, the strength value reaches a peak and then starts to decrease. Increasing the RH reduces shrinkage stress.

#### *2.2.1.2 Binder Content*

Binder content can influence the shrinkage cracking formation. High cement ratio causes problematic cracking in the base even if it is cured in good condition (Sebesta 2005a; Bofinger et al 1978), and there exists obvious relationship between cement content and shrinkage (Nakayama and Handy 1965). While other researchers find that shrinkage can be minimized at the optimum cement content (George 1968a; Scullion et al 2000).

Matthew et al. find that low strength ensures narrow and closely spaced shrinkage cracks that do not reflect through the wearing course. This finding is in line with that of Van Blerk and Scullion (1995) who conclude that high-strength CSL have wide cracks at large spacing and low strength CSL have fine cracks at close spacing.

#### *2.2.1.3 Host Materials*

The characteristics of host materials directly affect the shrinkage behavior of CSL. Norling (1973) found that increasing the clay content increases the occurrence of shrinkage. Van

Blerk and Scullion (1995) also indicate that an increase in the PI value increases the shrinkage potential. Smectite clay causes the most shrinkage. George (2002) finds that fine soil presents large crack width. And kaolinite soil-cement can shrink faster than montmorillonite soil-cement, maybe because larger particle size of kaolin clay makes moisture evaporate easily due to low water absorption energy (George 1968a). The linear shrinkage of the fine fraction of the aggregate is a good indicator of the ultimate drying shrinkage of the CSL. It is recommended that linear shrinkage of 1.5%, PI value of 4.0, passing #200 sieve of 7%, and shrinkage after 21 days of 250 microstrain are the maximum allowed.

Kodikara and Chakrabarti (2001) report that a clay size that is smaller than 0.08 mil is responsible for shrinking and swelling. Autogenous shrinkage is only 5% of the total shrinkage. The shrinkage potential of CSM is between that of clay and cement paste. Adding cement to clay reduces shrinkage due to the reduction in matric suction. However, after reaching a low point, adding more cement will induce higher shrinkage strain due to more gel particles. The restrained shrinkage cracks were examined with a microscope in the Kodikara and Chakrabarti study.

#### *2.2.1.4 Thermal Cooling*

Bonnot (1991) reports that factors that affect shrinkage include water content, thermal shrinkage, and the strength of the materials. Shrinkage cracking can result from thermal contraction. Cooling by 9°F to 18°F can cause thermal cracking in the laboratory. Shrinkage also can be increased by increasing the mixing temperature from 75°F to 100°F (George 1968a).

The values of coefficient of thermal expansion (COTE) of materials are highly variable. This means even at the same thermal variation condition, various layers can experience different shrinkage strain. Scullion and Harris (1998) report shrinkage cracking of CSL caused by the

difference of COTE between the lower cement stabilized recycled asphalt layer and upper cement stabilized limestone and sand layer. However, Otte (1978) indicates the thermal stress can be ignored after the initial cracks have formed, compared to the traffic-associated stress, as the cracks can release the stress and prevent the stress concentration. And placing a thick cover over the cement-treated base can mitigate the thermal stress.

### **2.2.2 Strength and Stiffness of CSM**

The strength of CSL directly controls their performance and thus affects overall pavement performance. The strength of CSM often is used in performance prediction models. The strength of CSM can be obtained from direct tensile, indirect tensile (IDT) strength, and UCS tests. UCS tests often are used for the purpose of mix design. Inadequate strength can result in crushing (compression) failure in the upper layer of CSL, especially for lightly stabilized deep layers (De Beer 1990). While high strength CSL is more likely to lead to cracking (George 2002).

George (2001) reports that a low strength or low modulus/strength ratio is beneficial in mitigating shrinkage cracking. The UCS after 7 days is recommended in the range of 300-400 psi to minimize surface cracking by Portland Cement Association (PCA) (Sebesta 2005a); and also Scullion (2002) suggests reducing the design strength from 500 to 300 psi to mitigate cracking. While other researchers argue the opposite view, Zube et al (1969) find that increasing the compressive strength can reduce block cracking, but transverse cracking is not significantly influenced by the increase of compressive strength.

Tensile strength and stiffness affect the development of shrinkage cracking in CSL. Little et al. (1995) report that shrinkage crack spacing depends on tensile strength and the friction

between the CSL and underlying layer. The width of the cracks depends on the tensile stiffness of the CSL. A maximum shrinkage strain of 250 microstrain is recommended.

Otte (1978) reports that the ratio between direct tensile strength and IDT strength is close to one. The Otte study also evaluates compressive strength, tensile strength, IDT strength, and bending strength. Pretorius et al. (1972) find that tensile strength is about one-tenth of UCS.

The strength of CSM is affected by many factors. Factors that affect the tensile strength of soil-cement include: molding water content, curing time, aggregate gradation, type of curing, aggregate type, curing temperature, compaction efforts, type of compaction, and cement content (Jayawickrama et al. 1998). It is reported that delayed compaction can reduce the strength of CSM. High levels of compactive effort lead to high UCS values. Increasing the water content decreases the UCS (Bhattacharja and Bhatty 2003). Increasing the cement content increases the UCS values (Arora and Aydilek 2005). Increasing the fines content up to 30% increases the UCS (Ashtiani et al. 2007).

The modulus of CSM is used in the shrinkage cracking model for the critical stress and strain analysis. In general, high stiffness stems from high additive content, which also may cause high shrinkage rates. Therefore, the impact of stiffness (or modulus) must be studied to develop an appropriate stiffness range for pavement application. For stabilized subbase, high stiffness is generally not a concern. The tensile modulus of CSM can be obtained by conducting IDT modulus tests. For Level 2, the modulus is predicted from the UCS. The modulus of CSM is affected by many factors, as follows (AustROAD 2008, Foley 2002, Marais et al. 1973, Yeo 2008, Khoury 2005, Arora and Aydilek 2005):

- proportion of coarse angular aggregate
- density

- compaction moisture content up to OMC
- binder content
- age
- efficiency of mixing
- field moisture content
- size of aggregate

Little (1999) provides the relationship between the IDT strength and UCS of soil-lime material, as follows.

$$IDT\ strength = 0.13 \times UCS \quad \text{Eq. (2-1)}$$

Figure 2-5 shows the relationship between UCS and IDT strength (Kennedy and Hudson 1973).

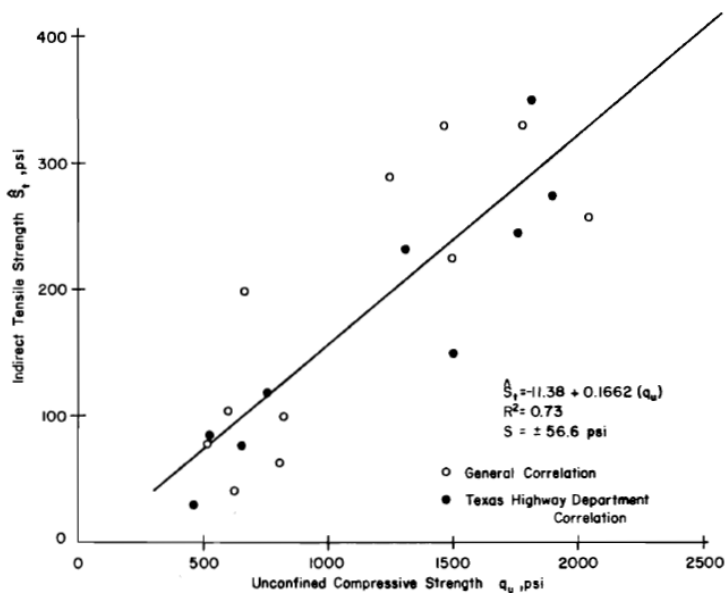


**Figure 2-5. Relationship between UCS and IDT Strength (Kennedy and Hudson 1973)**

Strength values obtained from different test modes can be related, but the modulus and strength values can only be related for a specific material (Carteret et al 2009). In addition, the strength and modulus of CSM continue to grow as the materials' age. Little and Nair (2007) report that for soil-lime, the UCS increases by 3.2 times from 28 days to 26 weeks and in another cases by 11 times from 60 days to 180 days.

Wang and Hudson (1972) use the following formula to predict the direct tensile strength of soil-cement.

$$\text{Direct tensile strength} = [0.5 + 60C^{1.33}/(32+C^{1.33})][1 + (2\log(t/92))^{2.67} + (\log(t))^{2.67}] \quad \text{Eq. (2-2)}$$

where

$C$  = cement content, %, and

$t$  = curing time, days.

The U.S. Air Force also provides a prediction equation to estimate the growth of UCS of soil-cement, as follows.

$$UCS(t) = UCS(t_0) + K \log(t/t_0) \quad \text{Eq. (2-3)}$$

where

$K = 70C$  for granular soils and  $10C$  for fine-grained soils,  $t$  is the number of curing days, and  $C$  is the cement content (%).

Lim and Zollinger (2003) developed a prediction equation to estimate initial strength of concrete based on 28-day strength:

$$f(t) = f(28)(t/[2.5 + 0.9t]) \quad \text{Eq. (2-4)}$$

where

$f(t)$  = UCS earlier than 28 days.

$t$  = days since the compaction of CSM within 28 days.

### **2.2.3 Interface Bond**

Even though it is not a material property, the interface bond between CSL and underlying material restrains the free movement of the CSL due to shrinkage or expansion. Interface bonding thereby affects shrinkage crack spacing and width.

Romanoschi and Metcalf (2001) report that the loss of a bond between HMA and CSL significantly increases the tensile strain at the bottom of the HMA layer. The bond between CSL and HMA is often lost due to the presence of water and erosion/crushing of the CSL surface. Shear failure occurs within the top of the CSL instead of at the interface of the CSL and HMA. The loss of the bond between the asphalt and CSL causes a shift in critical tension from the top of the subgrade to the bottom of the asphalt layer.

Wimsatt et al. (1987) report that increasing the interface bond strength between Portland concrete cement (PCC) and the base results in narrow crack spacing. The failure plane happens in CSL. The IDT strength of the CSL is correlated with the friction forces. Grogan et al. (1999) report that for concrete on top of CSL, asphalt emulsion does not work well as a bond breaker. Slippage and horizontal cracks are located below the interface of the concrete and CSL.

Wesevich et al. (1987) also report that for concrete pavement with CSL, friction at the interface results from adhesion, shearing and bearing. The soil cement base has the highest level of friction with a concrete surface, followed by the granular base, and asphalt and lime clay bases.

### **2.2.4 Techniques to Mitigate Shrinkage Cracking**

Shrinkage cracking occurs as a result of contraction of CSM that are restrained by the underlying materials. Shrinkage cracking can reflect through the surface layer and allow the

ingress of surface water. The shrinkage cracking of CSL can be reduced by (AustROAD 2008, George 1968a):

- the immediate application of a curing coat
- a lower binder content
- the use of slow-setting binder
- a lower fine clay content (<20% 0.003 in fines and PI <20)
- pretreating with lime or lime+cement
- adding gravel or rock.

Queensland in Australia uses the following specifications to reduce shrinkage (Scullion et al. 2005):

- Linear shrinkage of raw soil passing the #40 sieve: 2.5% maximum
- Plasticity index: 4% maximum
- Introduction of a fly-ash blend cement
- Percentage of fines passing #200 sieve: 7.0% maximum
- Linear shrinkage of cement-treated base material should not exceed 250 microstrain after 21 days.

Microcracking is an effective method to mitigate shrinkage cracking problems associated with the cement stabilized bases with no impact the pavement overall capacity or reduction of in-service modulus (Sebesta 2005a; Scullion 2002). Microcracking, which is formed by several vibratory roller passes to the cement-treated base at early curing age, can reduce both the total amount of cracking and the width of the cracks (Sebesta 2005a). Another solution to mitigate shrinkage cracking is to pre-crack the CSL by wet-forming transverse notches to 1/3-1/2 layer

thickness right after compaction (Thogersen and Bjulf 2005). Crack width of 0.1 in. is appropriate for load transfer and prevention of water infiltration (Kota et al 1995). In addition, slower strength gain associated with lime-Class F fly ash, compared to cement stabilized material, can prevent microcracks in CSL from developing into macrocracks by autogenous healing process, which is a benefit for the long-term performance of HMA pavements (Barstis and Crawley 2000; Thogersen and Bjulf 2005).

Scullion (2002) and George (2002) also find that the delay in placing the final HMA surface can reduce the extent and severity of the surface cracking.

Scullion et al. (2005) report that typical shrinkage cracking spacing is between 3 ft and 60 ft. The crack width is affected by temperature. Little (1999) finds that in summer, the backcalculated modulus value of CSL with a crack width less than 0.1 inch is about half of the backcalculated modulus value of CSL without cracks. However, in winter, the modulus value at a cracked area is one-third of the modulus value at an area without cracks.

## **2.3 SHRINKAGE CRACKING MODELS**

For the purpose of pavement design and performance prediction, shrinkage cracking model is needed to predict the time of occurrence of shrinkage cracking, crack spacing and width. Prediction of drying shrinkage strain as input to the shrinkage cracking model is also needed.

### **2.3.1 Drying Shrinkage Strain Model**

It is very time-consuming to measure drying shrinkage strain in the laboratory, especially the ultimate drying shrinkage strain (ARA 2004). Several drying shrinkage strain prediction models are available to predict the drying shrinkage strain of concrete. Mokarem et al. (2003) evaluated five drying shrinkage strain prediction models for concrete:

- American Concrete Institute – ACI 209
- Euro-International Concrete Committee - CEB 90 Code
- Bazant B3
- Gardner/Lockman
- Sakata

It is reported that the CEB 90 code model is the best for matching measured drying shrinkage strain. The current MEPDG provides a drying shrinkage strain prediction model for concrete that is similar to the CEB 90 code model (ARA 2004). The MEPDG drying shrinkage strain model is:

$$\varepsilon_{shr}(t) = \varepsilon_{su} \left\{ 1 - \left( \frac{RH_c}{100} \right)^3 \right\} \quad \text{Eq. (2-5)}$$

where

$\varepsilon_{shr}(t)$  = unrestrained drying shrinkage strain at any time  $t$  days from placement,  $\times 10^{-6}$

$\varepsilon_{su}$  = ultimate drying shrinkage strain

$RH_c$  = relative humidity, %,

where  $RH_c = RH_{ai} + (100 - RH_{ai})f(t)$

$RH_{ai}$  = atmospheric relative humidity, %

$f(t) = I/(I+t/b)$ ,

where  $t$  = time since placement in days

$$b = 35d^{1.35}(w/c - 0.19)/4$$

$d$  = half of depth of layer

$w/c$  = water cement ratio.

The ultimate drying shrinkage strain of concrete (ARA 2004) is:

$$\varepsilon_{su} = C_1 C_2 \left\{ 26w^{2.1} f_c^{'}^{-0.28} + 270 \right\} \quad \text{Eq. (2-6)}$$

where

$\varepsilon_{su}$  = ultimate shrinkage strain,  $\times 10^{-6}$

$C_1$  = cement type factor

$C_2$  = type of curing factor

$w$  = water content by weight

$f_c^{'}$  = 28-day PCC compressive strength.

### 2.3.2 Shrinkage Cracking Models

A few researchers have developed shrinkage cracking models for either CSL or concrete pavement. Due to the similarities between CSL and concrete pavement, the shrinkage cracking issues in both areas are considered here.

(a) Zhang and Li model

Zhang and Li (2001) derived a closed-form solution for shrinkage stress in concrete pavements. Based on their model, crack spacing and width can be derived, respectively, as:

$$L = \frac{1}{\beta} \cosh^{-1} \left( \frac{1}{\frac{S(t)}{E\varepsilon} + 1} \right) \quad \text{Eq. (2-7)}$$

$$W = \frac{2\varepsilon}{\beta} \tanh(\beta L) \quad \text{Eq. (2-8)}$$

where

$L$  = shrinkage crack spacing

$W$  = crack width

$$\beta = \sqrt{\frac{\tau_0}{EH\delta_0}}$$

$S(t)$  = tensile strength of CSL

$E$  = modulus of CSL

$\varepsilon$  = drying and thermal shrinkage strain

$\tau_0, \delta_0$  = maximum friction stress and displacement from slab friction test

$H$  = CSL thickness.

(b) George model

George (1968b) developed a simple model for crack spacing and width, as follows.

$$L = \frac{2\sigma_u}{\mu\gamma} \quad \text{Eq. (2-9)}$$

$$W = \varepsilon_c L - \frac{\mu\gamma L^2}{4E_t} \quad \text{Eq. (2-10)}$$

where

$L$  = shrinkage crack spacing

$W$  = crack width

$\sigma_u$  = ultimate tensile strength of CSL

$\mu$  = coefficient of sliding coefficient

$\gamma$  = unit weight of CSL

$E_t$  = modulus of elasticity of CSL

$\varepsilon_c$  = shrinkage strain.

## **2.4 TEST PROCEDURES FOR CSM PROPERTIES**

Based on the literature and parameters needed for the shrinkage cracking model, strength/stiffness, drying shrinkage (either free or restrained), and thermal shrinkage affect the shrinkage cracking of CSL. The proper characterization of the properties of CSM is important for selecting appropriate CSM and predicting the field performance of CSL. Different test procedures are available to measure these properties and need to be evaluated for selection.

### **2.4.1 Strength and Modulus Tests**

When the shrinkage stress exceeds the tensile strength of CSM, shrinkage cracks occur. The strength values of CSM can be obtained through direct tensile, IDT strength, or UCS test. The modulus can be obtained through IDT modulus test.

#### *2.4.1.1 Direct Tensile Strength Test*

Direct tensile strength is used to characterize CSM (Raad 1977, Otte 1978). Direct tensile strength tests subject a specimen to a tensile force with constant movement or load rate. The direct tensile test simulates the field conditions when the material is subjected to pure tension, such as thermal contraction or drying shrinkage (Hudson and Kennedy 1968). Direct tensile tests can be conducted in accordance with ASTM D2936–08, *Standard Test Method for Direct Tensile Strength of Intact Rock Core Specimens*. However, the test has many limitations, including a long preparation time (about 3 hours), misalignment for pure tension, and failure outside the central portion (Yeo et al. 2002). In addition, the method that is used to grip the specimen is also challenging (Gnanendran and Piratheepan 2008). All these factors contribute to lack of practicality and repeatability. Chakrabarti and Kodikara (2007) modified the tensile strength test setup (Figure 2-6). However, this configuration still is subjected to bending stress.

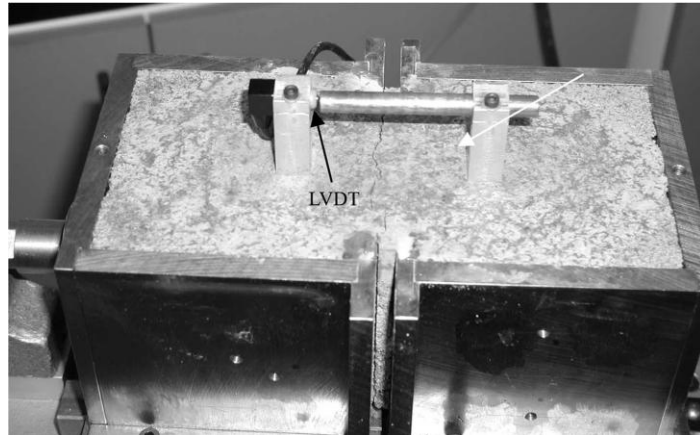


**Figure 2-6. Modified Tensile Strength Test (Chakrabarti and Kodikara 2007)**

#### 2.4.1.2 IDT Strength Test

The tensile strength of CSM can be obtained from indirect tensile strength test. The IDT strength test involves loading a cylindrical specimen with compressive loads distributed along two axial lines that are diametrically opposite, as shown in Figure 2-7. This loading setup results in a relatively uniform tensile stress perpendicular to and along the diametric plane. Failure occurs by splitting along this loaded plane.

The IDT strength can be calculated as follows:

$$S(t) = \frac{2P}{\pi l d} \quad \text{Eq. (2-11)}$$

where

$S(t)$  = IDT strength

$P$  = peak load

$l$  = height of specimen

$d$  = diameter of specimen.

From a review of the literature concerned with the evaluation and use of IDT strength, a number of advantages and disadvantages are found. The six major advantages attributed to the test are as follows (Hudson and Kennedy 1968):

- It is relatively simple.
- The type of specimen and equipment are the same as that used for compression testing.
- Failure is not seriously affected by sample end conditions.
- Failure is initiated in a region of relatively uniform tensile stress.
- The coefficient of variation (COV) of the test results is low.
- Mohr's theory is a satisfactory means of expressing failure conditions for brittle crystalline materials.

In addition, according to Yeo et al. (2002), the IDT strength test is practical, productive, economic, and user-friendly. Besides strength, the IDT strength test can also be used to measure the modulus, Poisson's ratio, fatigue, and permanent deformation (Gnanendran and Piratheepan 2008). The IDT test is also suitable for lightly stabilized materials (Yeo et al. 2002).

The IDT strength values for concrete can be obtained using AASHTO T198, *Splitting Tensile Strength of Cylindrical Concrete Specimens*, or ASTM C496, *Standard Test Method for Splitting Tensile Strength of Cylindrical Concrete Specimens*. The specimen geometry is 6 inches in diameter and 12 inches in height. The loading rate of the splitting tensile stress is 100-200 psi/min. The size and loading rate may not be appropriate, however, for soil-lime or soil-fly ash/lime, which is relatively weak material. The Australian method (Midgley and Yeo 2008) to test for IDT strength of stabilized materials uses specimens either 4 inches or 6 inches in diameter, which is dependent on the maximum particle size. The loading rate is  $4500 \pm 450$

lbs/min. For IDT testing, specimen length is not a factor for strength (Hudson and Kennedy 1968). For CSM, neither composition nor width of the loading strip makes any difference to the test results (Hudson and Kennedy 1968).



**Figure 2-7. IDT Test Setup (Yeo 2008)**

#### *2.4.1.3 Unconfined Compressive Test*

The UCS test is the most common test performed on CSM which can be used to correlate with direct or indirect tensile strength. It is also widely used to determine the suitability of the mixtures for uses such as in pavement bases and subbases, stabilized subgrades, and structural fills. Most state highway agencies use the UCS test for their mix designs and for quality assurance (QA) and quality control (QC) because of the simplicity of the test. The UCS test is well-established and meets all cost, practicality and availability requirements (Yeo et al. 2002). Tensile strength can be estimated conservatively as 10% of the UCS (Little 1999). Typically, AASHTO T22, ASTM D1633, AASHTO T220, and ASTM C593 are used to test lean concrete, soil cement, lime-stabilized materials, and fly ash-stabilized materials with or without lime, respectively.

The UCS value is the peak load divided by the cross-section of a cylindrical specimen, except for soil-lime for which the enlargement of the cross-section during loading is taken into account. The typical height-to-diameter ratio of a UCS specimen is two. Otherwise, a correction factor must be used to obtain a meaningful strength. Figure 2-8 presents the UCS test setup.

- For lean concrete, the loading rate in AASHTO T22 is displacement-controlled, which corresponds to 35+/-7 psi per second. The ratio of height to diameter is 1.75 or higher. Otherwise, a correction factor should be used.
- For soil-cement, the specimen size is either 4 inches in diameter by 4.6 inches in height or 2.8 inches in diameter and 5.6 inches in height according to ASDTM D1633. For the specimen with a 4-inch diameter and 4.6-inch height, a correction factor of 0.909 is used to convert the strength to that of a specimen with a height-to-diameter ratio of 2.0. The preparation of soil-cement specimens is based on ASTM D1632. Capping is required for soil-cement specimens. The test is conducted using either displacement-controlled, 0.05 in./min, or stress-controlled, 20 psi per second. Prior to the testing, the specimen is subjected to 4-hour soaking.
- For soil-lime, AASHTO T220 specifies a specimen size of 6 inches in diameter and 8 inches in height. The loading rate is 0.13-0.15 in./min. Prior to compression testing, the specimen is subjected to 7-day curing at room temperature, 6-hour drying at 140°F, and 10-day capillarity with confining pressure. The UCS is determined as follows:

$$UCS = \frac{Pd}{Ah} \quad \text{Eq. (2-12)}$$

where

$P$  = total vertical load

$d$  = deformation after testing

$A$  = cross-section of specimen before testing

$H$  = height of specimen before testing.

- For high calcium fly ash, such as Class C fly ash, or low calcium fly ash and lime-stabilized materials, ASTM C593 recommends the use of ASTM C39/C39M, *Test Method for Compressive Strength of Cylindrical Concrete Specimens*, which is equivalent to AASHTO T22. Prior to the UCS test, the specimen is subjected to 7-day curing at 100°F and 4-hour soaking. The specimen geometry is 4 inches in diameter and 4.6 inches in height.



**Figure 2-8. Unconfined Compressive Strength Test Setup**

#### 2.4.1.4 IDT Modulus Test

Tensile modulus of CSM is an important property in the shrinkage cracking model. The IDT modulus test involves placing a cylindrical sample horizontally along its axis with compression loading applied vertically across the diameter of the specimen. Induced tensile strains are measured horizontally across the diameter. The IDT modulus can be determined based on the following equation (Midgley and Yeo 2008):

$$E = P \times \frac{(v+0.27)}{H \times h_c} \quad \text{Eq. (2-13)}$$

where

$P$  = peak load

$v$  = Poisson's ratio

$H$  = recovered horizontal deformation of specimen after application of load

$h_c$  = height of specimen.

The IDT modulus value is higher than the beam modulus value (Yeo 2008). Yeo et al. (2002) report that the Australian IDT test is suitable for determining the strength and stiffness of stabilized materials. Cylindrical test specimens are considered to be the most practical both in terms of laboratory compaction and field sampling via coring techniques. In addition, this test is practical, cost-effective, has good equipment availability, requires basic sample preparation and provides for the preferred tensile mode of failure for both the strength and fatigue tests. On the other hand, use of such a test may be extremely difficult with brittle stabilized materials because once their ultimate load is exceeded, rapid cracking and sample failure is inevitable. Currently, there is no test standard to determine the IDT modulus. The Australian test method for the IDT modulus of CSM has been evaluated (Midgley and Yeo 2008). To determine the specimen IDT modulus, 50% or less of the ultimate failure load determined using the IDT strength test is used such that the material remains within its elastic range. The displacement is measured by linear variable differential transformer (LVDTs).

The COV of the IDT modulus is reported to be less than 20 percent (Carteret 2009). The location of the LVDTs is found to affect the test results significantly. By using internal LVDTs, the COV can be reduced significantly (Gnanendran and Piratheepan 2008).

## 2.4.2 Shrinkage Tests

Shrinkage of CSM can be characterized as free drying, restrained drying, and thermal shrinkage.

### 2.4.2.1 Free Drying Shrinkage Test

AASHTO T160, *Length Change of Hardened Hydraulic Cement*, can be modified to characterize the drying shrinkage of CSM. Different RH values can be used to obtain the drying shrinkage strain. Long-term curing also is needed to measure the ultimate drying shrinkage strain. Tex-107-E also allows users to determine the bar linear shrinkage of soils and is used for CSM (Si 2008, Guthrie et al. 2001).

Chakrabarti and Kodikara (2003) conducted drying shrinkage tests according to methods found in AS1012.13-1992. A known quantity of stabilized mix according to standard maximum dry unit weight was compacted in two layers into a rectangular steel mold measuring 3 in.  $\times$  3 in.  $\times$  11 in. A standard Proctor hammer with a maximum cross-sectional dimension of 2 inches (2.6 in., including the guide) was used to compact the material. Two gauge studs were placed at the middle of the end sections during compaction to facilitate shrinkage measurements. Specimens in duplicate per set were cured for 24 hours at 90% RH or above and at an air temperature of 70°F to 75°F. Subsequently, the specimens were dried in a controlled environment with 50% RH and at an air temperature of 71.6°F. Specimen lengths,  $l_i$  (in.), were recorded at gradually increasing intervals for up to 90 days while the specimens were kept in a controlled environment of 71.6°F and 50% RH. Shrinkage ( $\varepsilon_{sh}$ ) at any time in microstrain can be determined as follows:

$$\varepsilon_{sh} = (l_o - l_i) \times 10^6 / l_o \quad \text{Eq. (2-14)}$$

where,

$\varepsilon_{sh}$  = shrinkage strain at any time, microstrain

$l_o$  = specimen initial length, in.

$l_i$  = specimen length after drying process, in.

Figure 2-9 shows a free drying shrinkage test setup. The unrestrained or free shrinkage represents the full shrinkage potential of a geomaterial under a given environmental condition. In free drying shrinkage, no shrinkage stress is generated.



**Figure 2-9. Free Drying Shrinkage Test**

#### 2.4.2.2 Restrained Shrinkage Test

Tensile stress is generated when the changes of moisture or temperature cause a CSL to contract, and the underlying friction or self-restraint keeps the base from contracting. Shrinkage cracking occurs when the tensile stress exceeds the tensile strength of the cement-treated pavement layer (Cauley and Kennedy 1972). Because the restraint is in place either externally by the subgrade/surface layer or internally by differential shrinkage within different depths of the CSL due to the presence of humidity and temperature gradients in actual field conditions, the shrinkage cracking potential of each material in the CSL can be examined by restrained shrinkage testing.

In the concrete shrinkage cracking test, a ring of concrete is fabricated outside a steel ring. The internal steel ring hinders free drying and generates cracks. The onset of cracking and the development of the crack width are measured (Kodikara and Chakrabarti 2001).

The PCA recommends a drying shrinkage test on soil-cement beams restrained with a rough surface at their base (George 2002). This recommended procedure can be modified as a restrained shrinkage test for CSL. However, the bond condition recommended by the PCA, i.e., CSL on sand, does not generate shrinkage cracking within this 12-inch long beam. A typical shrinkage cracking spacing in the field is between 3 ft. and 60 ft. To generate shrinkage cracking in a laboratory-scale specimen, a strong bond must be created between the specimen and base. In addition, the length of the specimen must be increased.

Weiss et al. (1998) conducted restrained concrete slab tests to generate shrinkage cracking in a 39-inch long slab. The slab was fixed to the base, or to both ends and base, as shown in Figure 2-10. By restraining the movement of the slab, the shrinkage cracking spacing is significantly shorter than the field cracking spacing. The concrete slab was bonded to a steel tube to prevent curling.

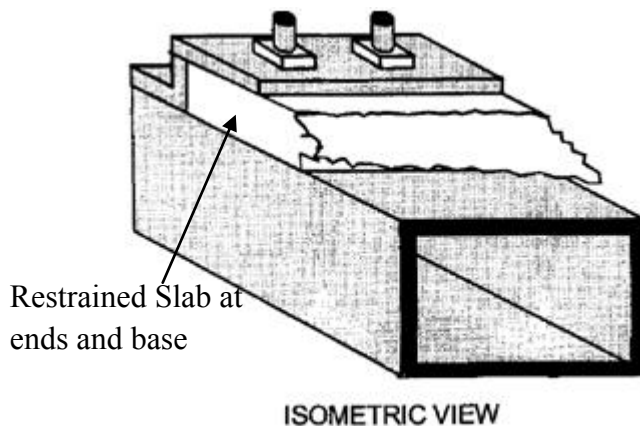


**Figure 2-10. Restrained Slab at Base and Ends (Weiss et al. 1998)**

#### 2.4.2.3 Thermal Shrinkage Test

The COTE is important for thermal strain determination, which is a key parameter in the shrinkage cracking model. AASHTO TP60, *Standard Method of Test for Coefficient of Thermal Expansion of Hydraulic Cement Concrete*, is a test method to determine the COTE of concrete. This method determines the COTE of a cylindrical concrete specimen, maintained in a saturated condition, by measuring the length change of the specimen due to a specified temperature change, as shown in Figure 2-11. The measured length change is corrected for any change in length of the measuring apparatus (previously determined), and the COTE is then calculated by dividing the corrected strain by the temperature change between 50°F and 122°F.

Cusson and Hoogeveen (2006) also recommend a test method for measuring the COTE, especially for early-age concrete. In their test, a concrete beam specimen is subjected to temperature cycles between 77°F and 86°F, including a 15-min temperature ramp followed by a 4-hour constant temperature. The cyclic strain, which does not include the permanent autogenous shrinkage strain, is used to determine the COTE.

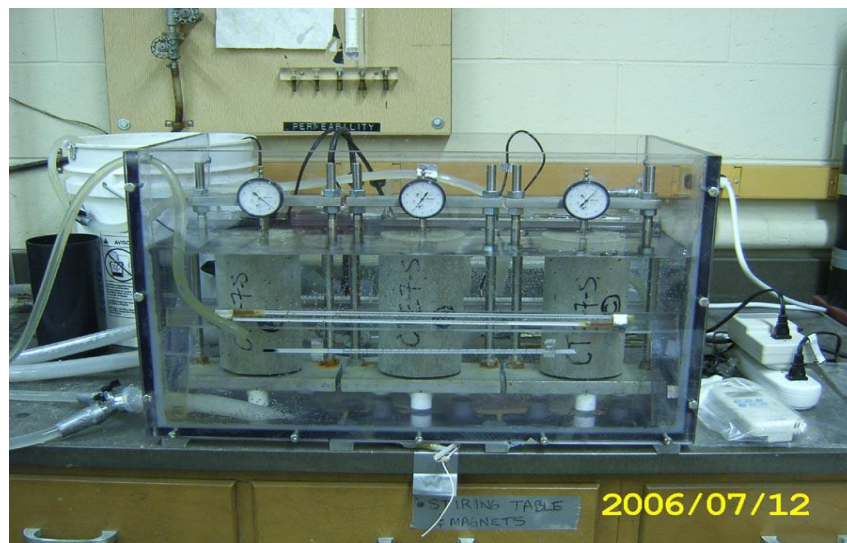


**Figure 2-11. Test Setup of Coefficient of Thermal Expansion (Naik et al. 2006)**

## **2.5 SUMMARY**

Block cracking and transverse cracking are the most severe distresses for pavements with CSL, according to the state agency survey results, which are due to the shrinkage cracking of CSL. When the tensile stress due to shrinkage is beyond the tensile strength, the shrinkage cracking occurs. The properties of CSL that can influence shrinkage cracking include the shrinkage of CSL, strength and stiffness of CSL, and the bonding condition between CSL and sublayer. The shrinkage cracking is influenced by several factors, like the moisture and curing condition, binder type and content, host material properties, and temperature variation. It is still unable to reach a consensus on how the strength and stiffness influence shrinkage cracking. Interface bonding affects shrinkage crack spacing and width. Several techniques to mitigate shrinkage cracking are mentioned in literature. Right now only drying shrinkage strain prediction models are available for concrete. CEB 90 model gives the best prediction. George (1968) gives a simple model for crack spacing and width of CSL. Zhang and Li (2001) introduces a closed-form solution for shrinkage crack spacing and width for concrete. These models will be evaluated in this research with both lab and field data. The test procedures that can identify CSM properties linked to shrinkage cracking include UCS, IDT strength and modulus, direct tensile strength, free drying shrinkage, restrained shrinkage, and thermal shrinkage test. These test procedures will be assessed in terms of their performance predictability, precision, accuracy, practicality, cost, and other pertinent factors.

## CHAPTER THREE

### SOIL PROPERTIES AND MIX DESIGN

This chapter presents the basic soil properties and mix design results for characterizing the properties of CSM for test procedure evaluation and model development. Four types of host material are used in this study for stabilization. The binders used for this study include cement, lime, and Class F and Class C fly ash. Totally nine different soil binder combinations are used in this study, which are the most common used according to the survey results from state agencies, as shown in Appendix A. These materials are used for test procedure evaluation and model development.

#### 3.1 BASIC SOIL PROPERTIES

The host soils are characterized in terms of moisture-density relationships, Atterberg limits, and gradation. Figure 3-1 presents the gradations of these four host soils. Table 3-1 presents the Atterberg limits and designations of these four host soils.

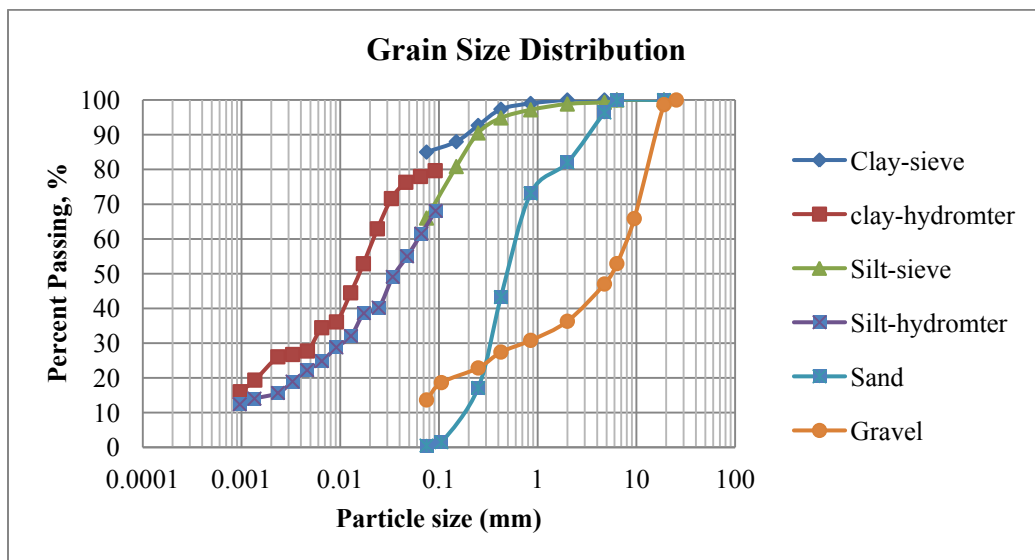


**Figure 3-1. Gradation of Host Soils**

**Table 3-1. Characteristics of Host Soils**

		<b>Clay</b>	<b>Silt</b>	<b>Sand</b>	<b>Gravel</b>
<b>Atterberg Limit</b>	LL	39	17	x	x
	PL	23	15	x	x
	PI	16	2	-	-
<b>Designation</b>	USCS	CL	ML	SP	GM
	AASHTO	A-6	A-4	A-1-b	A-1-a

## 3.2 MIX DESIGN

Mix designs were conducted to determine the appropriate binder contents. In this study, the methods developed by the National Lime Association (NLA) (2006) for soil-lime, the PCA (1992) for soil-cement, and the Federal Highway Administration (FHWA) (Veisi et al. 2010) guidelines for soil-fly ash were followed. Three replicates were used to measure UCS. It is noted that these mix design methods may be different from the methods used by other agencies. However, it is not the objective of this study to develop mix design methods. Instead, the mix designs were conducted to obtain representative mixes for test procedure evaluation and model development. In addition, depending on the location of a mix in a pavement, i.e., in the base or subbase, the binder content could be different for one type of soil.

### 3.2.1 Soil-Cement

Based on the soil designations, three trial cement contents were used to fabricate the soil-cement specimens, in accordance with the PCA method (PCA 1992). Among the trial contents, the minimum cement content that resulted in UCS values larger than 300 psi after 7-day curing was selected for that soil. It was found that a cement content of 3% is suitable for stabilizing gravel, 6% for sand, 8% for silt, and 12% for clay, as shown in Figure 3-2.

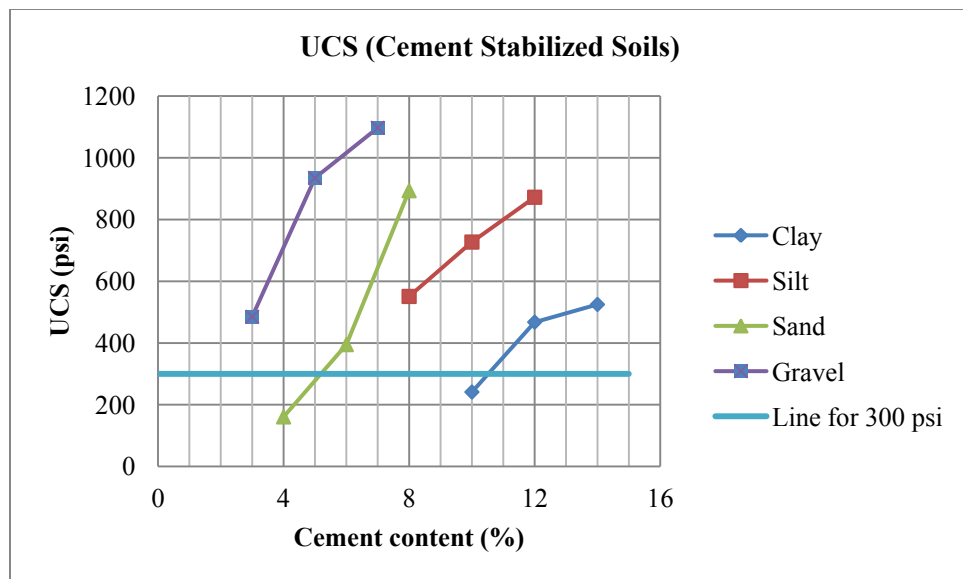


**Figure 3-2. Results for UCS after 7-day Curing for Cement-Stabilized Soils**

### 3.2.2 Soil-Fly Ash (Class C)

Three fly ash contents, 10%, 13% and 16% based on the dry weight of the soils, were used as the trial contents for silt, sand, and gravel, respectively. The 7-day UCS of 400 psi specified by the FHWA (Veisi et al. 2010) cannot be achieved for the gravel mixes or silt mixes, as shown in Figure 3-3. Increasing the fly ash content did not significantly increase the strength of the gravel or silt mixes. Instead, 13% fly ash was used for stabilizing the silt, sand, and gravel, because this percentage has been used successfully in past studies and is consistent with the content used by some agencies, such as the Oklahoma DOT.

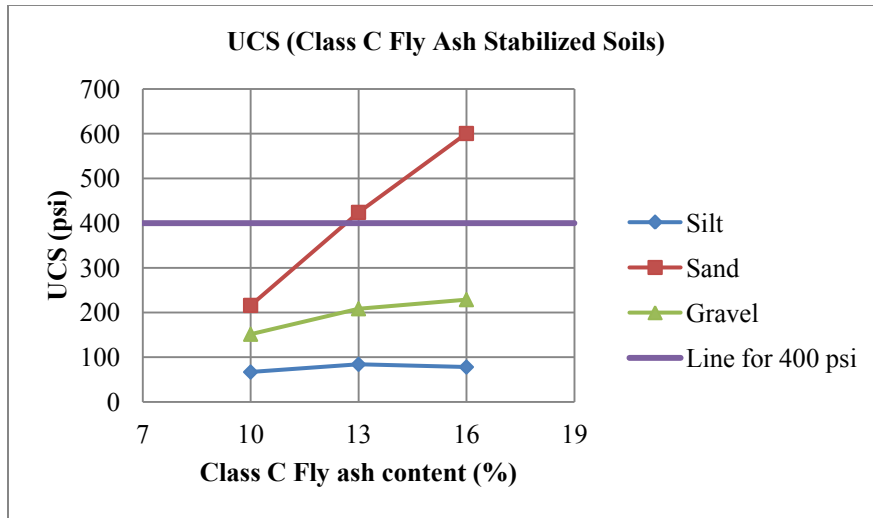


**Figure 3-3. Results for UCS after 7-day Curing for Class C Fly Ash-Stabilized Soils**

### 3.2.3 Soil-Lime

According to the design method developed by the NLA (2006), the initial lime content was determined based on the Eade and Grim method. Different lime contents were added to a soil and water solution. The lime content that led to a pH of 12.49 was the initial lime content used for further laboratory evaluation in terms of strength. For clay-lime, 2% lime, based on the dry mass of clay, is the lime content needed to reach a pH of 12.49 (Figure 3-4). Therefore, 2%, 4%, and 6% lime were used to fabricate specimens for strength testing to determine the minimum lime content for the clay-lime mix. It was found that 6% lime can lead to the UCS of 70 psi, which is specified by the NLA (2006) (Figure 3-5).

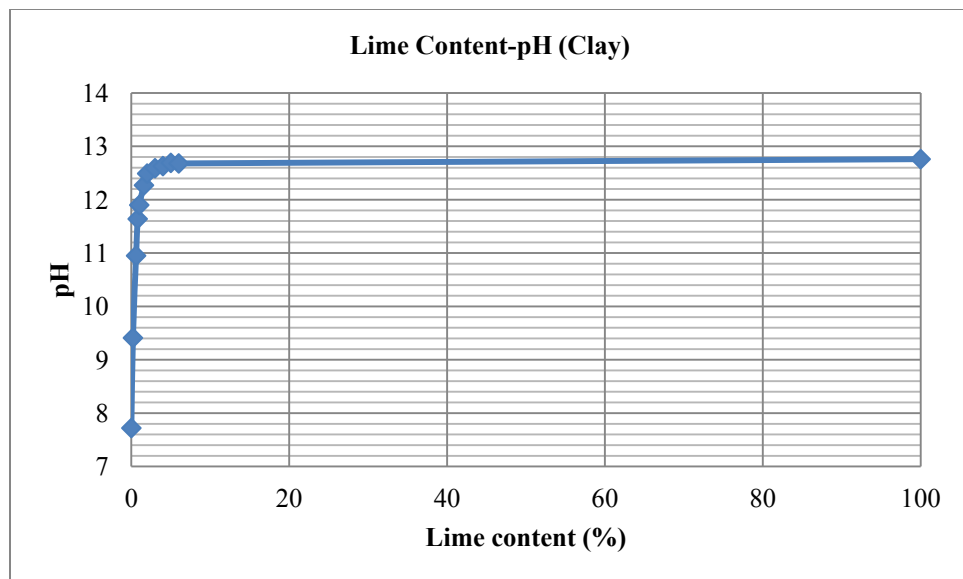


**Figure 3-4. pH Value vs. Lime Content**

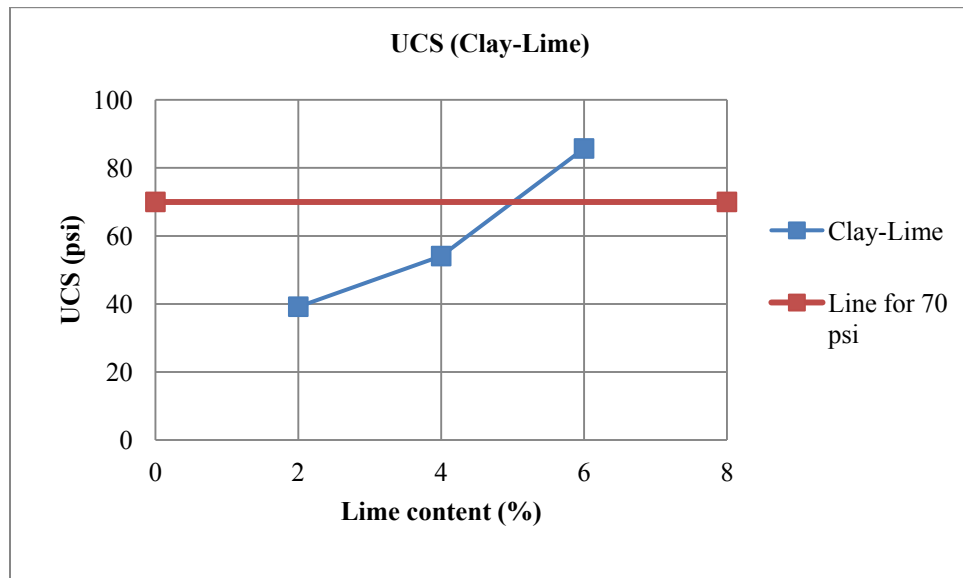


**Figure 3-5. Results for UCS after 7-day Curing for Clay-Lime Mix**

Because the plasticity index (PI) of the silt is less than 10, this silt is not suitable for lime stabilization, in accordance with the NLA design method (2006). This study used lime and Class F fly ash to stabilize the silt. In accordance with the MEPDG (ARA 2004), the UCS should be at

a minimum of 200 psi after 7-day curing and 4-hour soaking in water. This requirement can be achieved with 4% lime and 12% Class F fly ash, based on the dry mass of silt, as indicated in Figure 3-6.

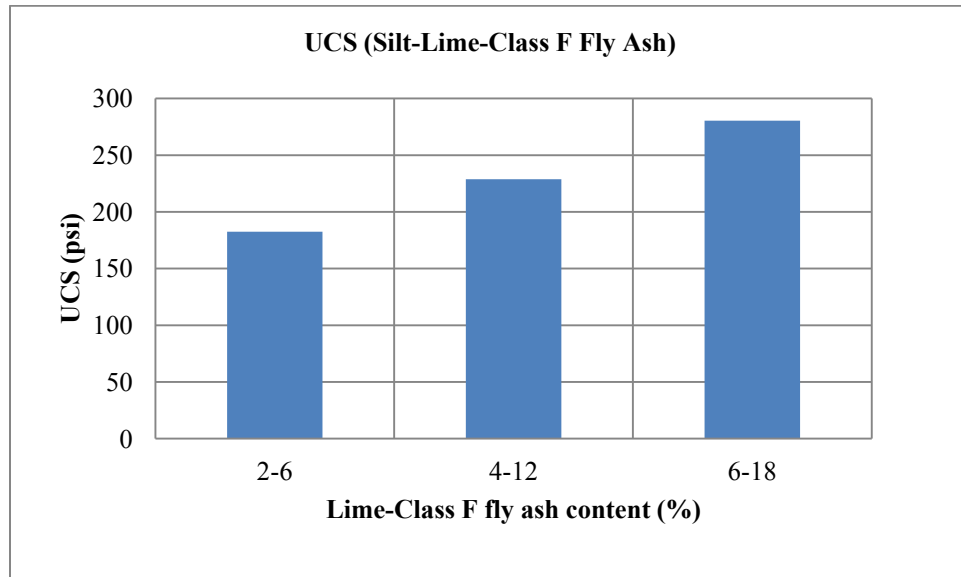


**Figure 3-6. Results for UCS after 7-day Curing for Silt-Lime-Class F Fly Ash**

Table 3-2 presents the final mix designs and Table 3-3 presents the maximum dry density (MDD) and optimum moisture contents (OMC). It is recommended a 7-day UCS of 200 psi as the criterion to distinguish between heavily and lightly stabilized materials. The heavily stabilized materials have a 7-day UCS that is 200 psi or higher, whereas lightly stabilized materials have a 7-day UCS that is lower than 200 psi (ARA 2004; Jameson 2013). Based on this criterion, the lime-clay and C fly ash-silt materials belong to the lightly stabilized group and the other seven materials are categorized as heavily stabilized materials.

**Table 3-2. Final Mix Design of Stabilized Mixtures**

	<b>Clay</b>	<b>Silt</b>	<b>Sand</b>	<b>Gravel</b>
<b>Cement</b>	12%	8%	6%	3%
<b>Lime</b>	6%	4% +12%*	Not applicable	Not applicable
<b>Fly ash</b>	Not applicable	13%	13%	13%

\*Note: 12% Class F Fly Ash

**Table 3-3. Maximum Dry Density and Optimum Moisture Content**

	<b>Clay</b>		<b>Silt</b>		<b>Sand</b>		<b>Gravel</b>	
	OMC (%)	MDD (lb/ft <sup>3</sup> )	OMC (%)	MDD (lb/ft <sup>3</sup> )	OMC (%)	MDD (lb/ft <sup>3</sup> )	OMC (%)	MDD (lb/ft <sup>3</sup> )
<b>No additive</b>	19.1	107.4	10.4	123.7	7.2	115.4	7.7	138.5
<b>Cement</b>	18.0	103.2	11.1	119.9	8.7	122.6	6.2	140.1
<b>Lime</b>	19.4	104.8	12.4*	118.6*	N/A		N/A	
<b>Class C fly ash</b>	N/A		10.0	121.2	7.3	135.2	7.4	139.3

\*Lime+Class F Fly Ash

### 3.3 SUMMARY

Four types of host material are used in this study for stabilization; they include high and low plasticity fine-grained soils (i.e., clay and silt) and granular materials (i.e., sand and gravel). The soil properties include gradation, Atterberg limits, and moisture-density relationship. The binders used for this study include cement, lime, and Class F and Class C fly ash. Totally nine mixtures were used in this study which are widely used in US. The optimum binder contents were determined according to UCS values. Different binder type requires different UCS criteria. The corresponding optimum moisture content and maximum dry density were also determined after mixing host soil and binder. These nine mixtures are used for test procedure evaluation and model development in this study.

## **CHAPTER FOUR**

### **TEST PROCEDURE EVALUATION**

This chapter presents the appraisal of test procedures linked to the properties of CSM shrinkage and cracking. These test procedures were appraised in terms of their performance predictability, precision, accuracy, practicality, cost, and other pertinent factors. Promising test procedures were evaluated in the laboratory to determine their applicability to CSM. One heavily stabilized material, i.e. cement-stabilized gravel, and one lightly stabilized material, i.e. lime-stabilized clay, are selected to evaluate the test procedures. Both materials are widely used by state highway agencies.

#### **4.1 APPRAISAL OF TEST PROCEDURES**

A level system is used to select or determine the design inputs for materials in the MEPDG. The hierarchical level is consistent with the relative importance, size, and cost of the design project. Level 1 is the input through comprehensive laboratory or field test or measurement. Level 2 requires the correlations with other material properties that are determined in the laboratory or field. Inputs at Level 3 are estimated from national or regional default values with little or no testing (ARA 2004).

The test procedures needed to characterize the material properties are appraised in the following sections. These appraisals are based either on the literature review, or the author's experience or understanding. These test procedures were then evaluated in the laboratory.

#### **4.1.1 Strength and Modulus Tests**

The types of strength and modulus tests for shrinkage cracking model of CSM include UCS, IDT strength, tensile strength, and IDT modulus. Table 4-1 presents the appraisal and recommendations of these test procedures that are relevant to the strength and modulus for shrinkage cracking model of CSM.

Indirect Tensile Strength Test: IDT strength testing is recommended for measuring tensile strength for Level 1 input to the shrinkage cracking model for both heavily and lightly stabilized materials, because direct tensile strength is difficult to measure. The IDT strength value is close to that of tensile strength and the test correlates well with other strength tests. Furthermore, the IDT test procedure is practical and repeatable.

The IDT strength can be obtained in accordance with the splitting test: AASHTO T198, *Splitting Tensile Strength of Cylindrical Concrete Specimens*, which specifies the specimen geometry of 6 inches in diameter and 12 inches in height. The specified loading rate of the splitting tensile stress by AASHTO T198 is 100-200 psi/min. The size and loading rate may not be appropriate for soil-lime or soil-fly ash/lime, which are relatively weak materials. The Australian method (Midgley and Yeo 2008) used to determine the IDT strength of stabilized materials is recommended. The specimen sizes are either 4 inches in diameter and 2.4 inches in height or 6 inches in diameter and 3.3 inches in height, depending on the size of the soil/aggregate particles. The loading rate is 4500 lbs/min.

Unconfined Compressive Strength Test: UCS testing correlates well with other strength and modulus tests for Level 2 input. Most state highway agencies use UCS tests for mix design and for quality assurance/quality control (QA/QC) because of the simplicity of the tests. UCS testing

is well-established and meets all cost, practicality and availability requirements (Yeo et al. 2002). UCS also is used in CSM mix design procedures. AASHTO T22, ASTM D1633, ASTM D5102, and ASTM C593 are test methods used for lean concrete, soil cement, lime-stabilized materials, and fly ash-stabilized materials with or without lime, respectively.

Indirect Tensile Modulus Test: IDT modulus testing is recommended for measuring the tensile modulus for Level 1 input to the shrinkage cracking model for stabilized materials. The IDT modulus test procedure is practical and repeatable, compared to direct tensile testing. The IDT modulus can be determined by cyclic load, in accordance with the Australian method (Medgley and Yeo 2008). The typical peak load applied on specimens is at 50% or less of the ultimate failure load determined using the IDT strength testing. The specimen sizes are same to the IDT strength testing.

**Table 4-1. Appraisal of Material Strength/Modulus Tests**

	Unconfined Compressive Strength (UCS)	Indirect Tensile Strength (IDT Strength)	Direct Tensile Strength (DT)	Indirect Tensile Modulus (IDT Modulus)
<i>Performance Predictability</i>	<b>Good</b> (a key parameter in the top-down compressive fatigue model; correlates well with modulus and other strength tests)	<b>Good</b> (predicts direct tensile strength well, which correlates with shrinkage cracking potential)	<b>Good</b> (predicts shrinkage cracking potential well, which is a key parameter in prediction model)	<b>Average</b> (simulates shrinkage/tensile behavior of CSL)
<i>Precision</i>	<b>Average</b> (COV typically below 20%) (White et al. 2005)	<b>Good</b> (COV typically below 10%) (White et al. 2005, Hudson and Kennedy 1968)	<b>Unknown</b>	<b>Average</b> (mixed results) (White et al. 2005)
<i>Accuracy</i>	<b>Good</b> (correlates well with modulus and strength tests)	<b>Good</b> (0.9-1.1 of direct tensile strength) (Bonnot 1991)	<b>Good</b> (direct measurement of tensile strength) (Hudson and Kennedy 1968)	<b>Good</b> (direct measurement of tensile behavior)
<i>Practicality</i>	<b>Good</b> (well established strength test, and meets cost, practicality, and availability requirements; not for tensile strength and fatigue) (Yeo et al. 2002)	<b>Good</b> (practical, productive, economic, and user friendly) (Yeo et al. 2002); same type of specimen and equipment as that used for compression testing (Hudson and Kennedy 1968)	<b>Poor</b> (misalignment for pure tension, failure outside central portion (Yeo et al. 2002); gripping specimen is difficult (Hudson and Kennedy 1968)	<b>Average</b> (relatively practical and user friendly; stress/strain control is difficult with brittle stabilized materials; suitable for lightly stabilized materials) (Yeo et al. 2002)
<i>Machine Costs</i>	<b>Low</b>	<b>Low</b>	<b>Average</b>	<b>High</b>
<i>Time</i>	<b>Short</b>	<b>Short</b>	<b>Average</b> (3 hr preparation of specimens)	<b>Long</b>
<i>Recommendation</i>	<b>Recommended</b> for Level 2 for prediction of IDT strength and modulus tests	<b>Recommended</b> for shrinkage cracking as Level 1	<b>Not recommended</b> due to operational difficulties	<b>Recommended</b> for shrinkage cracking modeling

Note: Cost Ratings: High: >\$50,000; Medium: \$20,000 to \$50,000; Low: <\$20,000; Very Low: <\$5,000

#### **4.1.2 Shrinkage Tests**

The shrinkage tests of CSM are evaluated for shrinkage cracking development. Table 4-2 presents the appraisal and recommendations for the tests procedures.

Free Drying Shrinkage Test: This test is recommended for the free drying shrinkage strain prediction model development for the shrinkage cracking prediction. There is no standard for the free drying shrinkage of CSM; however, AASHTO T160, *Length Change of Hardened Hydraulic Cement*, can be modified for CSM. Long-term drying also is needed to measure the ultimate drying shrinkage strain and develop the ultimate shrinkage strain prediction model.

Free Autogenous Shrinkage Test: This test is recommended for measuring the autogenous shrinkage strain. During the test, the specimen should be sealed well to prevent any loss of moisture so that the shrinkage strain is due only to the hydration of the cementitious binder. There is no standard for the autogenous drying shrinkage of CSM. This test will be developed and evaluated in this research.

Gradient Drying Shrinkage Test: This test is recommended for the drying shrinkage strain gradient model development for the shrinkage cracking prediction. This test can simulate field conditions, as the four sides of the surface of the beam specimen are sealed and only the top surface is subjected to drying. The shrinkage strain at different depths is measured to represent the shrinkage gradient in the field. This test was first developed by Xiaojun Li at Washington State University, and will be evaluated in this research.

Restrained Drying Shrinkage Test: This test is recommended to induce shrinkage cracking for model development. The increase in friction between the CSL and underlying material will

reduce the shrinkage crack spacing and crack width. By artificially creating a high level of bond, shrinkage cracking can be generated in a lab specimen for model development. This method is evaluated in terms of size, base restraint, RH and temperature so that cracking occurs in laboratory-scale beams. There is no test standard for restrained drying shrinkage cracking testing. However, concrete researchers have conducted restrained slab tests at the base layer (Weiss et al. 1998). The slab is fixed to the base and subjected to drying to generate shrinkage cracking in a lab-scale specimen. These test procedures developed by Weiss et al. (1998) are modified for laboratory evaluation in this study.

Thermal Shrinkage/Expansion Test: The thermal shrinkage/expansion property is recommended as Level 1 input to determine thermal strain, which is a key parameter in the shrinkage cracking model. AASHTO TP 60, *Standard Method of Test for Coefficient of Thermal Expansion of Hydraulic Cement Concrete*, is designed to determine the COTE of concrete only. This test will be developed and evaluated in this research. The method developed by Cusson and Hoogeveen (2006) will be evaluated for CSM.

#### **4.1.3 Friction/Bond**

Even though the interface friction/bond is not a property of CSM, it significantly affects shrinkage cracking and thus is an important parameter in the shrinkage cracking model. Typical crack spacing in the field is between 3 ft and 60 ft, which is difficult to achieve in the lab. Therefore, the shrinkage cracking model is based on the large-scale restrained drying shrinkage test conducted in the lab. Epoxy and cement slurry are proposed to create a strong bond between the CSL and mold base so that shrinkage cracking can be generated within the lab specimen. The

bond strength is characterized in accordance with the Iowa shear test (Iowa DOT 2000), which separates the CSL and base along the interface.

After the placement of the CSL in the field, the bond between the CSL and underlying material is typically strong, such that bond failure often occurs in the weak material between the CSL and underlying materials (Romanoschi and Metcalf 2001). The friction/bond input can be based on the shear strength of these weak materials, such as sand and gravel, which are readily available for use in the shrinkage cracking model.

**Table 4-2. Appraisal of Test Methods for Shrinkage and Swelling**

	Free Drying Shrinkage	Autogenous Drying Shrinkage	Gradient Drying Shrinkage	Restrained Drying Shrinkage	Thermal Shrinkage/Expansion
<b>Performance Predictability</b>	<b>Good</b> (key parameter in shrinkage cracking model)	<b>Good</b> (key parameter in shrinkage cracking model)	<b>Good</b> (key parameter in shrinkage cracking model)	<b>Good</b> (models behavior of restrained drying shrinkage cracking)	<b>Good</b> (key parameter for thermal shrinkage prediction)
<b>Precision</b>	<b>Unknown</b>	<b>Unknown</b>	<b>Unknown</b>	<b>Unknown</b>	<b>Unknown</b>
<b>Accuracy</b>	<b>Good</b> (direct measurement)	<b>Good</b> (direct measurement)	<b>Good</b> (direct measurement)	<b>Good</b> (direct measurement; fixed base creates shrinkage cracking in a lab-scale slab)	<b>Good</b> (direct measurement)
<b>Practicality</b>	<b>Unknown</b>	<b>Unknown</b>	<b>Unknown</b>	<b>Average</b> (application of bond and specimen is time-consuming)	<b>Good</b>
<b>Machine Costs</b>	<b>Very low</b>	<b>Very low</b>	<b>Very low</b>	<b>Low</b>	<b>Low</b>
<b>Time</b>	<b>Long</b>	<b>Long</b>	<b>Long</b>	<b>Long</b>	<b>Average</b>
<b>Recommendation</b>	<b>Recommended</b> for unrestrained shrinkage strain prediction model development	<b>Recommended</b> for unrestrained shrinkage strain prediction model development	<b>Recommended</b> for unrestrained shrinkage strain prediction model development	<b>Recommended</b> for shrinkage cracking prediction model development	<b>Recommended</b> for thermal cracking strain prediction

Note: Cost Ratings: High: >\$50,000; Medium: \$20,000 to \$50,000; Low: <\$20,000; Very Low: <\$5,000

## 4.2 LABORATORY TEST PROCEDURE EVALUATION

Test procedures shown in Table 4-3 are evaluated for their applicability to CSM, because many of these procedures were originally designed for materials other than CSM. Proper selection of test procedures to characterize the material properties is important and needs to consider the application of a specific material in a pavement structure. One heavily stabilized material, i.e. cement-stabilized gravel, and one lightly stabilized material, i.e. lime-stabilized clay, are selected to evaluate the test procedures. Both materials are widely used by state highway agencies, based on the survey results.

**Table 4-3. Test Procedures Selected for Evaluation**

Test Procedures for Evaluation	Evaluation Variables	Number of Tests
IDT strength	Applicability	$2 \text{ mixtures} \times 1 \text{ test} \times 3 \text{ replicates} = 6$
IDT modulus	Two stress levels: 20% ~ 30% of strength	$2 \times 2 \times 3 = 12$
Coefficient of thermal expansion	Applicability	$2 \times 1 \times 3 = 6$
Bond strength	Bond conditions: epoxy and cement slurry	$2 \times 2 \times 3 = 12$
Free drying shrinkage	Free drying shrinkage at relative humidity: 65% at 68°F and ultimate shrinkage after long-term curing	$2 \times 2 \times 3 = 12$
Free autogenous shrinkage	Free autogenous shrinkage at 68°F	$2 \times 1 \times 3 = 6$
Gradient drying shrinkage	Gradient drying shrinkage at relative humidity: 40% and 65% at 68°F	$2 \times 1 \times 1 = 2$
Restrained drying shrinkage	Slab length: 48 in. and two bond conditions: epoxy and cement slurry	$2 \times 2 \times 1 = 4$
<b>Total</b>		<b>60</b>

IDT Strength/Modulus Test: IDT strength/modulus tests will be conducted for the clay-lime and cement-gravel materials. According to the Australian test standard, the maximum stress levels of the model test should not be more than 50% of the strength for the IDT test. Therefore, the two stress levels for the IDT modulus are 20% and 30% of the IDT strength for the IDT modulus tests.

Coefficient of Thermal Expansion (COTE) Test: The applicability of AASHTO TP60 to CSM will be evaluated. AASHTO TP60 specifies the use of a water bath for temperatures between 50°F and 122°F. Unlike concrete, CSM are sensitive to water, especially for lightly stabilized materials. A temperature cycling method will be evaluated.

Bond Strength Test: Bond strength tests will be conducted in accordance with the Iowa shear test (Iowa DOT 2000). Two CSL will be bonded to the metal base to be used for the restrained drying shrinkage test, using epoxy and cement slurry. The bond strength and displacement values that correspond to the peak load will be recorded.

Free Drying Shrinkage Test: This test will be evaluated in terms of RH for curing. AASHTO T160 specifies 50% RH during evaluation. For this study, a different curing RH will be evaluated: 65% at 68°F. The 65% RH is equivalent to field bituminous curing.

Free Autogenous Shrinkage Test: This test will be evaluated at room temperature (68°F) for both heavily and lightly stabilized materials. The specimens will be sealed with wax to prevent any evaporation.

Gradient Drying Shrinkage Test: This test will be evaluated in terms of RH for curing. For this study, two RH values, 40% and 65%, will be evaluated.

Restrained Drying Shrinkage Test: This method will be evaluated in terms of beam length, the bonding condition between the beam and underlying material, and RH.

Typical shrinkage crack spacing for CSL is between 3 ft and 60 ft. If the bond strength is increased, the shrinkage crack spacing can be reduced to that for a lab-scale beam. Two bonding agents will be used, epoxy and cement slurry, which create a strong bond (Atkinson 1990). The specimen length greatly affects shrinkage cracking. The restrained slab at the base is recommended to be 4 in. × 6 in. × 48 in. to create shrinkage cracking. The restrained slab will be subjected to 65% RH drying at room temperature.

#### **4.2.1 IDT Test**

This investigation was conducted in order to (i) determine the IDT strength, and (ii) determine an appropriate stress level for the IDT modulus test, using a lightly stabilized mixture (clay-lime) and a heavily stabilized mixture (gravel-cement). The dimensions of the cylindrical specimens used for this study are 6 inches in diameter and 3.1 inches in length. The specimens were kept in an environment of 68°F and 65% RH for 14 days prior to testing.

##### **(a) Indirect Tensile Strength (IDT) Test**

The Australian method (Midgley and Yeo 2008) for determining the IDT strength of stabilized materials was used with modifications. The IDT strength tests of moisture-cured specimens were performed within 30 minutes after removing the specimens from the curing room. The IDT strength test involves loading a cylindrical specimen with compressive loads distributed along two axial lines that are diametrically opposite, as shown in Figure 4-1. Two loading strips that are slightly longer than the specimen were provided for each specimen. The width of the loading strips is 0.75 inch. This condition results in a relatively uniform tensile stress perpendicular to and along the loading diametric plane. Failure occurs due to splitting along this loaded plane.



**Figure 4-1. Indirect Tensile (IDT) Strength Test Setup**

The loading rate for the IDT strength test is 15 psi/min. The IDT strength value is computed using Eq. (4-1).

$$S_{IDT} = \frac{2P}{\pi l d} \quad \text{Eq. (4-1)}$$

where

$S_{IDT}$  = IDT strength, psi

$P$  = maximum applied load, lb

$l$  = height of the specimen, in.

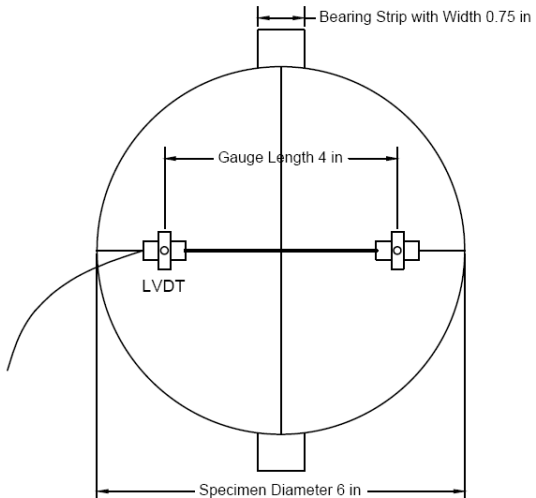
$d$  = diameter of the specimen, in.

### (b) IDT Modulus Test

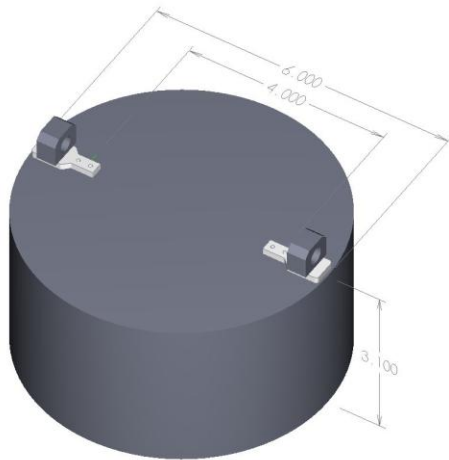
The same setup as used for the IDT strength test was followed for IDT modulus testing. LVDTs were fixed on both sides of the cylinder to measure the horizontal displacement, as shown in Figure 4-2. For fine materials, LVDTs were mounted on the specimen using screws (Figure 4-3), whereas epoxy was used to mount the LVDTs for the granular materials (Figure 4-4). The gauge length is 4 inches in the horizontal direction.



(a) IDT Modulus Test Setup

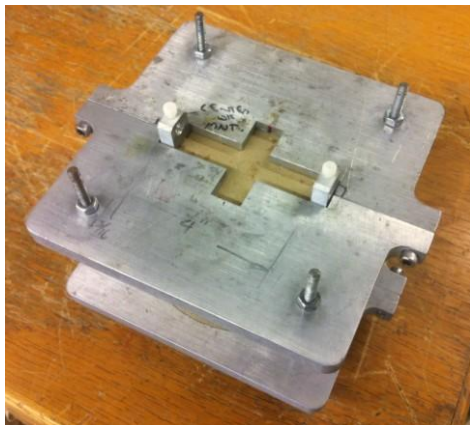


(b) 2D Schematic View of IDT Modulus Test

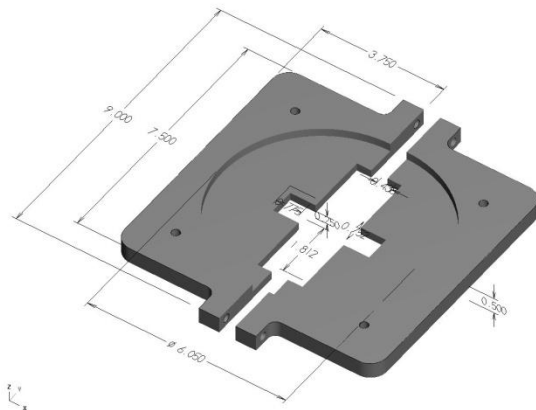


(c) 3D Schematic View of IDT Modulus Test

**Figure 4-2. IDT Modulus Test Setup**



(a) Outside of the Aligning Jig

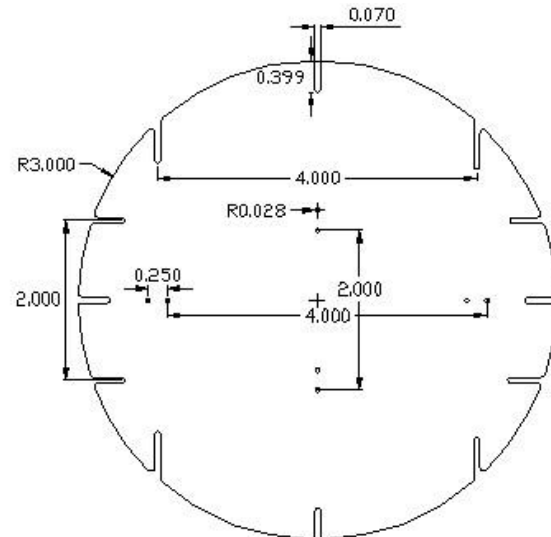


(b) Schematic View the Aligning Jig

**Figure 4-3. Aligning Jig for Gluing LVDT Mounts on the Specimen**



(a) Drill Press and Specimen



(b) Schematic View of the Aligning Jig

**Figure 4-4. Drill Press and Aligning Jig for Fastening LVDT Mounts with Screws**

The IDT modulus test was conducted at a frequency of 1 Hz. A cyclic haversine load pulse of 100 ms duration followed by a 900 ms rest period was applied for each cycle. A contact load of approximately 10 lbs was applied to the specimen. Cyclic haversine loading was applied for 100 load pulses. Both the maximum force applied to the specimen and the peak displacement for each pulse cycle were recorded. The first 90 cycles were considered preconditioning. The data from the last 10 consecutive cycles were used to calculate the IDT modulus value of the specimen based on Eqs. (4-2) through (4-4) (Wen and Kim 2002):

$$\sigma = \frac{2P}{\pi l d} \quad \text{Eq. (4-2)}$$

$$\varepsilon = U(t) \frac{\gamma_1 + \gamma_2 v}{\gamma_3 + \gamma_4 v} \quad \text{Eq. (4-3)}$$

$$E_t = \frac{\sigma}{\varepsilon} \quad \text{Eq. (4-4)}$$

where

$\sigma$  = tensile stress, psi

$P$  = maximum applied load indicated by the testing machine, lbs

$l$  = height of the specimen, in.

$d$  = diameter of the specimen, in.

$U(t)$  = horizontal displacement, m, 1 m = 0.0254 in.

$\varepsilon$  = cyclic horizontal tensile strain

$v$  = Poisson's ratio, assuming 0.2 for CSM

$E_t$  = indirect tensile modulus, psi

$\gamma_1, \gamma_2, \gamma_3, \gamma_4$  = constants.

Table 4-4 shows the values of  $\gamma_1$ ,  $\gamma_2$ ,  $\gamma_3$ ,  $\gamma_4$  when the load strip width is 0.75 inch. For different diameters, gauge lengths, and load strip widths,  $\gamma$  can be found in Wen and Kim (2002), or calculated with the MATLAB codes, as introduced in Appendix B.

**Table 4-4. Parameters for IDT Modulus Test**

$\gamma_1$	$\gamma_2$	$\gamma_3$	$\gamma_4$
12.27	37.34	0.7781	2.7269

Tables 4-5 and 4-6 summarize the results of the IDT tests for IDT strength and modulus, respectively. The average IDT strength of the clay-lime specimens is 13.9 psi with good repeatability. While the average value of cement-gravel specimens is 117.4 psi, the COV value of cement-gravel material is higher than the one of lime-clay, maybe because the specimen variation of granular material is greater than fine material. The averaged IDT modulus values of lime-clay were obtained as 110,611 psi and 102,000 psi for the stress levels of 20% and 30% of IDT strength, respectively. And the averaged IDT modulus values of cement-gravel were 1562,986 psi and 1442,013 psi, respectively. The 20% and 30% stress levels resulted in comparable modulus values. However, during the test, it was noted that the 20% results were affected by the specimen setup and signal noise from the machine. Thus, 30% IDT strength is recommended for IDT modulus testing. Therefore, the IDT strength and modulus tests are recommended to determine the tensile strength and stiffness of the CSM.

**Table 4-5. Summary of IDT Strength Test Results**

Test Item	Material	Specimen No.	IDT Strength (psi)	Coefficient of Variation (COV)
IDT Strength	Lime-Clay	S <sub>IDT</sub> -LC-1	14.5	3.67%
		S <sub>IDT</sub> -LC-2	13.8	
		S <sub>IDT</sub> -LC-3	13.5	
	Gravel-Cement	S <sub>IDT</sub> -CG-1	117.1	7.43%
		S <sub>IDT</sub> -CG-2	108.9	
		S <sub>IDT</sub> -CG-3	126.3	

**Table 4-6. Summary of IDT Modulus Test Results**

Test Item	Material	Specimen No.	Stress Level by Percentage of IDT Modulus, %	IDT Modulus (psi)	COV
IDT Modulus	Lime-Clay	E <sub>IDT</sub> -LC-20-1	20	117014	9.09%
		E <sub>IDT</sub> -LC-20-2	20	115795	
		E <sub>IDT</sub> -LC-20-3	20	99025	
	Cement-Gravel	E <sub>IDT</sub> -LC-30-1	30	107394	7.99%
		E <sub>IDT</sub> -LC-30-2	30	105974	
		E <sub>IDT</sub> -LC-30-3	30	92631	
	Cement-Gravel	E <sub>IDT</sub> -CG-20-1	20	1586031	8.23%
		E <sub>IDT</sub> -CG-20-2	20	1424448	
		E <sub>IDT</sub> -CG-20-3	20	1678480	
		E <sub>IDT</sub> -CG-30-1	30	1490241	11.32%
		E <sub>IDT</sub> -CG-30-2	30	1260163	
		E <sub>IDT</sub> -CG-30-3	30	1575636	

#### 4.2.2 Shrinkage and Cracking

The objective of the shrinkage test evaluation is to investigate the test methods that are input factors for the shrinkage strain and shrinkage cracking models.

##### 4.2.2.1 Coefficient of Thermal Expansion (COTE) Test

The COTE is a key parameter in the shrinkage cracking model. The originally proposed test method for the COTE of concrete, based on AASHTO TP60, *Standard Method of Test for*

*Coefficient of Thermal Expansion of Hydraulic Cement Concrete*, is not suitable for measuring the COTE of lightly stabilized materials or the early-age (e.g., 2 days) COTE of heavily stabilized materials which is critical for early-age shrinkage cracking. The saturation method recommended in AASHTO TP60 would severely damage the lightly stabilized materials or the early-age specimens of heavily stabilized materials. In addition, thermal expansion is coupled with autogeneous and drying shrinkage for early-age stabilized materials. A test method for COTE, recommended by Cusson and Hoogeveen (2006), which was specifically designed for early-age concrete, is evaluated in this study based on temperature cycling. The shrinkage of a CSL specimen includes autogenous, drying, and thermal shrinkage. The use of temperature cycling can separate the thermal shrinkage/expansion from autogenous and drying shrinkage.

Prism specimens with dimensions of 4 in.  $\times$  4 in.  $\times$  11.25 in. were placed in an environmental chamber at an initial ambient temperature of 77°F and 98% RH. The chamber cycled the temperature between 77°F and 86°F using a saw-tooth pattern while the RH was kept constant. After the target temperature in the chamber was reached, which takes about 20 minutes, the temperature was kept constant for 4 hours, resulting in three full cycles (or six steps) per day. The constant temperature period is long enough to ensure a stable and uniformly distributed temperature in the prism sample. The amplitude of the temperature cycle (9°F) is selected to be small enough to maximize the number of cycles per day and obtain more COTE values at early ages. With such small temperature changes, the temperature effect on the change in COTE over time can be considered small (Cusson and Hoogeveen 2006).

The displacements were measured by LVDTs. The temperatures inside the specimens and environmental chamber were monitored by thermal couples. Figure 4-5 shows the COTE test setup. Figure 4-6 shows the typical change in strain with temperature cycles.



**Figure 4-5. COTE Test Setup (Left: Gravel-Cement; Right: Clay-Lime)**

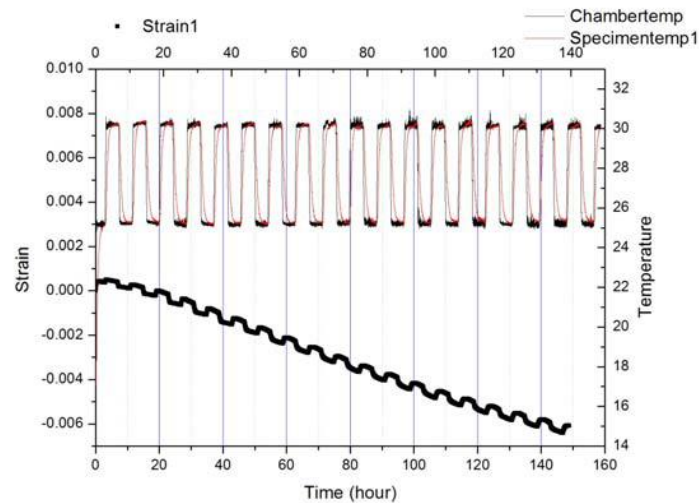


**Figure 4-6. COTE Test of Clay-Lime between 77°F and 86°F**

Figures 4-7 and 4-8 show the test results and COTE of the clay-lime and gravel-cement specimens, respectively. The COTE of the clay-lime specimens increased within the first two days and then stabilized at about  $4.7 \times 10^{-5}/^{\circ}\text{F}$ . However, the COTE of the gravel-cement samples was relatively stable at about  $1.4 \times 10^{-5}/^{\circ}\text{F}$ , which is about one-third of that of the clay-lime specimens.

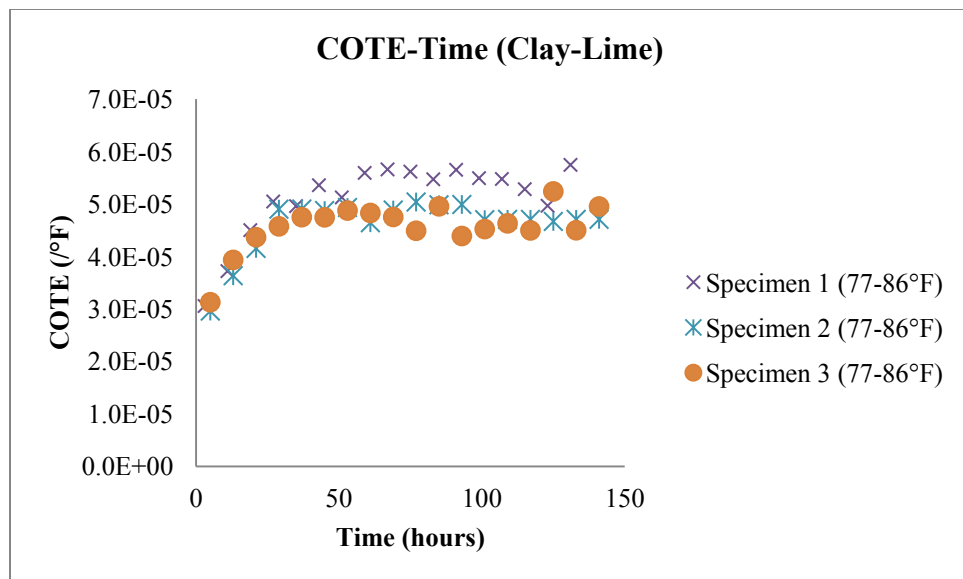


**Figure 4-7. COTE Development of Clay-Lime Specimens**

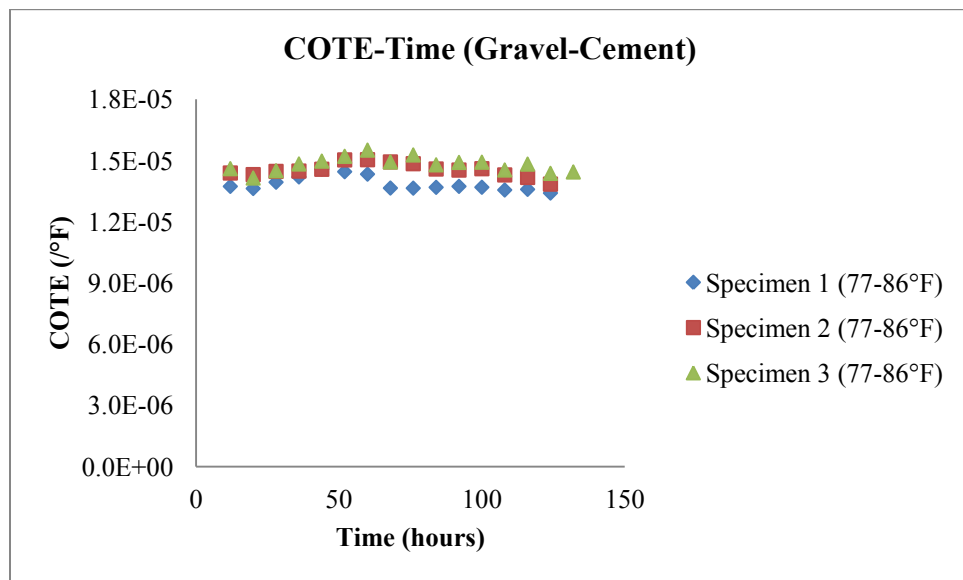


**Figure 4-8. COTE Development of Gravel-Cement Specimens**

Overall, the COTE test, which is based on temperature cycling, is capable of measuring the COTE of both lightly and heavily stabilized materials and is recommended for model development.

#### *4.2.2.2 Free Autogenous Shrinkage*

Autogenous shrinkage is the shrinkage due to hydration of the binder in CSL. Autogenous shrinkage can be measured when specimens are wrapped with plastic to prevent loss of moisture. However, it is cumbersome to wrap specimens with plastic and difficult to prevent moisture loss and drying shrinkage. Instead, wax was used in this study to seal the specimens. Specimens of clay-lime and gravel-cement were fabricated and placed in plaster molds, as shown in Figure 4-9. Hot liquid wax was poured into each plaster mold. After the excess liquid wax was drained, the specimen was covered with a thin layer of wax. The plaster mold was removed and the specimens and wax were cooled to room temperature. A plastic pad was glued onto the sides of the specimen in order to prevent permanent deformation caused by the tips of the dial gauges. The shrinkage was then measured, as shown in Figure 4-10.



**Figure 4-9. Plaster Mold**



**Figure 4-10. Autogenous Shrinkage Test Setup**

Figure 4-11 shows the free autogenous shrinkage test results. The clay-lime specimens show large autogenous shrinkage, which continued to increase even after 8 days; whereas the autogenous shrinkage of gravel-cement specimens was small and stabilized after about 3 days. This phenomenon might be due to the fact that the reaction time for the clay-lime is longer than for the gravel-cement mixture.

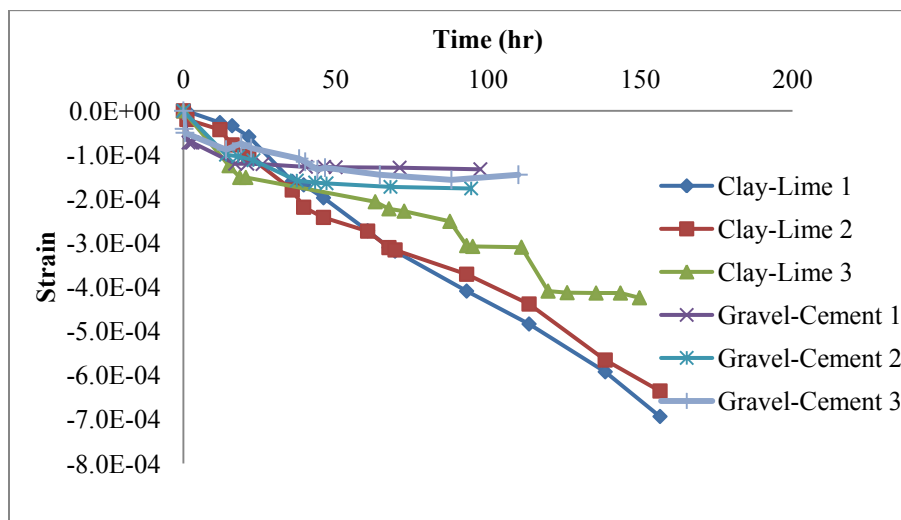


**Figure 4-11. Autogenous Shrinkage Results of Clay-Lime and Gravel-Cement Specimens**

Based on the test results, it seems that the autogenous shrinkage of CSL can be measured using this test.

#### *4.2.2.3 Free Drying Shrinkage*

This test aims to measure free drying shrinkage due to moisture loss. Free drying shrinkage tests were conducted on both lightly stabilized materials (clay-lime) and heavily stabilized materials (gravel-cement). For measuring the drying shrinkage, clay-lime and gravel-cement specimens were fabricated with dimensions of 4 in.  $\times$  4 in.  $\times$  11.25 in., as shown in Figure 4-12. The specimens were air-dried and the displacements were measured from both ends. Two dial gauges were placed on the ends to measure the displacements. The total shrinkage strain is the sum of the two measured strains. The drying shrinkage strain is equal to the total shrinkage strain minus the autogenous shrinkage strain, because the specimen is simultaneously subjected to autogenous shrinkage as well.

Each specimen was placed on a solid plate and lubricant was applied between the specimen and solid plate to allow free movement of the specimen. In addition, in order to allow the specimen to dry in 3 dimensions (6 surfaces), another specimen was placed on a metal plate with numerous small holes for moisture to evaporate from the bottom as well. Lubricant was applied between the specimen and metal plate to allow free movement of specimen. The third method that was evaluated in this study was to reduce the height of specimen (for fine-grained materials only) to mitigate the effect of the moisture gradient inside the specimen, without the need for the metal plate with holes. A 2-inch high specimen was used. The shrinkage of the three specimens was measured side by side, as shown in Figure 4-13. Figure 4-14 shows the test results and indicates that the shrinkage of these three specimens is very similar to each other.

Therefore, the effect of specimen dimension and evaporation from the bottom of the specimen is negligible. It is recommended that the drying shrinkage test should be conducted on specimens with dimensions of 4 in.  $\times$  4 in.  $\times$  11.25 in. on a solid plate and that lubricant should be applied between the specimen and plate.



**Figure 4-12. Compaction Mold for Free Shrinkage Test**



**Figure 4-13. Test Setup to Evaluate the Effects of Specimen Dimension and Bottom Surface (left: 4 in. high on porous plate; middle: 4 in. high on solid plate; right: 2 in. high on solid plate)**

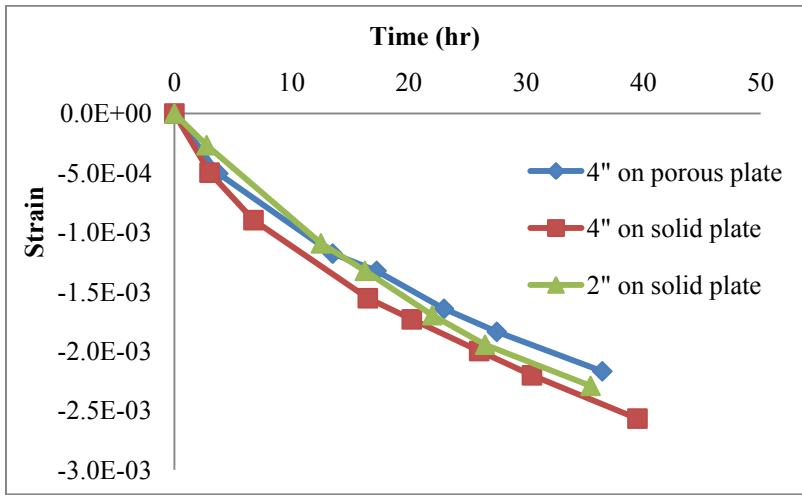


**Figure 4-14. Effects of Specimen Dimension and Bottom Surface**

Lime-stabilized clay and cement-stabilized gravel specimens were fabricated, as shown in Figure 4-15. Figure 4-16 presents the test results and indicates that the results for lime-stabilized clay are very close and repeatable compared to those of cement-stabilized gravel. The shrinkage of lime-stabilized clay continued to increase, whereas the shrinkage of the cement-stabilized gravel stabilized after three days.



(a) Clay-Lime

(b) Gravel-Cement

**Figure 4-15. Drying Shrinkage Test**

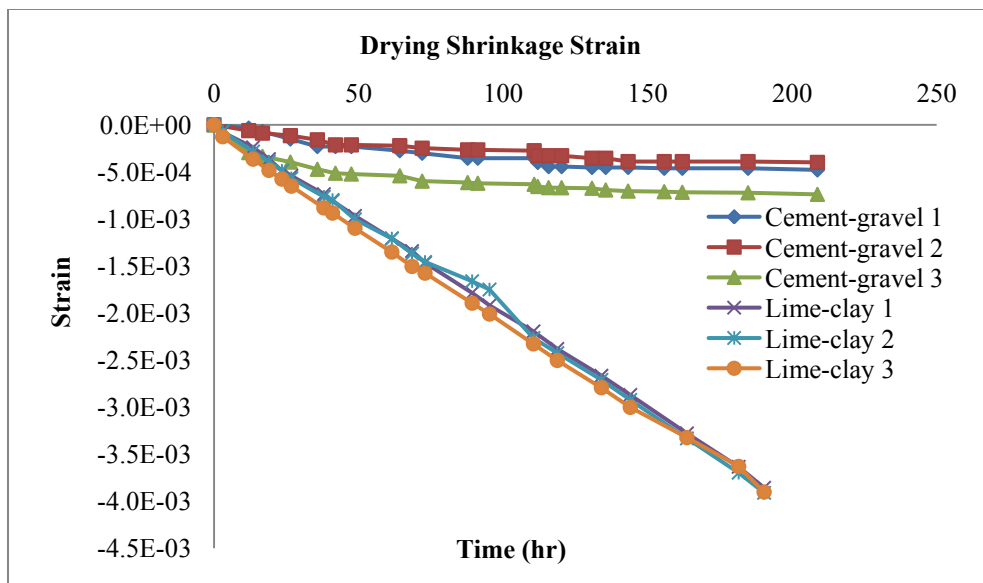


**Figure 4-16. Test Results for Drying Shrinkage Evaluation**

The drying shrinkage and autogenous shrinkage results are plotted together in Figures 4-17 and 4-18 for the clay-lime and gravel-cement specimens, respectively. Free drying shrinkage is significantly larger than the autogenous shrinkage for both materials. Based on the test results, the free drying shrinkage test used in this study can be used to measure the drying shrinkage of both lightly and heavily stabilized materials and is recommended for model development.

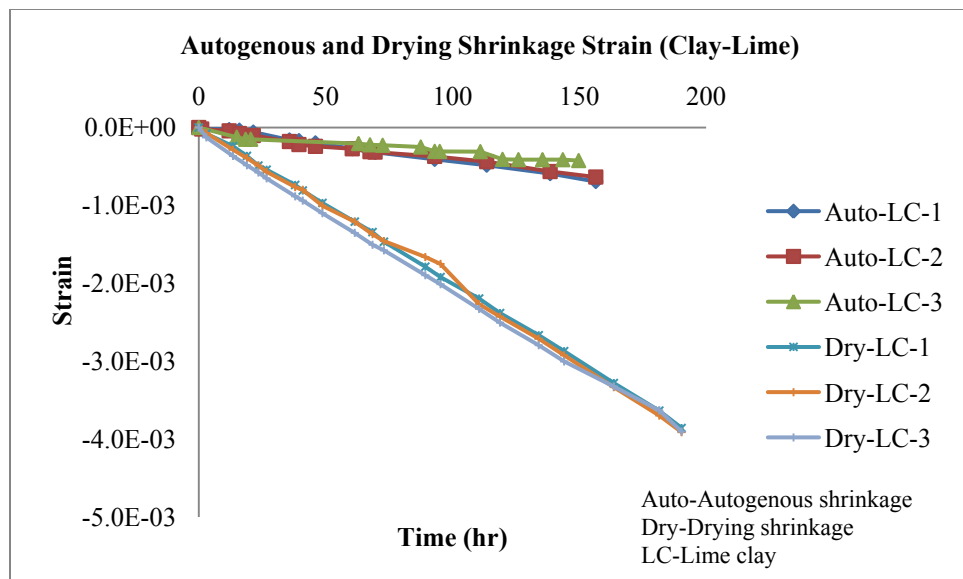


**Figure 4-17. Free Drying and Autogenous Shrinkage Results for Clay-Lime Specimens**

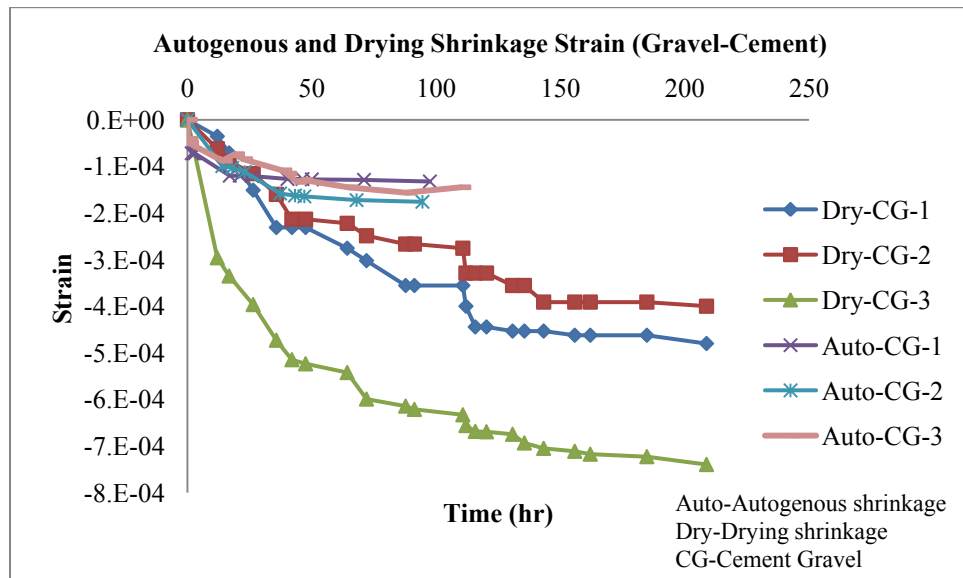


**Figure 4-18. Free Drying and Autogenous Shrinkage Results for Gravel-Cement Specimens**

#### 4.2.2.4 Restraint Drying Shrinkage Cracking

Tensile stress is produced when moisture or temperature changes cause the CSL base or subbase to contract or shrink with restraint. Shrinkage cracking occurs when the tensile stress

exceeds the tensile strength of the cement-treated pavement layer (Cauley and Kennedy 1972). Because shrinkage cracking occurs when the CSL are restrained, the shrinkage cracking potential of each CSL material can be examined using the restrained shrinkage cracking test. The increase in friction between the CSL and underlying material reduces the shrinkage crack spacing. By artificially creating a high level of bond, shrinkage cracking can be generated in a laboratory-scale specimen for model development. The CSL slab is bonded to a steel tube to prevent curling.

Clay-lime and gravel-cement beams with dimensions of 48 in.  $\times$  6 in.  $\times$  4 in. were glued onto a steel tube using either epoxy or cement mortar. The beams were air-dried to generate drying shrinkage as well as autogenous shrinkage. The clay-lime beam that was glued to the steel tube with epoxy generated one shrinkage crack (Figure 4-19). Another clay-lime beam was bonded to the base using cement mortar and generated two shrinkage cracks one day after casting (Figure 4-20). Figures 4-21 and 4-22 present the growth of the cracks (in terms of width) as measured at the top and mid-span of the specimens over time.



**Figure 4-19. Restrained Shrinkage Test for Clay-Lime when Epoxy is used as Bonding**

**Agent (48 in. Long)**

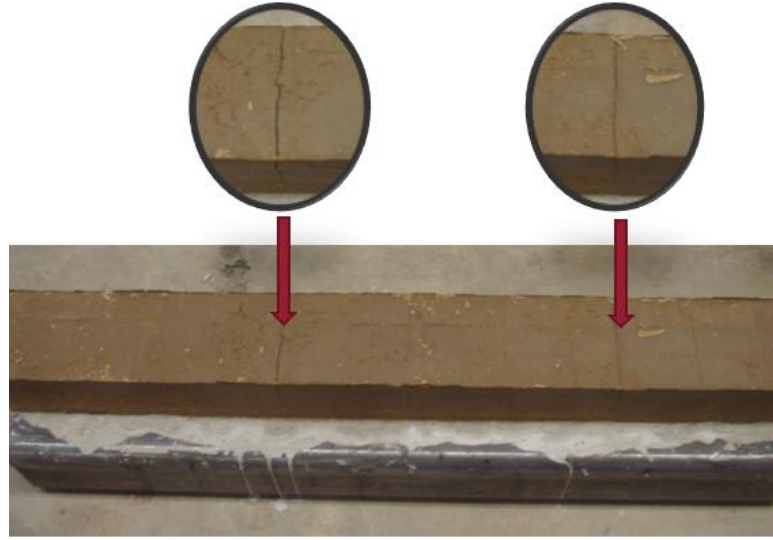


**Figure 4-20. Restrained Shrinkage Test for Clay-Lime when Cement Mortar is used as Bonding Agent (48 in. Long)**

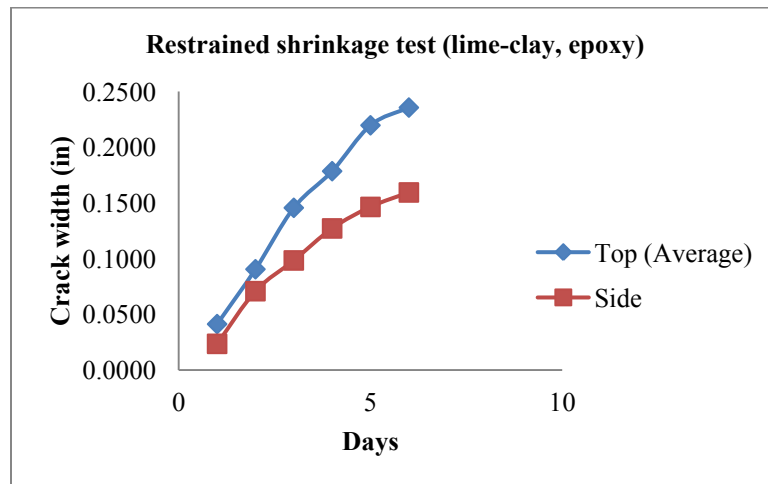


**Figure 4-21. Crack Width Increase over Time for Clay-Lime Specimen when Epoxy is used as Bonding Agent**

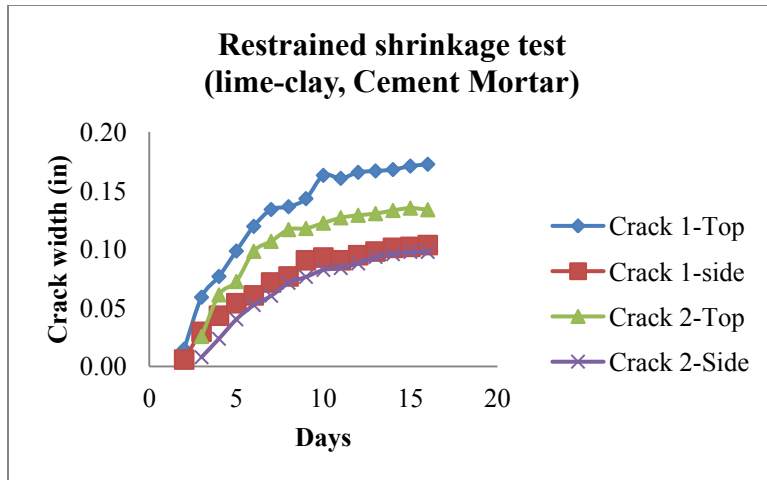


**Figure 4-22. Crack Width Increase over Time for Clay-Lime Specimen when Cement Mortar is used as Bonding Agent**

The gravel-cement specimens, on the other hand, did not generate any shrinkage cracking when either epoxy or mortar was used as the bonding agent. This outcome is likely due to the low molding moisture content and low drying and autogenous shrinkage of the gravel-cement mixture. Three longer gravel-cement (3%, 5%, and 7% cement, respectively) beams with dimensions of 92 in.  $\times$  6 in.  $\times$  4 in. were fabricated and glued onto a concrete floor using epoxy (Figure 4-23). However, still no shrinkage cracking was observed.



**Figure 4-23. Restrained Shrinkage for Gravel-Cement when Epoxy is used as Bonding Agent (92 in. Long)**

The clay-lime beams experienced shrinkage cracking. However, the gravel-cement used in this study was found not to be prone to shrinkage cracking. To simulate field conditions, the side surfaces of the beam specimens were sealed in a later study and used for the cracking model development. The restrained shrinkage test is recommended for evaluating the potential of CSM for shrinkage cracking and for developing a shrinkage cracking model.

#### *4.2.2.5 Bond Strength Test*

Bond strength is an input to the restrained shrinkage cracking model. Because the beam specimen for restrained shrinkage cracking is glued onto a steel substrate with epoxy or cement mortar, the bond strength between the CSM and steel substrate is measured when epoxy or cement mortar are used as bonding agents.

The bond strength tests were conducted in accordance with the Iowa shear test (Iowa DOT 2000), which separates the CSL and base along the interface, as shown in Figure 4-24. Two materials, i.e., clay-lime and gravel-cement, were used and compacted at the optimum moisture content. The mixed materials were compacted by standard Proctor compaction in a 4-inch diameter mold. The specimens were cured at 100% RH at room temperature (68°F) for 7 days and were glued to a steel substrate with epoxy or cement mortar. The cement mortar was prepared with a sand:cement:water ratio of 6:2:2.



**Figure 4-24. Coefficient of Friction Test Setup**

The bond strength tests were conducted at a constant loading rate (71.6 psi/min) or constant deformation rate (0.065 in./min). Figures 4-25 and 4-26 show the test results for the constant loading rate and constant deformation rate for the cement-gravel specimens, respectively. Due to abrupt failure during the constant loading rate tests, a constant deformation rate is recommended for the purpose of safety. However, the repeatability of the deformation control (0.065 in./min) is poor. Thus, the load speed was increased to 0.65 in./min, which improved the repeatability.

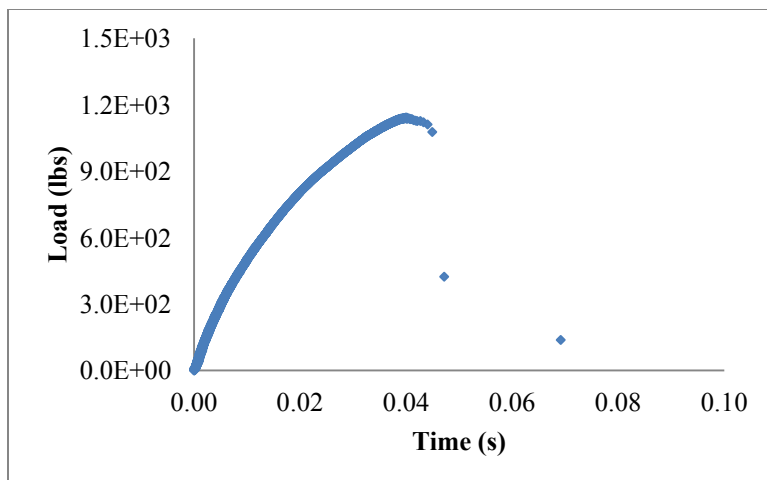


**Figure 4-25. Bond Strength under Constant Loading Rate for Cement-Gravel (71.6 psi/min)**

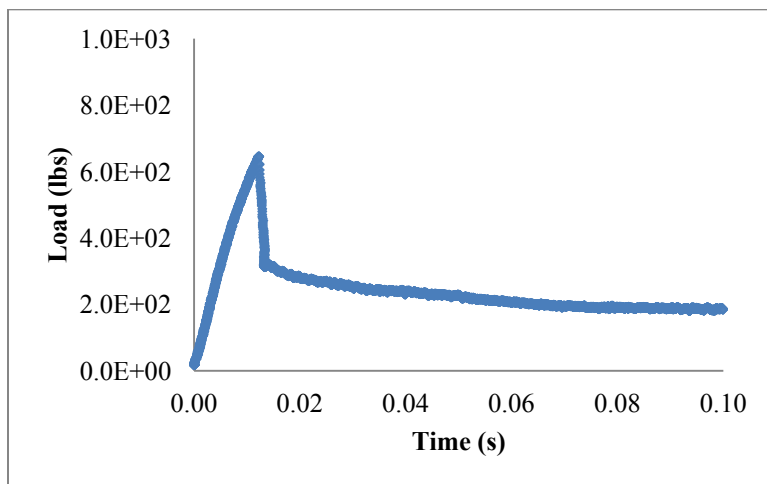


**Figure 4-26. Bond Strength under Constant Deformation Rate for Cement-Gravel (0.065 in./min)**

Table 4-7 and Figures 4-27 and 4-28 present the test results for three clay-lime and three gravel-cement specimens that use epoxy or cement mortar as bonding agents, respectively. Some variability is seen in the bond strength measured. As shown in Figure 4-27, when cement mortar is used as the bonding agent, the bond strength values for the clay-lime and gravel-cement specimens are very close to each other, around 3 psi, because the failure occurred within the mortar. That is, the bond strength was controlled by the strength of the cement mortar. Therefore,

the clay-lime and gravel-cement specimens have similar bond strength values when cement mortar is used as the bonding agent.

When epoxy is used as the bonding agent, the bond strength values of the clay-lime specimens are significantly lower than those of the gravel-cement specimens, as shown in Figure 4-28. Shear failure occurred inside the clay-lime specimen, as shown in Figure 4-29 (a). Therefore, the bond strength that was measured is actually the shear strength of the clay-lime. The failure plane for the gravel-cement specimen is located at the interface between the epoxy and soil specimen in Figure 4-29 (b). Therefore, this measured strength is the bond strength at the interface.

**Table 4-7. Results of Bond Strength Tests**

Binder	Materials	Shear Strength (psi)	COV
Mortar	Clay-Lime	2.53	26.2%
		2.43	
		3.80	
	Gravel-Cement	2.68	27.9%
		2.57	
		4.14	
Epoxy	Clay-Lime	19.1	32.1%
		14.0	
		26.8	
	Gravel-Cement	206.8	10.5%
		224.5	
		181.8	

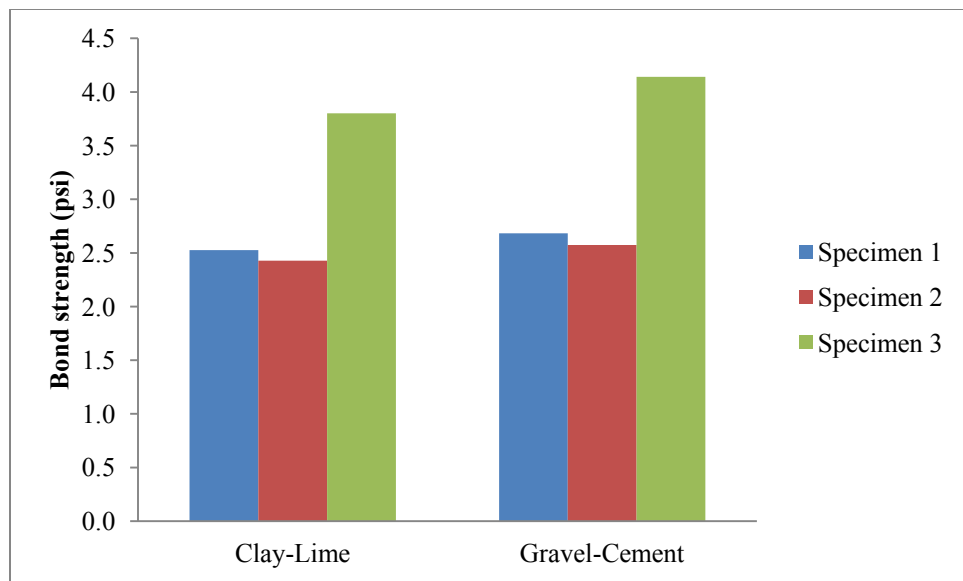


**Figure 4-27. Bond Strength Test when Cement Mortar is used as Bonding Agent**

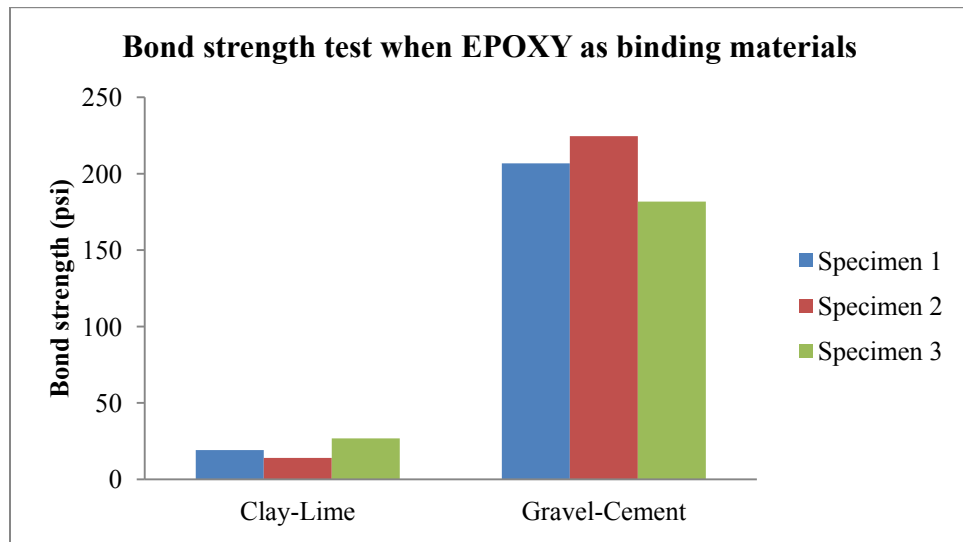


**Figure 4-28. Bond Strength Test when Epoxy is used as Bonding Agent**



(a) Clay-Lime Specimen after Test



(b) Gravel-Cement Specimen after Test

**Figure 4-29. Failure Surfaces after Bond Strength Tests**

Even though some variability was found between the bond strength of the replicates, the Iowa shear test is capable of measuring the bond strength for modeling shrinkage cracking and is recommended for model development.

### 4.3 SUMMARY

The test procedures were assessed in terms of their performance predictability, precision, accuracy, practicality, cost, and other pertinent factors. These appraisals are based either on the literature review, or my experience or understanding. One heavily stabilized material, i.e. cement-stabilized gravel, and one lightly stabilized material, i.e. lime-stabilized clay, are selected to evaluate these test procedures in the lab. UCS, IDT strength and modulus tests are suitable for strength and stiffness tests of CSM. Free drying shrinkage, free autogenous shrinkage, and COTE tests are recommended to identify the shrinkage properties of CSM. Free gradient drying shrinkage test is developed to simulate the loss of moisture in field condition. Restrained drying

shrinkage test is recommended to induce shrinkage cracking for model development. The increase in friction between the CSL and underlying material will reduce the shrinkage crack spacing and crack width. By artificially creating a high level of bond, shrinkage cracking can be generated in a lab specimen for model development. The interface friction/bond can be measured by bond strength test. The high level of bond in lab can be created when epoxy or cement slurry as bonding agents. The evaluation results show that all of these aforementioned test procedures are suitable for identifying the CSM properties and are recommended for establishing shrinkage cracking models.

## CHAPTER FIVE

### EXPERIMENTAL RESULTS

This chapter summarizes the experimental results, which are used to develop models for strength and modulus growth, and shrinkage cracking. Table 5-1 provides a list of recommended material properties and test procedures.

**Table 5-1. Material Properties and Performance Tests**

Distress Model	Shrinkage Cracking
Material Properties	<ul style="list-style-type: none"><li>• Unconfined compressive strength</li><li>• Indirect tensile strength</li><li>• Indirect tensile modulus</li><li>• Ultimate drying shrinkage strain</li><li>• Gradient drying shrinkage strain</li><li>• Coefficient of thermal expansion</li><li>• Coefficient of friction</li></ul>
Tests for Model Development or Calibration	Restrained shrinkage cracking test

#### 5.1 STRENGTH AND MODULUS GROWTH TESTS

The strength/modulus growth rate of CSL was studied. If cement is used as a binder, a relative high strength/modulus can form fairly quickly. For lime and/or fly ash, the early-age strength/modulus value is relatively low when compared to that of cement. However, the strength/modulus can grow for years due to additional pozzolanic reactions. Different curing periods were used to evaluate the mechanisms of strength gain: 3, 7, 28, 90, 180, and 360 days. Table 5-2 shows the test matrix for the strength growth model development, which includes UCS and IDT strength. All the specimens were cured at 68°F and 100% RH. For IDT strength/modulus, different combinations of temperature and RH were used.

**Table 5-2. Strength of Mixtures**

Material Characterization				
		Purpose		Symbol
Properties	Unconfined Compressive Strength	Level 2 for correlation with other strength/moduli values, and catalogue of Level 3 default values		UCS
	IDT Strength	Level 1 for cracking model and catalogue of Level 3 default values		S <sub>IDT</sub>
Factors	Curing time	Long-term behavior: 3, 7, 28, 90, 180, and 360 days.		C
	Clay	Silt	Sand	Gravel
Cement	UCS, S <sub>IDT</sub>	UCS, S <sub>IDT</sub>	UCS, S <sub>IDT</sub>	UCS, S <sub>IDT</sub>
Lime	UCS, S <sub>IDT</sub>	UCS, S <sub>IDT</sub>	(N/A)	(N/A)
Class C fly ash	(N/A)	UCS, S <sub>IDT</sub>	UCS, S <sub>IDT</sub>	UCS, S <sub>IDT</sub>
Replicates	1			
Strength	6 curing times × (2UCS+2 S <sub>IDT</sub> ) × 1 replicate = 24	6 × (3+3) × 1 = 36	6 × (2+2) × 1 = 24	6 × (2+2) × 1 = 24
<b>Total</b>	<b>54 UCS + 54 S<sub>IDT</sub> tests</b>			

### 5.1.1 UCS and IDT Strength at 68°F and 100% RH

The UCS test is the most common test performed on CSM for mix designs for use in pavement bases and subbases. The test methods for the different mixtures follow the recommendations in the MEPDG (ARA 2004). The specimens for all nine types of mixtures were compacted using standard Proctor compaction in a mold 4 inches in diameter and 4.6 inches in height. At the end of the moist-cure periods, all of the specimens except the lime-clay specimens were soaked in water for 4 hours prior to testing.

For the cement-stabilized fine-grained materials (clay, silt and sand), the ASTM D1633 test method was followed. The compression tests were conducted as soon as possible after removing the specimens from the water. The tests were conducted using a servo-hydraulic

machine with the loading rate of 20 psi/sec. The AASHTO T22 test method was followed to test the cement-gravel specimens with the loading rate of 35 psi/sec. For the fly ash-stabilized soils, the ASTM C593 method was followed, and the loading rate was 35 psi/sec.

The lime-clay specimens were capillary-soaked for 24 hours prior to testing. The capillary soaking process is conducted by wrapping the specimens with wet absorptive fabric and placing them on a porous stone. The water level reaches the top of the stone and comes in contact with the fabric wrap throughout the capillary soaking process. However, the specimen is not in direct contact with the water, following the NLA procedure (NLA 2006). During the test, the load is applied with an axial deformation rate of approximately 2.0%/min, in accordance with the ASTM D5102 test method.

Figures 5-1 and 5-2 present the UCS and IDT strength results for all nine mixtures, respectively.

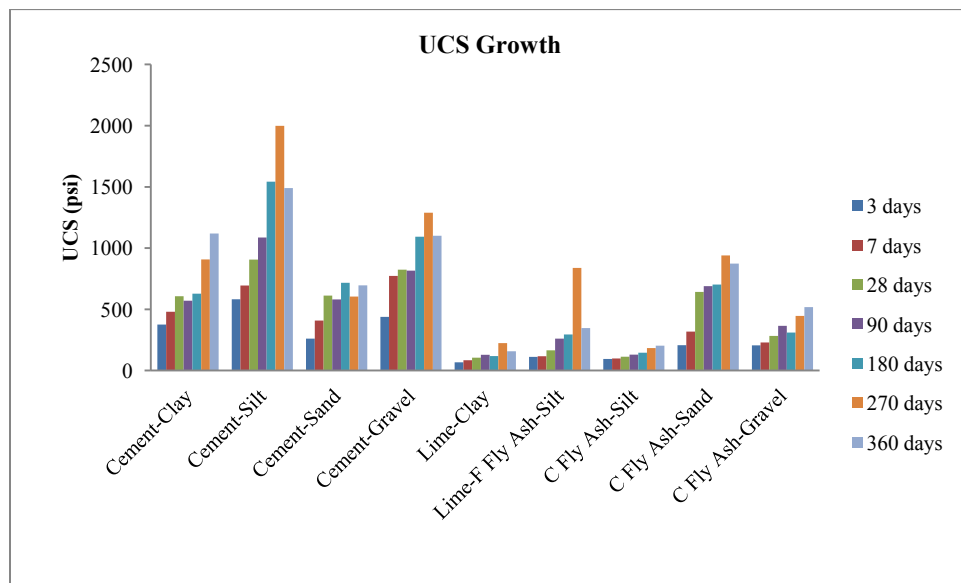


**Figure 5-1. UCS Growth with Curing Age**

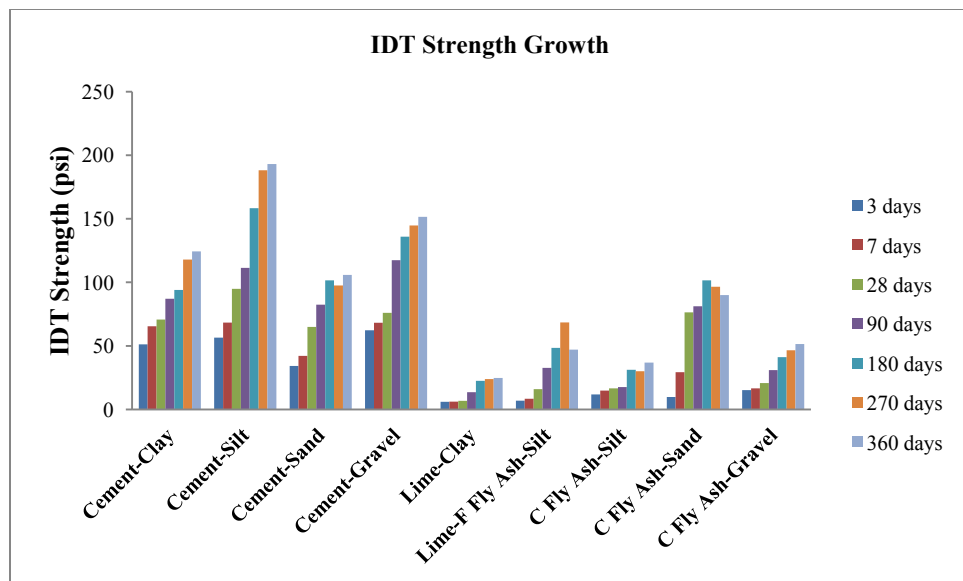


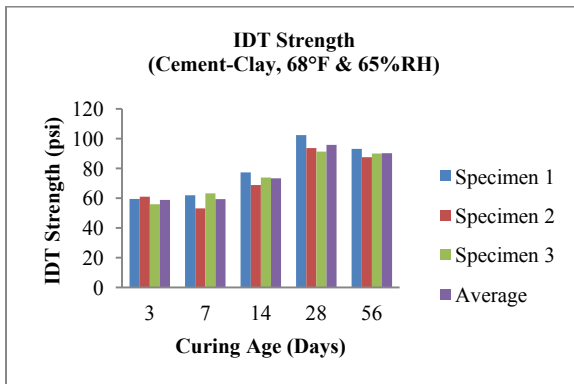
**Figure 5-2. IDT Strength Growth with Curing Age**

### 5.1.2 IDT Strength and Modulus at Various RH and Temperatures

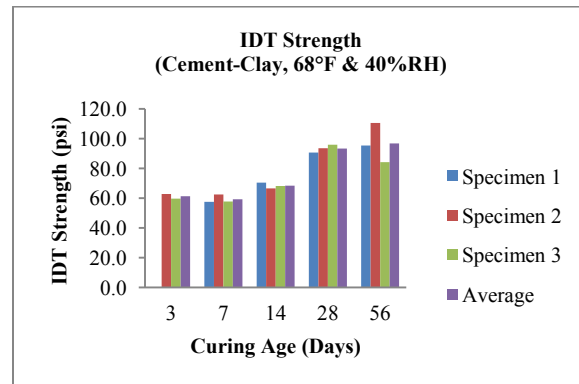
In order to establish the shrinkage cracking model, the IDT strength/modulus specimens were prepared for 3, 7, 14, 28, and 56 days curing at various RH and temperatures, because early-stage shrinkage cracking and the IDT strength/moduli are sensitive to environmental conditions. Five mixtures were tested with three replicates, including cement-clay, cement-silt, cement-gravel, lime-clay, and C fly ash-silt, as shown in Table 5-3. Figures 5-3 and 5-4 present the IDT strength and IDT modulus growth test results, respectively.

**Table 5-3. IDT Strength and Modulus of Mixtures**

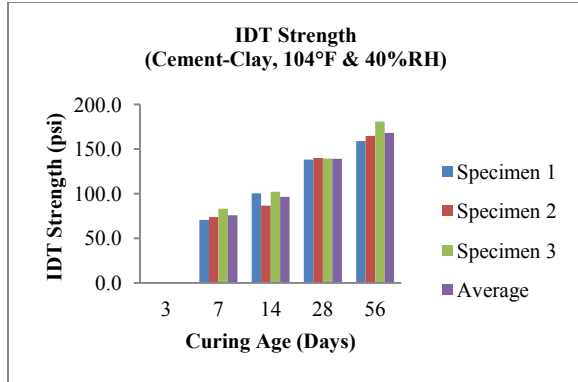
Material Characterization				
		Purpose	Symbol	
Properties	IDT Strength	Level 1 for cracking response model and catalogue of Level 3 default values	$S_{IDT}$	
	IDT Modulus	Level 1 for cracking response model and catalogue of Level 3 default values	$E_T$	
Factors	Curing time	Long-term behavior: 3, 7, 14, 28, and 56 days at various temperatures and RH	C	
	Clay	Silt	Sand	Gravel
Cement	$S_{IDT}, E_t$	$S_{IDT}, E_t$	-	$S_{IDT}, E_t$
Lime	$S_{IDT}, E_t$	-	(N/A)	(N/A)
Class C fly ash	(N/A)	$S_{IDT}, E_t$	-	-
Replicates	3			
<b>Total</b>	<b>12 materials/environment × 5 curing time × 3 replicates =180 IDT Strength and 180 IDT Modulus Tests</b>			



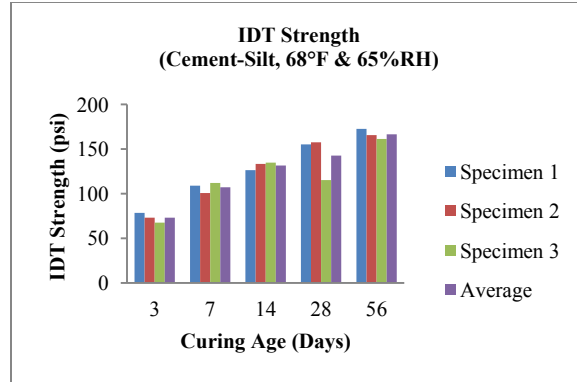
(a) Cement-Clay, 68°F & 65%RH



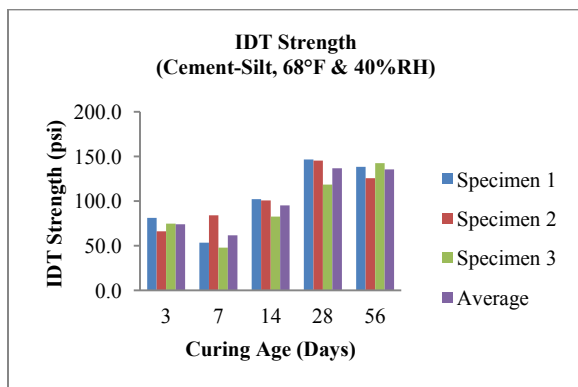
(b) Cement-Clay, 68°F & 40%RH



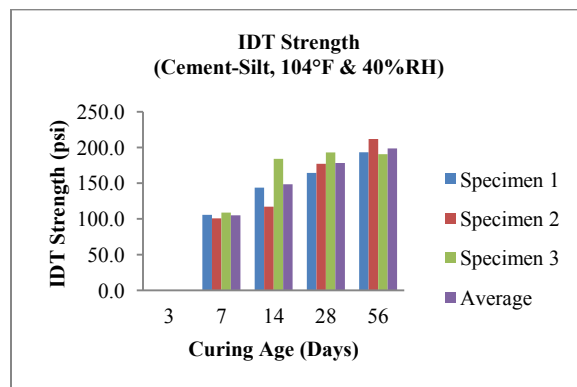
(c) Cement-Clay, 104°F & 40%RH



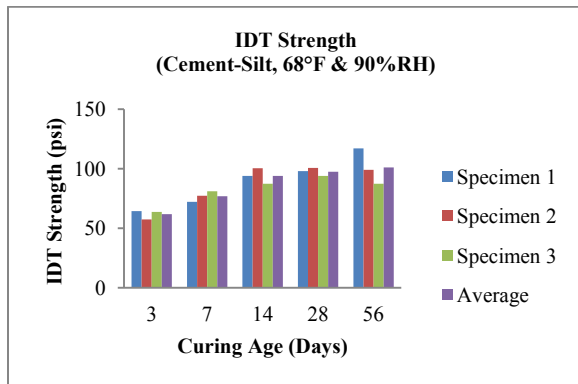
(d) Cement-Silt, 68°F & 65%RH



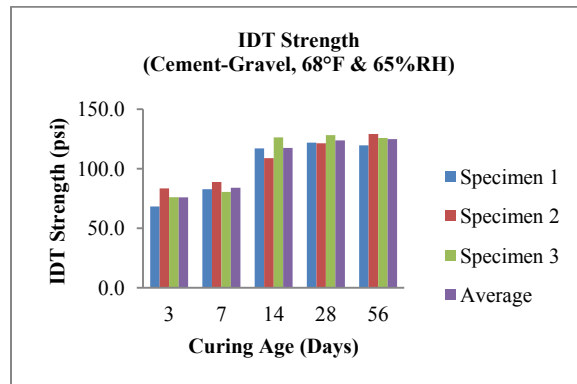
(e) Cement-Silt, 68°F & 40%RH



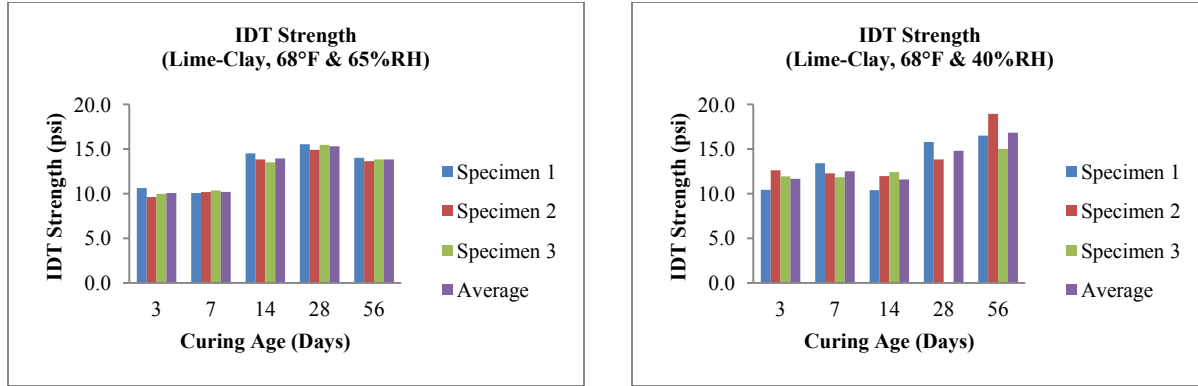
(f) Cement-Silt, 104°F & 40%RH



(g) Cement-Silt, 68°F & 90%RH

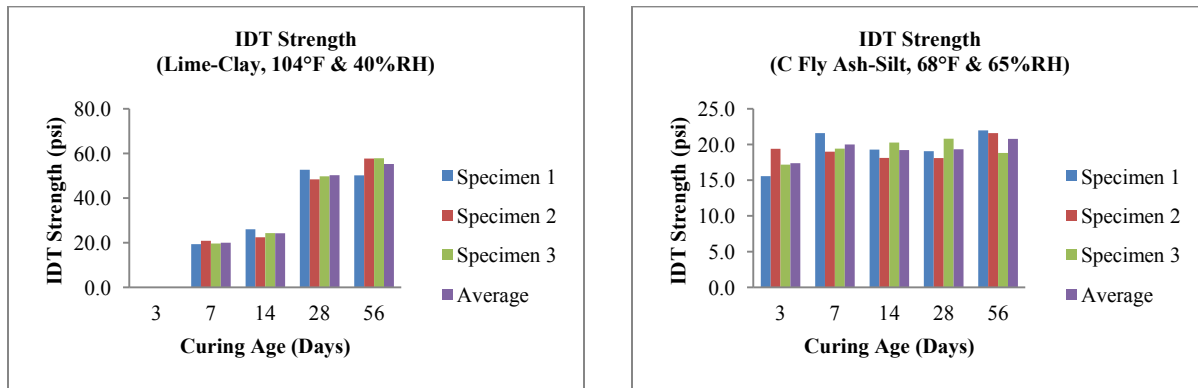


(h) Cement-Gravel, 68°F & 65%RH



(i) Lime-Clay, 68°F & 65%RH

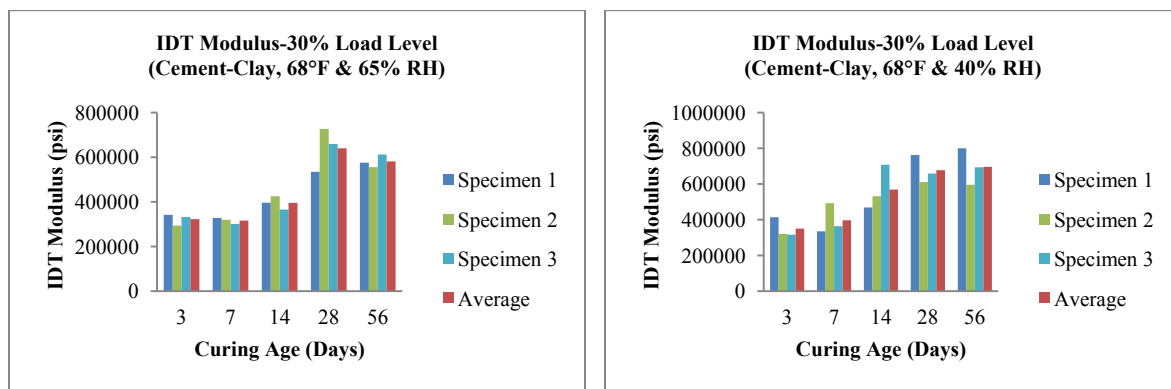
(j) Lime-Clay, 68°F & 40%RH



(k) Lime-Clay, 104°F & 40%RH

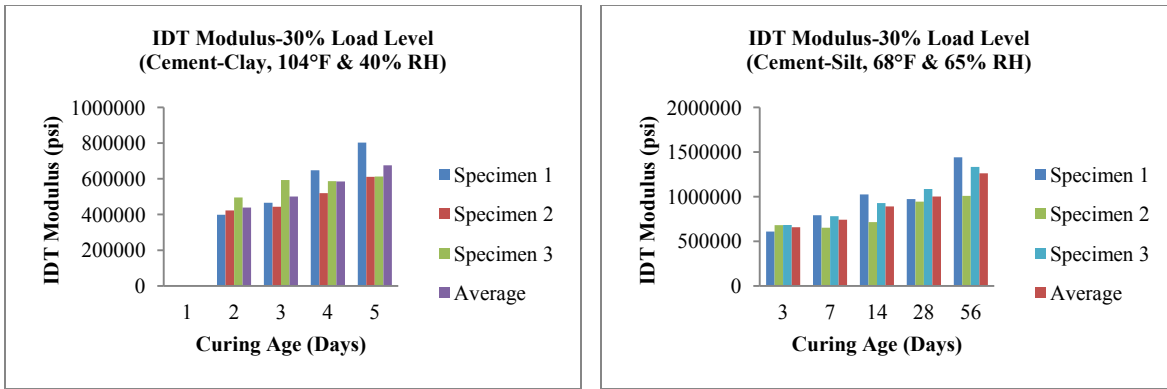
(l) C Fly Ash-Silt, 68°F & 65%RH

**Figure 5-3. IDT Strength Values at Various RH and Temperatures with Curing Age**



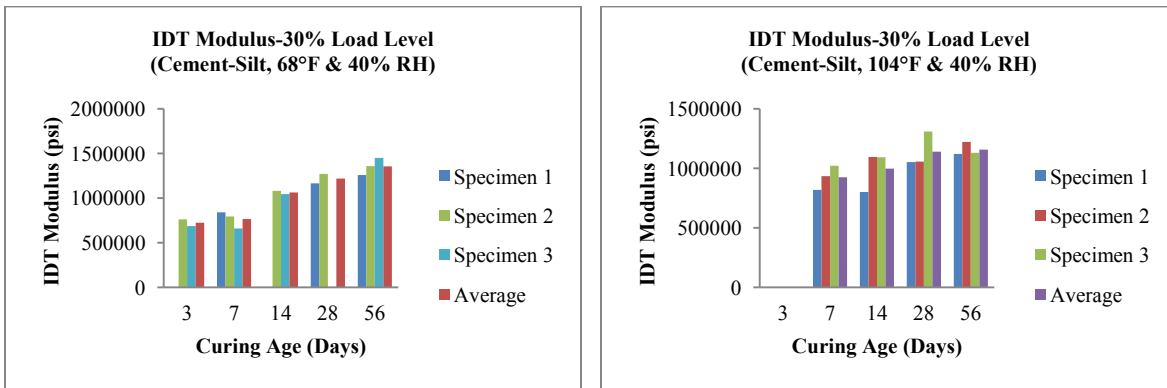
(a) Cement-Clay, 68°F & 65% RH

(b) Cement-Clay, 68°F & 40% RH



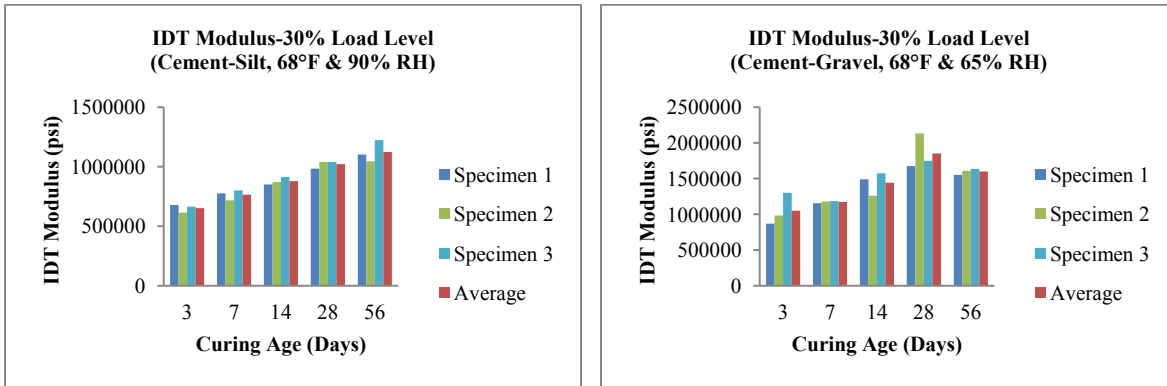
(c) Cement-Clay, 104°F & 40% RH

(d) Cement-Silt, 68°F & 65% RH



(e) Cement-Silt, 68°F & 40% RH

(f) Cement-Silt, 104°F & 40% RH



(g) Cement-Silt, 68°F & 90% RH

(h) Cement-Gravel, 68°F & 65% RH

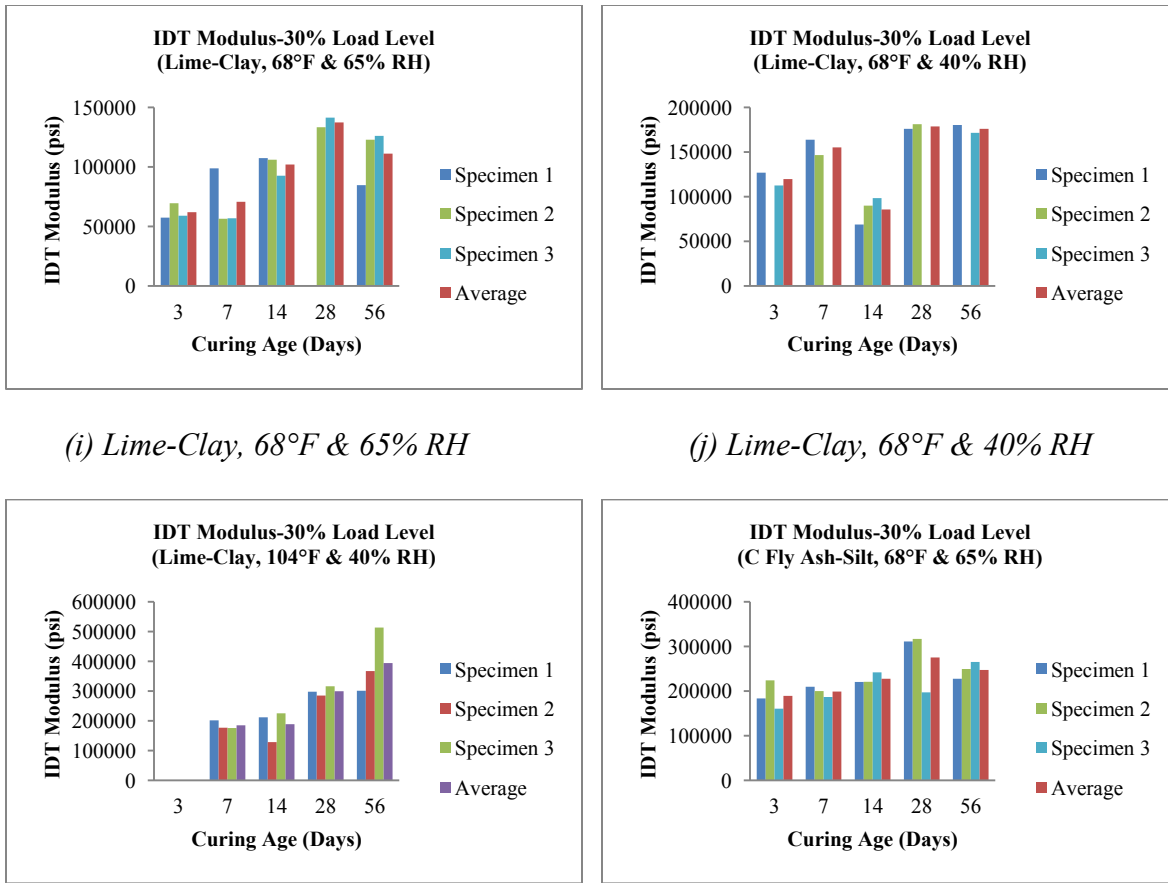


**Figure 5-4. IDT Modulus Values at Various RH and Temperatures with Curing Age**

## 5.2 SHRINKAGE AND CRACKING TESTS

Shrinkage cracking test sets were conducted on cement-clay, cement-silt and lime-clay at various RH values and temperatures (68°F and 65% RH, 68°F and 40% RH, and 104°F and 40% RH). These tests include the COTE, ultimate drying shrinkage strain, drying shrinkage strain gradient, large-scale restrained shrinkage cracking (using epoxy as bonding agent), coefficient of friction, and IDT strength and modulus values. The sides of the beams used for the restrained shrinkage cracking tests were sealed, and only the top surface was exposed to air to simulate field drying. The shrinkage strain was measured by a LVDT. The IDT strength/modulus

specimens were tested after 3, 7, 14, 28, and 56 days of curing for model development. Table 5-4 presents the laboratory test plan for the shrinkage model.

**Table 5-4. Laboratory Test Plan for Shrinkage Model**

Shrinkage Model				
		Purpose		Symbol
Material Properties	IDT Modulus	Material property in the cracking spacing and width model		$E_t$
	IDT Strength	Material property in the cracking spacing and width model		$S_{IDT}$
Model Development Tests	Ultimate Drying Shrinkage	Input to shrinkage strain model		$\epsilon_{su}$
	Gradient Drying Shrinkage Strain	Shrinkage strain model development		$\epsilon_g$
	Restrained Shrinkage Cracking	Shrinkage cracking model development		$R$
	Interface Friction	Input to shrinkage cracking model		$\mu$
	Thermal Shrinkage	Thermal shrinkage measurement		$\epsilon_T$
	Clay	Silt	Sand	Gravel
Cement	$E_t, S_{IDT}, \epsilon_{su}, R, \mu, \epsilon_T$	$E_t, S_{IDT}, \epsilon_{su}, \epsilon_g, R, \mu, \epsilon_T$	-	$E_t, S_{IDT}, \epsilon_{su}, \mu, \epsilon_T$
Lime	$E_t, S_{IDT}, \epsilon_{su}, \epsilon_g, R, \mu, \epsilon_T$	-	(N/A)	(N/A)
Class C fly ash	(N/A)	$E_t, S_{IDT}, \epsilon_{su},$	-	$\epsilon_{su},$
<b>Subtotal</b>	$90E_t + 90S_{IDT} + 2\epsilon_{su} + \epsilon_g + 6R + 9\mu + 12\epsilon_T$	$75E_t + 75S_{IDT} + 2\epsilon_{su} + \epsilon_g + R + 12\mu + 6\epsilon_T$	-	$15E_t + 15S_{IDT} + 2\epsilon_{su} + 0\epsilon_g + 0R + 3\mu + 6\epsilon_T$
<b>Total</b>	<b>180 IDT modulus + 180 IDT strength + 2 gradient drying shrinkage + 7 restrained drying shrinkage + 24 bond strength tests + 24 thermal shrinkage/expansion</b>			

### 5.2.1 Coefficient of Thermal Expansion (COTE)

The COTE is important for thermal strain determination, which is a key parameter in the shrinkage cracking model. Temperatures were cycled and the displacements were measured by LVDTs. The temperatures inside the specimens and in the environmental chamber were

monitored by thermal couples. Cyclic strain, which does not include strain due to autogenous and/or drying shrinkage, is used to determine the COTE.

The amplitude of the temperature cycles was set to 9°F, with constant RH. Table 5-5 presents the COTE for the cement-clay, cement-silt, lime-clay, and cement-gravel at different temperatures and RH values.

**Table 5-5. COTE Test Results**

Materials	Temperature Cycles	Relative Humidity (%)	COTE ( $\times 10^{-6}/^{\circ}\text{F}$ )
<b>Cement-Clay</b>	68-77°F	65	12.6
<b>Cement-Silt</b>	68-77°F	65	9.3
	104-113°F	65	9.5
<b>Lime-Clay</b>	68-77°F	65	13.1
	77-86°F	98	46.7
	36-45°F	98	29.2
<b>Cement-Gravel</b>	77-86°F	98	14.4
	36-45°F	98	2.6

### **5.2.2 Ultimate Drying Shrinkage**

Ultimate drying shrinkage strain is the shrinkage strain that the CSL develops upon prolonged exposure to drying conditions, and constitutes a material property in the drying shrinkage model. The ultimate drying shrinkage strain test was conducted using beam specimens with dimensions of 11.25 in. $\times$ 4 in. $\times$ 4 in. The shrinkage of the specimen was measured under room conditions (68°F and about 40% RH) from dial gauges on both sides. The shrinkage strain was monitored until it became stable.

Ultimate drying shrinkage strain is an input for the gradient drying shrinkage, crack spacing and width models. Table 5-6 presents the measured ultimate shrinkage strain results.

**Table 5-6. Measured Ultimate Shrinkage Strain**

Material	Optimum Moisture Content (%)	Measured Ultimate Strain ( $\times 10^{-6}$ )
C Fly Ash-Silt	10.0	1313
C Fly Ash-Gravel	7.4	628
Cement-Gravel	6.2	1467
Cement-Clay	18.0	12430
Cement-Silt	11.1	3259
Lime-Clay	19.4	14438

### 5.2.3 Gradient Drying Shrinkage

Pavement can lose its moisture by evaporation from the top surface, which results in a moisture gradient. The moisture gradient can lead to self-sustained drying shrinkage stress and early-age cracking in CSL. Therefore, this gradient is an important factor that can affect the shrinkage cracking distress.

The gradient drying shrinkage test was first developed with 4 in.  $\times$  4 in.  $\times$  11.25 in. specimen, by Xiaojun Li at Washington State University. In order to investigate the moisture gradient and resultant shrinkage strain gradient in a specimen, the four sides of beam specimens were sealed with wax, and only the top surface was exposed to air. In order to measure the shrinkage strain at more depths, the specimen height was increased to 8 in. tall in this research, with 4 in. wide and 11.25 in. long. Figure 5-5 shows the test setup. The drying shrinkage strain values were measured at four depths from the exposed surface, i.e., 0, 2.25, 4.5 and 6.75 inches, respectively. The results of gradient drying shrinkage test are shown in Section 6.2.2.



**Figure 5-5. Free Drying Shrinkage with Moisture Gradation Test Setup**

#### **5.2.4 Restrained Shrinkage Cracking**

Shrinkage cracking occurs when CSL are restrained by the underlying layer and/or are self-restrained (i.e., strain gradient). The shrinkage cracking potential of each CSL material can be examined by restrained shrinkage testing. The increase in friction between the CSL and underlying material reduces the shrinkage crack spacing. By artificially creating a high level of bonding, shrinkage cracking can be generated in a laboratory-scale specimen for model development. To simulate the field pavement conditions, the beams were side-sealed as in the gradient drying shrinkage strain test. Figure 5-6 presents the test setup.

Clay-cement, clay-lime, and silt-cement beams with dimensions of 48 in. $\times$ 6 in. $\times$ 4 in. were glued on a steel tube using epoxy. One replicate was used for each of the combinations. The restrained shrinkage was monitored by a LVDT, and the crack spacing and crack widths were measured from the top surface. Three environmental conditions, 68°F and 65% RH, 68°F and 40% RH, and 104°F and 40% RH, were used for the restrained shrinkage cracking tests.

Figure 5-7 shows typical cracking in the beam specimen. Seven specimens experienced shrinkage cracking.



**Figure 5-6. Restrained Shrinkage Test Setup with Sides Sealed**

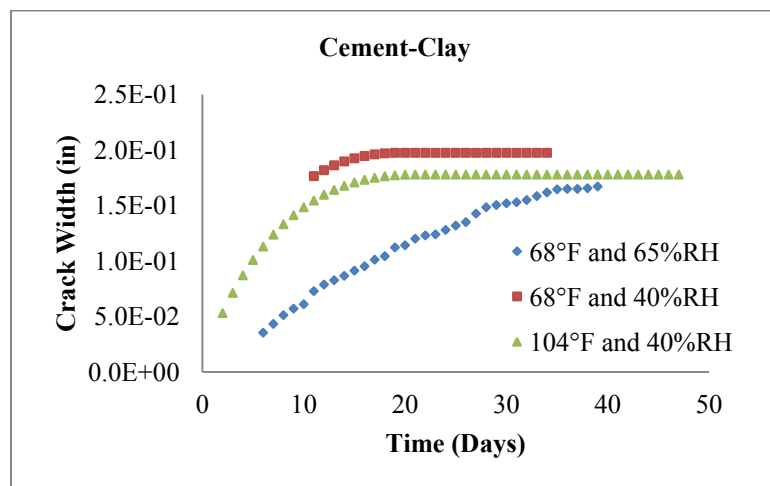


**Figure 5-7. Transverse Crack in Lime-Clay Specimen (View from Top)**

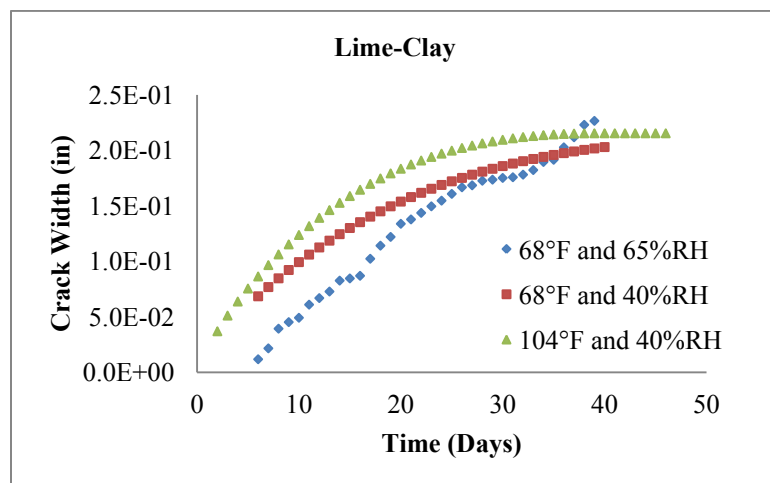
Table 5-7 provides a summary of the number of cracks, crack spacing and age when cracking occurred. And Figure 5-8 shows the measured crack width results.

**Table 5-7. Laboratory Restrained Cracking Summary**

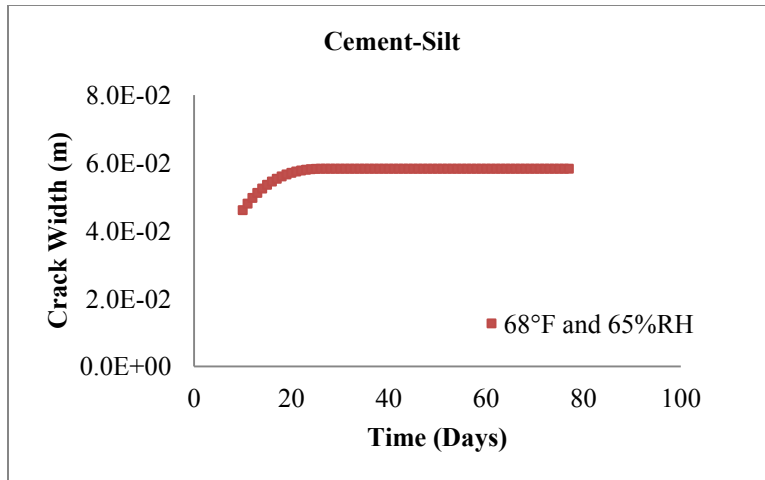
Materials	Environment	No. of Cracks	Crack Spacing (in.)	Age when Crack Occurred (days)
Cement-Clay	68°F and 65% RH	1	24	6
	68°F and 40% RH	2	16	11
	104°F and 40% RH	2	16	2
Lime-Clay	68°F and 65% RH	1	24	6
	68°F and 40% RH	1	24	4
	104°F and 40% RH	1	24	2
Cement-Silt	68°F and 65% RH	1	24	10



(a) Cement-Clay



(b) Lime-Clay



(c) Cement-Silt

**Figure 5-8. Measured Crack Width**

### 5.2.5 Coefficient of Friction

Even though the interface friction/bond is not a CSM property, it significantly affects shrinkage cracking and is an important parameter in the shrinkage cracking model. Because the beam for the restrained shrinkage cracking tests was glued on a steel substrate using epoxy, the coefficient of friction between the CSM and steel substrate was measured when the epoxy was used as the bonding agent. The coefficient of friction is defined as the slope of stress-displacement relationship curve (linear portion). The coefficient of friction tests were conducted in accordance with the Iowa shear test (Iowa DOT 2000), which separates the CSL and base layer along the interface. The Iowa shear test is similar to a direct shear test. The coefficient of friction tests were conducted under a constant deformation rate (0.65 in./min). The coefficient of friction can be calculated as the slope of the stress and displacement curve.

When epoxy is used as the bonding agent in the laboratory, it is found that the coefficient of friction has a linear relationship with the IDT strength of the CSM, as shown in Figure 5-9. In

the field, the CSL bond well with the underlying layer, and the failure interface related to shrinkage usually occurs in the weaker material between the CSM and the underlying material (Romanoschi and Metcalf 2001). Therefore, the slope of the stress and displacement curve in a direct shear test can be used to determine the coefficient of friction for field cases. Figure 5-10 shows the relationship between the IDT strength of the CSM and the coefficient of friction determined in direct shear testing, which can be used as the Level 2 input for the coefficient of friction.

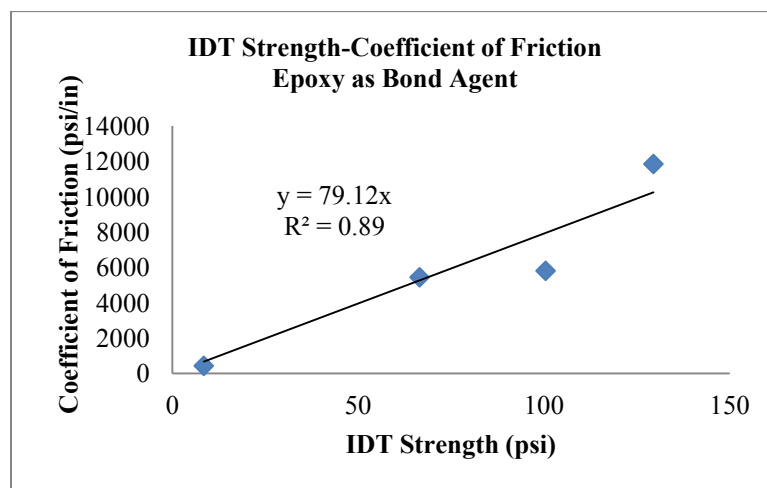


**Figure 5-9. Relationship between IDT Strength of CSM and Coefficient of Friction when Epoxy is used as Bonding Agent**

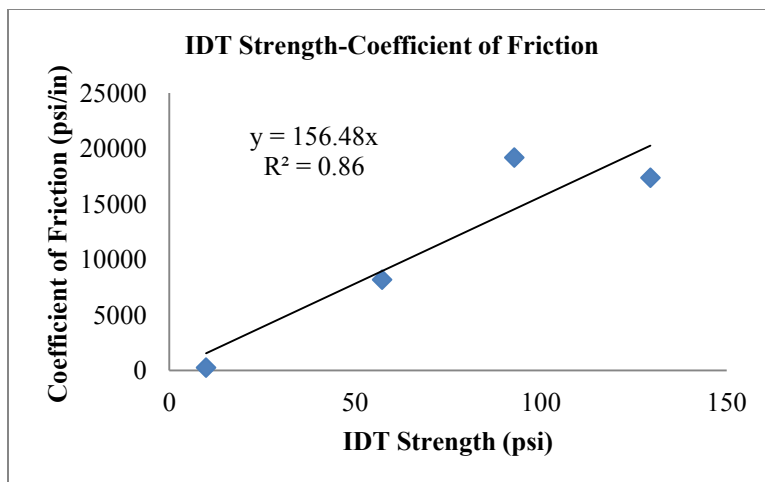


**Figure 5-10. Relationship between IDT Strength and Coefficient of Friction in a Direct Shear Test**

### 5.3 SUMMARY

The experimental results are summarized in this chapter. The strength and modulus gain tests were conducted after different curing periods. The UCS and IDT strength test specimens were cured after 3, 7, 28, 90, 180, and 360 days. In order to establish the shrinkage cracking model, the IDT strength/modulus specimens were prepared for 3, 7, 14, 28, and 56 days curing at various RH and temperatures, because early-stage shrinkage cracking and the IDT strength/moduli are sensitive to environmental conditions. The results show that different binders lead to various strength/modulus growth rates. Cement results in strength growth fairly quickly. For lime and/or fly ash, the early-age strength/modulus value is relatively low when compared to that of cement. Tests related to shrinkage cracking include COTE, ultimate drying shrinkage, gradient drying shrinkage, restrained shrinkage cracking, and coefficient of friction tests. These tests were conducted at various temperature and/or RH values. The large-scale restrained shrinkage cracking (using epoxy as bonding agent) is different from the one in the test procedure

evaluation section (Section 4.2.2.4). To simulate the field pavement conditions, the beams were side-sealed as in the gradient drying shrinkage strain test. These results are used to develop strength and modulus growth, and shrinkage cracking models.

# **CHAPTER SIX**

## **MODEL DEVELOPMENT**

This chapter presents correlations of UCS, IDT strength and modulus; and the strength and modulus growth model, and shrinkage cracking models based on the laboratory results.

### **6.1 STRENGTH AND MODULUS GROWTH MODELS**

If cement is used as the binder, relatively high strength/modulus can form fairly quickly. For lime and/or fly ash stabilized CSM, the early-age strength/modulus is relatively low when compared to cement stabilized CSM, but can grow for years due to pozzolanic reactions. The strength/modulus growth of CSM is examined in this study.

#### **6.1.1 Correlations between UCS and IDT Tests**

The strength and modulus characteristics of CSM include UCS, IDT strength, and IDT modulus. Figures 6-1 and 6-2 and Eqs. (6-1) through (6-3) show the correlations between the different types of strength and modulus. These correlations can be used to predict the strength and modulus as Level 2 inputs in the MEPDG (ARA 2004).

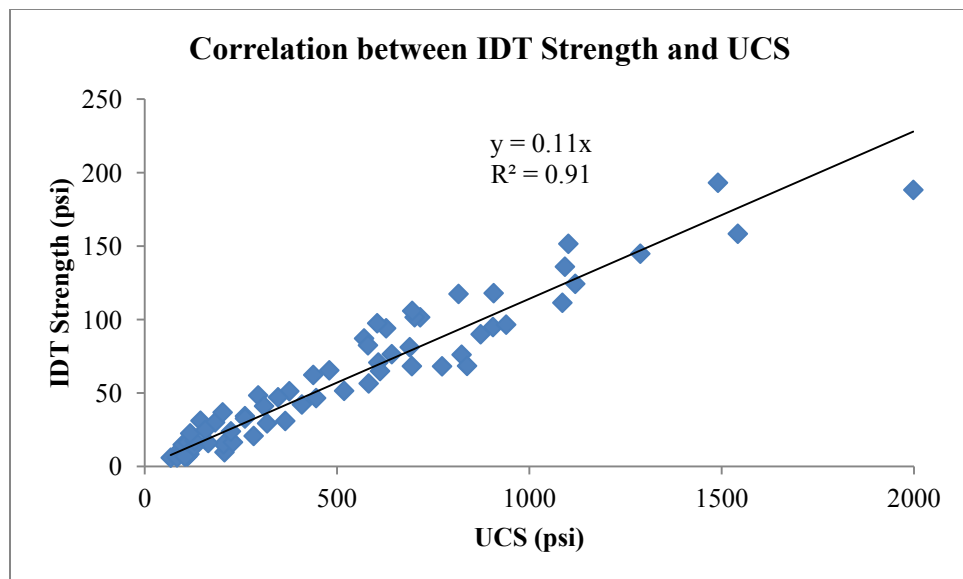


**Figure 6-1. Correlation between IDT Strength and UCS**

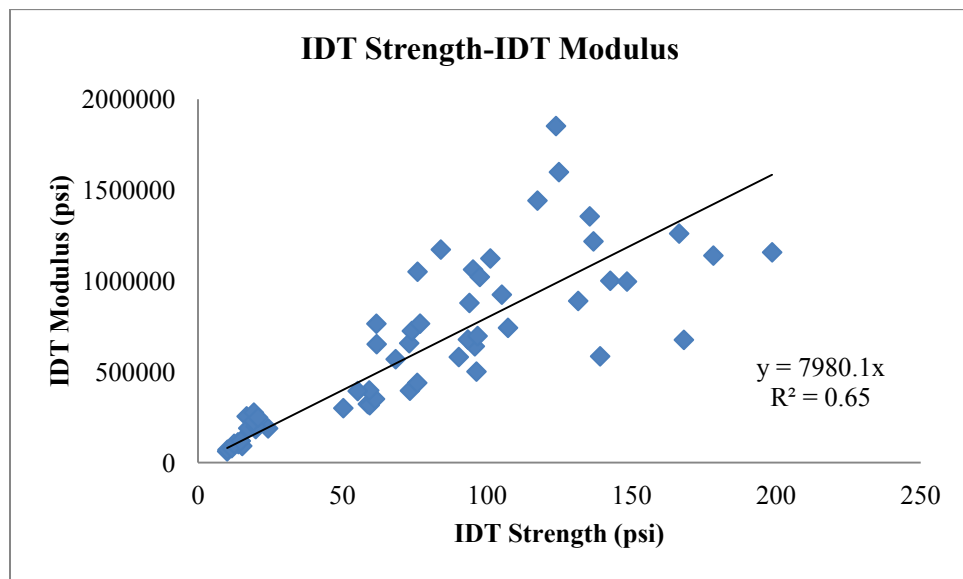


**Figure 6-2. Correlation between IDT Strength and IDT Modulus**

$$S_{IDT} = 0.11 \times UCS \quad \text{Eq. (6-1)}$$

$$E_t = 7980.1 \times S_{IDT} \quad \text{Eq. (6-2)}$$

$$E_t = 910.5 \times UCS \quad \text{Eq. (6-3)}$$

where

$S_{IDT}$  = indirect tensile strength, psi

$UCS$  = unconfined compressive strength, psi

$E_t$  = indirect tensile modulus, psi

### 6.1.2 Strength Growth Model

The growth of CSL strength also is examined based on different curing periods. Because the 28-day strength is a commonly used material property for performance prediction and quality control, a strength growth model was developed based on 28-day strength, which can be used to predict the corresponding strength at a time at 68°F and 100% RH curing condition. Eq. (6-4) shows the strength growth model and Figure 6-3 presents a comparison of the predicted and measured strength values.

$$S_t(t) = (S_{28}) \left[ p_1^{1 - \frac{1}{(1 + \frac{(t-t_0)}{p_2})}} \right] \quad \text{Eq. (6-4)}$$

where

$S_t(t)$  = UCS and IDT strength at age  $t$  months, psi

$S_{28}$  = UCS and IDT strength after 28-day curing at 68°F and 100% RH;  $S_t$  and  $S_{28}$  should be the same type of strength, psi

$t$  = time corresponding to  $S_t$ , month

$t_0$  = time corresponding to  $S_{28}$ , equals to 28/30.5 (assume each month has 30.5 days), month

$p_1, p_2$  = regression parameters; 1.59 and 1.61, respectively, in this study.

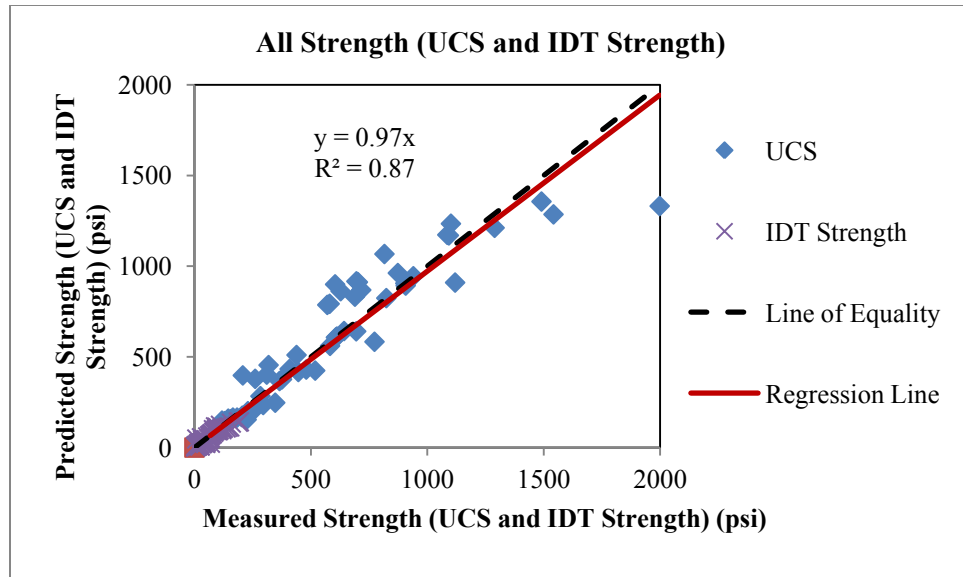


**Figure 6-3. Comparison of Predicted and Measured Strength Values at Different Ages**

### 6.1.3 IDT Strength and Modulus Growth Model Considering Temperature and RH Effect

The early-age tensile strength/modulus is critical to shrinkage cracking. Shrinkage cracking is sensitive to environmental conditions, including temperature and RH. Thus, the IDT strength/modulus growth models were established with consideration of temperature and RH effects. The IDT strength/modulus values were measured after 3, 7, 14, 28, and 56 days of curing. Growth models were developed to predict the IDT strength and modulus values at various temperatures and RH, as shown in Eq. (6-5),

$$S_{IDT} = p_5(UCS_{28}) \left[ p_1 \frac{1 - \frac{1}{\left(1 + \frac{t-28/30.5}{p_2}\right) \left(\frac{1+RH}{100}\right)^{\frac{p_3}{2}} \left(\frac{T-32}{1.8} + 273.15\right)^{\frac{p_4}{293.15}}}} \right] \quad \text{Eq. (6-5-a)}$$

$$E_t = q_5(UCS_{28}) \left[ p_1 \frac{1 - \frac{1}{\left(1 + \frac{t-28/30.5}{p_2}\right) \left(\frac{1+RH}{100}\right)^{\frac{p_3}{2}} \left(\frac{T-32}{1.8} + 273.15\right)^{\frac{p_4}{293.15}}}} \right] \quad \text{Eq. (6-5-b)}$$

where

$S_{IDT}$  = IDT strength at age  $t$  months, psi

$E_t$  = IDT modulus at age  $t$  months, psi

$UCS_{28}$  = unconfined compressive strength after 28-day curing at 68°F and 100% RH, psi

$t$  = curing time, months; assuming each month has 30.5 days

$RH$  = curing relative humidity, %

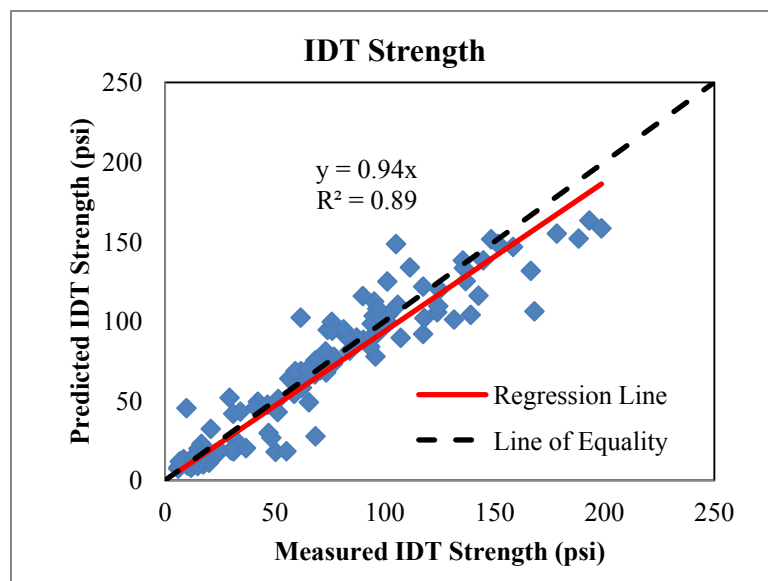
$T$  = temperature, °F

$p_1, p_2, p_3, p_4, p_5$  = regression parameters.

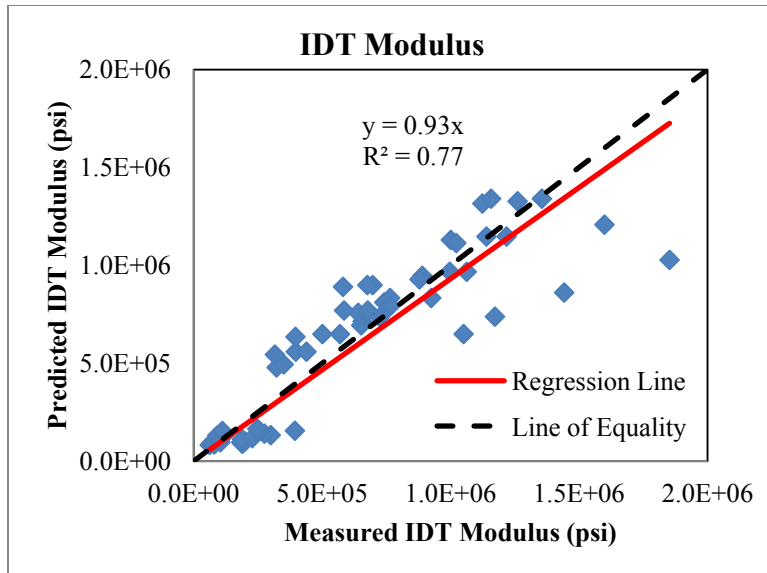
Table 6-1 presents the model parameters. Figure 6-4 presents a comparison of the measured and predicted IDT strength and modulus values.

**Table 6-1. Parameters for IDT Strength/Modulus Model**

Model	Parameter	1	2	3	4	5
<b>IDT strength</b>	$p$	1.59	1.61	-1.50	23.41	0.11
<b>IDT modulus</b>	$q$	1.59	1.61	-0.23	0	1223



(a) IDT Strength



(b) IDT Modulus

**Figure 6-4. Comparison of Measured and Predicted IDT Strength/Modulus Values**

## 6.2 SHRINKAGE STRAIN MODELS

Shrinkage strain is a key parameter in the models developed by both Zhang and Li (2001) and George (1968b). Shrinkage strain primarily consists of drying and thermal shrinkage strain. Currently, there is no drying shrinkage strain for CSL to be developed.

### 6.2.1 Ultimate Drying Shrinkage Strain Model

In this study, ultimate shrinkage models are modified using the lab results of CSM testing, as shown in Eq. (6-6)

$$\varepsilon_{su} = C_1 \cdot [w^{m_1} + m_2] \quad \text{Eq. (6-6)}$$

where

$\varepsilon_{su}$  = ultimate drying shrinkage strain,  $\times 10^{-6}$

$w$  = optimum water content, lb/ft<sup>3</sup>

$C_1$  = binder type factor

0.993 for cement

1.026 for lime

0.366 for C fly ash

$m_1, m_2$  = regression parameters,  $m_1 = 3.17, m_2 = 313.76$ .

Figure 6-5 presents the measured and predicted ultimate drying shrinkage results.

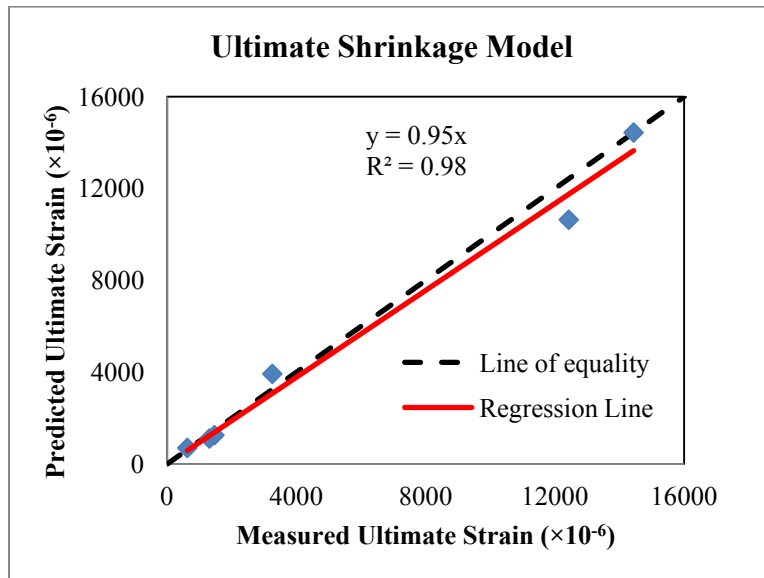


**Figure 6-5 Measured and Predicted Ultimate Drying Shrinkage Results**

### 6.2.2 Gradient Drying Shrinkage Strain Model

The gradient drying shrinkage model was developed based on the measured drying shrinkage strain at four depths from the exposed surface, i.e., 0, 2.25, 4.5 and 6.75 inches, respectively. Two beam specimens were fabricated for this test at room temperature (68°F), a cement-silt specimen was monitored at 65% RH, and a lime-clay specimen was monitored at 40% RH.

The drying shrinkage strain of CSL with moisture gradient is modified based on the MEPDG model for concrete. Eq. (6-7) shows the drying shrinkage strain model at a certain depth from the surface.

$$\varepsilon_g(t) = \varepsilon_{su} \left[ 1 - \left( \frac{RH_c}{100} \right)^{a_6} \right] \quad \text{Eq. (6-7)}$$

where

$\varepsilon_g(t)$  = drying shrinkage strain with moisture gradient at  $t$  days from placement,  $\times 10^{-6}$

$\varepsilon_{su}$  = ultimate drying shrinkage strain,  $\times 10^{-6}$ , which can be estimated from Eq. (6-6)

$RH_c$  = calculated relative humidity, %

where,  $RH_c = RH + (100 - RH)f(t)^{a_5}$

$RH$  = atmospheric relative humidity, %

$f(t) = I/(I+t/b)$

where  $t$  = time since placement in days

$b = a_1(d + a_2)^{a_3}(w/c)^{a_4}$

$d$  = depth from evaporation surface, ft

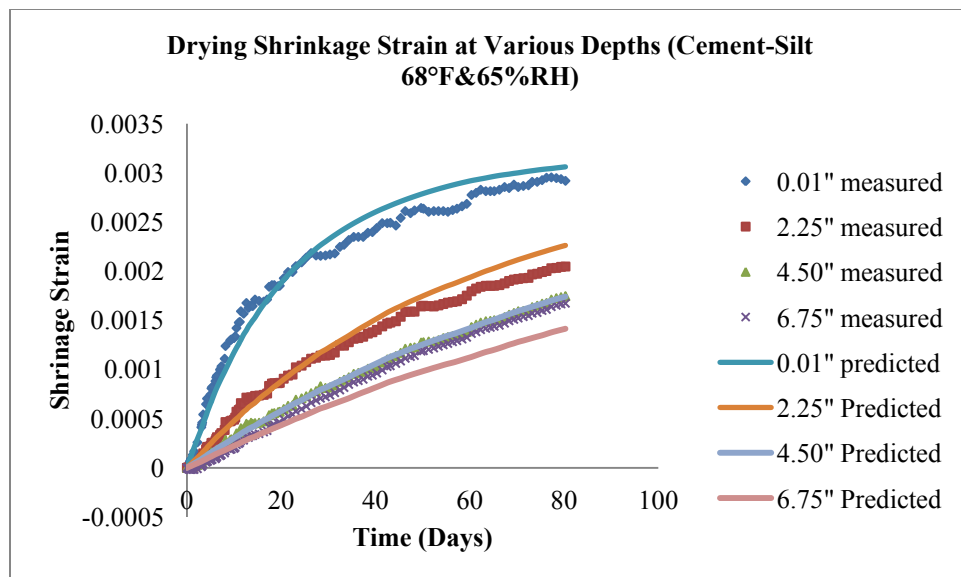
$w/c$  = water/calcium ratio in mass

$a_i$  = parameters,  $i = 1, 2, 3, 4, 5$ , and 6, as shown in Table 6-2.

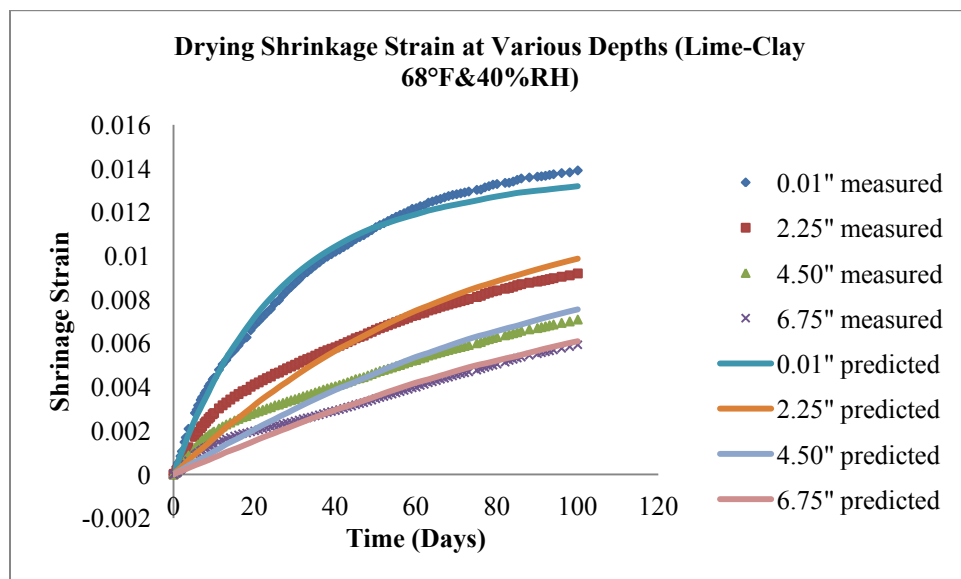
Figure 6-6 presents a comparison between the measured and predicted drying shrinkage strain values at various depths.

**Table 6-2. Parameters for Drying Shrinkage Strain Gradient Model**

$a_1$	$a_2$	$a_3$	$a_4$	$a_5$	$a_6$
1289202	0.085	0.94	1.24	10209.3	4.51



(a) Cement-Silt at 68°F and 65% RH



(b) Lime-Clay at 68°F and 40% RH

**Figure 6-6. Comparison of Measured and Predicted Gradient Drying Shrinkage Strain Values at Various Depths**

### 6.2.3 Thermal Shrinkage Strain Model

The thermal contraction/expansion strain for concrete (ARA 2004) is:

$$\varepsilon_T = \alpha_C \Delta T \quad \text{Eq. (6-8)}$$

where

$$\alpha_C = \text{COTE, } ^\circ\text{F}$$

$$\Delta T = \text{temperature difference, } ^\circ\text{F}$$

### 6.3 SHRINKAGE CRACKING MODELS

Shrinkage cracking is one of the most critical distresses found in CSL and must be considered in a pavement design. Shrinkage cracking often occurs at the early stage of pavement life and significantly affects the performance of the pavement. Shrinkage cracking is not considered in the MEPDG, even though it is the most recognized distress for CSL.

The aforementioned models have been evaluated in terms of the lab shrinkage test results and field data obtained from the literature. The common limitation of the aforementioned cracking models is that they do not consider the effect of moisture gradient and drying shrinkage gradient along the depth of CSL for shrinkage cracking, which could be one of the major causes of cracking in the field. Also, the George model (1968b) does not consider the bond condition between the CSL and sublayer that is used in the Zhang and Li model (2001).

Therefore, a shrinkage cracking model is developed in this study based on the strain gradient formulation developed by Westergaard (1927) for concrete. Given a cementitiously-stabilized slab with constant thickness  $H$ , as shown in Figure 6-7, and given the slab is completely free of bottom restraint, then the loss of moisture from the slab's top surface will result in a moisture gradient, which in turn, causes the shrinkage gradient through the thickness/depth of the CSL. The shrinkage at any depth,  $\varepsilon(y)$ , can be calculated from Eqs. (6-6) and (6-7).

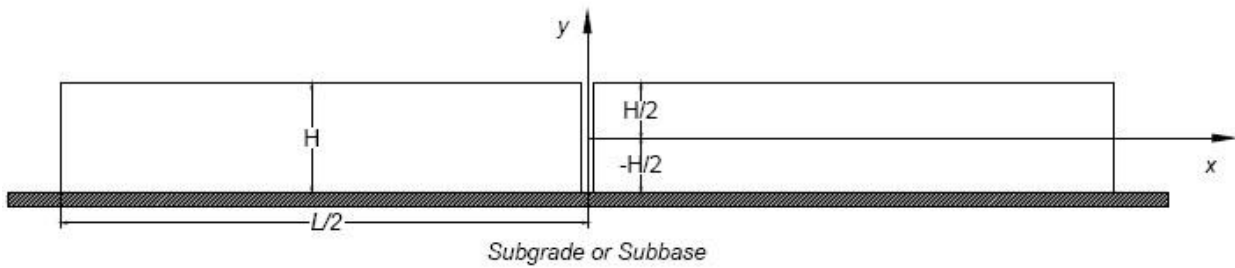


**Figure 6-7. Schematic Diagram of Slab Drying from Top Surface Only**

Then, the tensile stress  $\sigma(y)$  can be expressed by Eq. (6-9), as shown by Westergaard (1927):

$$\sigma(y) = \frac{1}{1-\nu} \left( E_t \cdot \varepsilon(y) - \frac{E_t}{H} \int_{-\frac{H}{2}}^{\frac{H}{2}} \varepsilon(y) dy - \frac{12 \cdot E_t \cdot y}{H^3} \int_{-\frac{H}{2}}^{\frac{H}{2}} \varepsilon(y) y dy \right) \quad \text{Eq. (6-9)}$$

where

$\nu$  = Poisson's ratio, assuming 0.2 for cementitiously-stabilized material

$H$  = thickness of slab, in.

$\varepsilon(y)$  = strain at depth  $y$

$y$  = distance from the half depth of thickness, in.

The restraint from the underlying layer beneath the CSL hinders shrinkage. The restrained stress has a linear relationship with slab slippage, and the slope is the coefficient of friction (Zhang and Li 2001). The boundary conditions include that slippage is at its maximum at the end of the slab and is zero at the center. Thus, the shear stress  $\tau$  can be expressed as Eq. (6-10).

$$\tau = \frac{1}{1-\nu} \cdot \mu \cdot \varepsilon \left( -\frac{H}{2} \right) \cdot x \quad \text{Eq. (6-10)}$$

where

$$\varepsilon \left( -\frac{H}{2} \right) = \text{strain at bottom of the slab}$$

$x$  = distance from the center of slab in horizontal direction, in.

$\mu$  = coefficient of friction, psi/in., equals to  $77.12 \times \text{IDT strength}$ , which is determined in the lab when epoxy is used as bonding agent.

From Eq. (6-10), the restrained force,  $F_{re}$ , can be obtained, as shown in Eq. (6-11).

$$F_{re} = \int_0^L \tau dx = \frac{\mu \cdot \varepsilon \left( -\frac{H}{2} \right) L^2}{1-\nu} \quad \text{Eq. (6-11)}$$

where

$F_{re}$  = restrained force, lbs

$L$  = slab length, in.

From Eqs. (6-9) and (6-11), the stress distribution  $\sigma(y)$  can be obtained by the superposition of stress levels due to the shrinkage gradient and restraint, as shown in Eq. (6-12).

$$\sigma(y) = \frac{1}{1-\nu} \left( E_t \cdot \varepsilon(y) - \frac{E_t}{H} \int_{-\frac{H}{2}}^{\frac{H}{2}} \varepsilon(y) dy - \frac{12 \cdot E_t \cdot y}{H^3} \int_{-\frac{H}{2}}^{\frac{H}{2}} \varepsilon(y) y dy \right) + \frac{F_{re}}{H} \quad \text{Eq. (6-12)}$$

Replace  $\sigma(y)$  with tensile strength  $S_t$ , and reform Eq. (6-12), and the restraint stress  $\sigma_{re}$  can be obtained as Eq. (6-13).

$$\sigma_{re} = \frac{F_{re}}{H} = S_t - \frac{1}{1-\nu} \left( E_t \cdot \varepsilon(y) - \frac{E_t}{H} \int_{-\frac{H}{2}}^{\frac{H}{2}} \varepsilon(y) dy - \frac{12 \cdot E_t \cdot y}{H^3} \int_{-\frac{H}{2}}^{\frac{H}{2}} \varepsilon(y) y dy \right) \quad \text{Eq. (6-13)}$$

Therefore, the crack spacing and crack width can be obtained from Eqs. (6-14) and (6-15).

MATLAB codes in Appendix C were used to calculate the shrinkage cracking models.

$$\text{Crack Spacing} = \frac{L}{2} = \frac{1}{2} \sqrt{\frac{8F_{re}}{\mu \varepsilon \left( -\frac{H}{2} \right)}} \quad \text{Eq. (6-14)}$$

$$\text{Crack Width} = \varepsilon \left( \frac{H}{2} \right) \cdot L - \frac{F_{re} \cdot (1-\nu)}{H \cdot E_t} \cdot L \quad \text{Eq. (6-15)}$$

The mechanism of shrinkage cracking can be expressed by Figure 6-8.

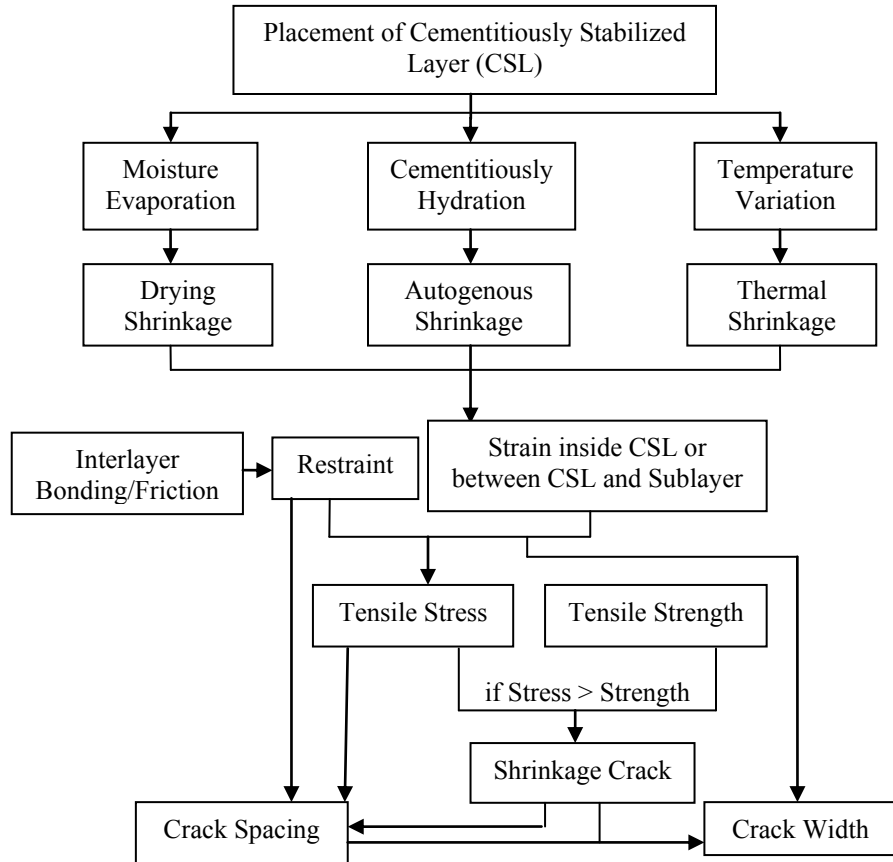
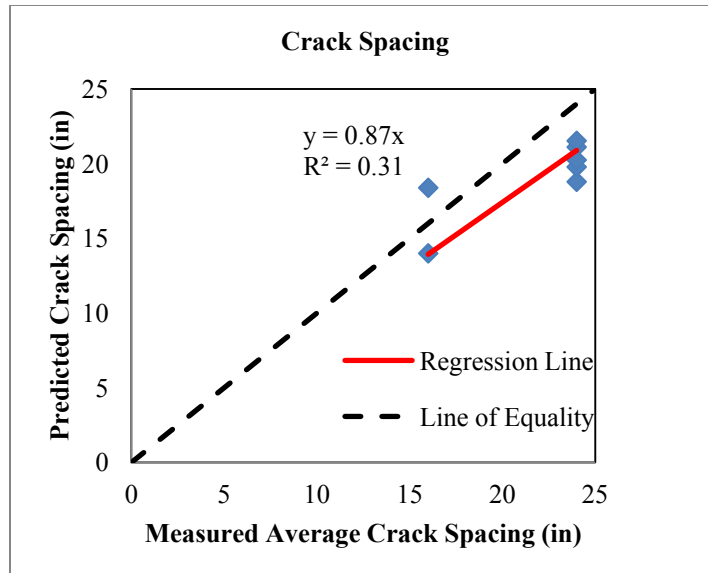
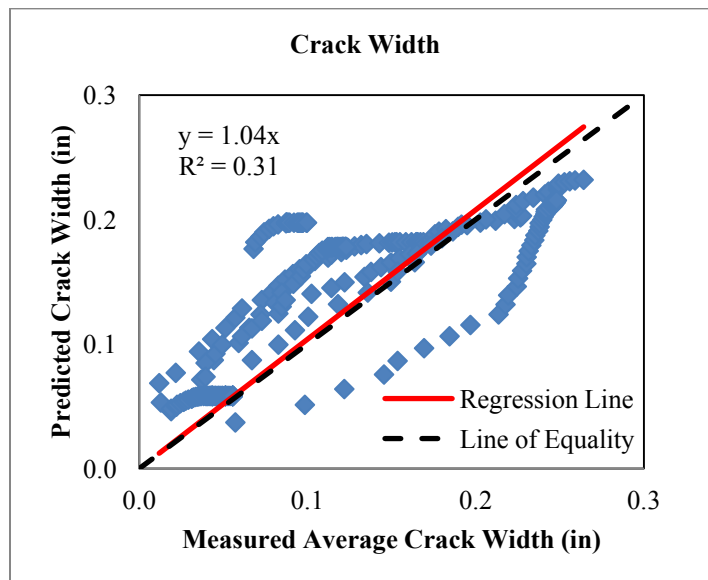


**Figure 6-8. Mechanism of Shrinkage Cracking**

Figure 6-9 presents the comparison of measured and calculated crack spacing and width based on the restrained shrinkage cracking tests in the laboratory, in which the temperature and RH are controlled at constant value. It shows that the mechanical model can predict the crack spacing and width very well in lab conditions, for which  $R^2$  is 0.31 for both spacing and width.



(a) Crack Spacing



(b) Crack Width

**Figure 6-9. Comparison of Measured and Predicted Crack Spacing and Width from Lab Tests**

However, there are limitations to these models, as follows:

(1) The shrinkage strain model was developed based on two materials (cement-silt and lime-clay), at two RH values (65% and 40%), but only at one temperature level (68°F). Temperature is not included in the shrinkage strain model. More tests are necessary for improving the shrinkage strain model based on more materials, more RH values, especially at various temperatures.

(2) Creep compliance is not considered in the shrinkage cracking models. In general, the creep effect has significant influence on the stress and strain distributions at early age. The specimen right after compaction acts as an unbound soil. The bonding between particles gradually forms due to hydration process and the creep effect reduces. The creep effect of CSM shall be studied by conducting creep or relaxation test at various curing ages and conditions, and incorporated into the mechanical models.

#### **6.4 SUMMARY**

The correlations of UCS, IDT strength, and IDT modulus are presented in this chapter. The test results show that the IDT strength is about 0.11 times UCS value, which is consistent with literature findings. IDT modulus can be predicted from IDT strength. A strength growth model was developed to predict UCS and IDT strength based on 28-day strength. The IDT strength and modulus models were developed to predict the IDT strength and modulus at various temperatures and RH values. Ultimate shrinkage model, developed from several materials after long-term monitoring, was developed to estimate shrinkage potential which is an important input for the gradient drying shrinkage strain model. A gradient drying shrinkage strain model was proposed to determine the shrinkage strain at different depths when only the top surface is exposed to air. The shrinkage cracking models in the literature do not consider the moisture

gradient and drying shrinkage gradient along the depth of CSL for shrinkage cracking, and cannot predict shrinkage crack spacing and width with laboratory or field data. Therefore, shrinkage cracking models were developed based on the strain gradient formulation in this study. The new models can predict the shrinkage crack spacing and width in the laboratory, though they can be improved from several aspects.

# CHAPTER SEVEN

## MODEL CALIBRATION WITH FIELD DATA

This chapter introduces the model calibration results using field data found in the literature and from field experiments and the shrinkage cracking models developed with dimensional analysis.

### 7.1 DATA COLLECTION

For the sections used for model calibration, material properties, such as water content, density, CSL thickness, UCS, and the actual local daily average temperature and RH data, were collected. Table 7-1 shows the summary of the field data related to CSL shrinkage cracking. Very limited field data were available for shrinkage cracking in CSL. Therefore, the restrained shrinkage cracking test results in the laboratory also were used for calibrating the shrinkage cracking model. The field data that were used for model development were obtained based on the following procedures.

#### 1) Calculation of Crack Spacing and Width

For some of the field sections, the crack spacing and crack width could be obtained directly. However, for a few sections, only the total crack length is reported. First, it was assumed that there were no longitudinal cracks, only the transverse cracks that extend throughout the whole pavement width. The crack spacing is calculated by Eq. (7-1-a).

$$\text{Crack Spacing} = \frac{\text{section length}}{\frac{\text{total crack length}}{\text{pavement width}}} \quad \text{Eq. (7-1-a)}$$

**Table 7-1. Summary of Literature Data Related to CSL**

Literature	Highway	Section	Host Material	Binder	Underlying Layer
George (2001)	Highway #302 (Mississippi)	Section 1A	A-2-4	cement (5.5%)	lime (4%) treated subgrade
		Section 3A	A-2-4	cement (5.5%)	lime (4%) treated subgrade
		Section 4	A-2-4	cement 3.5% and fly ash 8%	lime (4%) treated subgrade
		Section 6	A-2-4	lime 3% and fly ash 12%	lime (4%) treated subgrade
Gaspard (2002)	LA 89 (Louisiana)	Section 1	A-4	cement (9%)	natural silt
		Section 4	A-4	cement (5%)	natural silt
		Section 9	A-4	cement (9%)	natural silt
Sebesta and Scullion (2004), Sebesta (2005b)	TAMU Campus (Texas)	4% dry cure	marginal river gravel	cement (4%)	natural gravel
		4% prime cure	marginal river gravel	cement (4%)	natural gravel
		4% moisture cure	marginal river gravel	cement (4%)	natural gravel
		8% dry cure	marginal river gravel	cement (8%)	natural gravel
		8% prime cure	marginal river gravel	cement (8%)	natural gravel
		8% moisture cure	marginal river gravel	cement (8%)	natural gravel
Monlux (Unpublished)	Highway #143 (Montana)	Section 2001	A-4	cement 8.7%	natural silt

If the crack spacing is smaller than the pavement width, longitudinal cracking is likely to occur, and block (square) cracking is the cracking pattern. The crack spacing is calculated using Eq. (7-1-b).

$$\text{Crack Spacing} = \frac{\text{section length}}{\frac{\text{total crack length}}{2 \cdot \text{pavement width}}} \quad \text{Eq. (7-1-b)}$$

The crack width is obtained from Eq. (7-2).

$$\text{Crack Width} = \frac{\sum_i^n \text{average crack width of } i^{\text{th}} \text{ group} \times \text{crack length of } i^{\text{th}} \text{ group}}{\text{total crack length}} \quad \text{Eq. (7-2)}$$

where

$n$  = total number of groups.

For those sections for which the number of cracks is reported, the average crack spacing is calculated using Eq. (7-3).

$$\text{Crack Spacing} = \frac{\text{section length}}{\text{No of crack}} \quad \text{Eq. (7-3)}$$

## 2) Coefficient of Friction

After the placement of CSL in the field, the bond between the CSL and underlying material is typically strong, such that bond failure often happens in the weak material that lies between the CSL and underlying materials (Romanoschi and Metcalf 2001). Thus, the Level I input for the coefficient of friction is based on the direct shear strength test results for those weak materials between the CSM and underlying material. For the Level 2 input, the coefficient of friction can be predicted from the IDT strength, as shown in Figure 3-24. Zhang and Li (2001) provide typical coefficient of friction values for the various materials in an underlying layer, as shown in Table 7-2; these values are used in this study.

**Table 7-2. Typical Coefficient of Friction Values (Zhang and Li 2001)**

<b>Material in Underlying Layer</b>	<b>Coefficient of Friction (psi/in.)</b>
Cement Stabilized	13415
Granular	169
Lime Treated Clay	146
Clay	22

### 3) Age of CSL

The age of the CSL is determined as the number of days between the construction date and the date when shrinkage cracking in the field was measured.

### 4) Material Properties of CSL

Density, water content, binder content, and CSL thickness data were obtained from literature. The calcium contents by mass for cement, lime, C fly ash, and F fly ash are assumed to be 63%, 90%, 27% and 2.7%, respectively (Ramme and Tharaniyil 2004).

The 28-day UCS values in the field were obtained from most of the literature references directly. However, in the case that only 7-day UCS values for the lab were provided, the 28-day UCS values were predicted based on the growth model, as shown in Eq. (6-4). The COTE of CSM is not available in the literature and is assumed based on the COTE of the CSM used in this study.

### 5) Daily Climate Information

Daily climate information was collected from <http://www.wunderground.com/history/> and includes the daily maximum temperature, minimum temperature, and average RH.

### 6) Prediction of IDT Strength and Modulus Growth

The cumulative IDT strength/modulus growth is determined using the growth model presented in Eq. (6-5) and the daily temperature and RH. The MATLAB codes in Appendix C are used to calculate the cumulative IDT strength/modulus with daily climate information.

## 7) Prediction of Ultimate Shrinkage Strain and Shrinkage Strain on Top of CSL

Ultimate shrinkage is determined based on Eq. (6-6). The cumulative shrinkage strain of the top CSL is obtained based on Eq. (6-7) on a daily basis. The MATLAB codes in Appendix C are used to calculate the shrinkage strain with daily climate information.

### 7.2 CALIBRATION PROCEDURES

Different mechanistic models of shrinkage cracking were evaluated without success. Chapter 6 presents the detailed evaluation results. Therefore, dimensional analysis (Palmer 2007) was conducted to develop shrinkage cracking and width models, based on the data collected. The fundamental dimensions, including dry density ( $\rho$ ), thickness of CSL ( $H$ ), age ( $t$ ), COTE, ultimate drying shrinkage ( $\epsilon_{ult}$ ), and IDT strength ( $S_{IDT}$ ), and the other properties or factors expressed by the fundamental dimensions, were used to form dimensionless groups.,

### 7.3 CALIBRATION RESULTS

It is found that no existing, modified, or new mechanistic models developed were found to be able to predict field shrinkage crack spacing and width, which might be due to the differences between lab and field conditions. These differences include the following two aspects:

(1) The environmental conditions in the field are not constant. The temperature and RH values change all the time. In addition, the wind and sunshine can accelerate the moisture evaporation. The CSL lose moisture not only from top surface, but also from the bottom also. On the other hand, precipitation can infiltrate into the CSL. Therefore, the field shrinkage is much more complicated than the laboratory conditions. It is necessary to improve the shrinkage strain model with field collected data.

(2) The restraint conditions are different between the field and the laboratory. In the laboratory, the epoxy creates stronger bond condition than the interlayer friction in field. In addition, the CSL in field is much longer than the laboratory beam. The restraint in the field can be from the CSL itself horizontally.

Thus, the shrinkage crack spacing and width models for the CSL were developed based on dimensional analysis. Because the fine host material and coarse host material show different shrinkage cracking behaviors (Kodikara and Chakrabarti 2001), the calibration was carried out for both fine host material and coarse host material, as shown in Eqs. (7-4) and (7-5), respectively. Figures 7-1 and 7-2 show comparisons of the predicted and measured shrinkage crack spacing in the CSL for the stabilized fine and coarse soils, respectively. Figures 7-3 and 7-4 show the predicted and measured shrinkage crack widths for the CSL for the stabilized fine and coarse soils, respectively. Tables 7-3 and 7-4 present the model parameters for crack spacing and crack width for stabilized fine and coarse materials, respectively.

$$\log \left( \frac{L}{H} \right) = \left[ \left( \frac{\mu}{\rho \cdot H \cdot t^{-2}} \right)^{l_1} \cdot (c\%)^{l_2} \cdot \left( \frac{\omega}{\rho} \right)^{l_3} \cdot (\Delta T \cdot COTE)^{l_4} \cdot \left( \frac{UCS_{28}}{\rho \cdot H^2 \cdot t^{-2}} \right)^{l_5} \cdot (RH\%)^{l_6} \cdot \left( \frac{\varepsilon_{top}}{\varepsilon_{ult}} \right)^{l_7} \cdot \left( \frac{\varepsilon_{top} \cdot E_t}{S_{IDT}} \right)^{l_8} \right] \cdot l_9 \quad \text{Eq. (7-4)}$$

$$W = \left[ \left( \frac{\mu}{\rho \cdot H \cdot t^{-2}} \right)^{w_1} \cdot (c\%)^{w_2} \cdot \left( \frac{\omega}{\rho} \right)^{w_3} \cdot (\Delta T \cdot COTE)^{w_4} \cdot \left( \frac{UCS_{28}}{\rho \cdot H^2 \cdot t^{-2}} \right)^{w_5} \cdot (RH\%)^{w_6} \cdot \left( \frac{\varepsilon_{top}}{\varepsilon_{ult}} \right)^{w_7} \cdot \left( \frac{\varepsilon_{top} \cdot E_t}{S_{IDT}} \right)^{w_8} \right] \cdot w_9 \quad \text{Eq. (7-5)}$$

where

$L$  = crack spacing, in.

$W$  = crack width, in.

$H$  = thickness of CSL layer, in.

$\mu$  = coefficient of friction, psi/in., lab from Figure 3-23, field from Table 4-3

$\rho$  = dry density, lb/ft<sup>3</sup>

$t$  = age when crack survey conducted, days

$c\%$  = calcium content, %

$\omega$  = water content, lb/ft<sup>3</sup>

$\Delta T$  = average daily maximum temperature variation, °F

$COTE$  = coefficient of thermal expansion, /°F, from Table 3-8

$UCS_{28}$  = 28-day UCS at 68°F and 100% RH

$RH$  = average atmosphere relative humidity, %

$\varepsilon_{ult}$  = ultimate drying shrinkage, calculated by Eq. (6-5)

$\varepsilon_{top}$  = shrinkage on the top surface, step-by-step calculated by Eq. (6-6) with daily environmental conditions

$S_{IDT}$  = IDT strength, calculated by Eq. (6-4-a), psi

$E_t$  = IDT modulus, calculated by Eq. (6-4-b), psi

$l_i$  = regression parameters for crack spacing model, i = 1, 2, 3, 4, 5, 6, 7, 8, and 9

$w_i$  = regression parameters for crack width model, i = 1, 2, 3, 4, 5, 6, 7, 8, and 9.

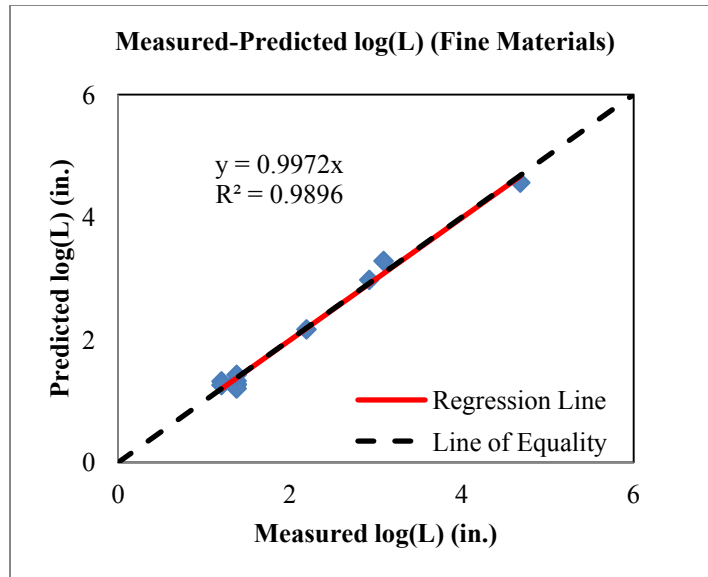


**Figure 7-1. Comparison of Predicted and Measured CSL Shrinkage Crack Spacing for Stabilized Fine Materials**

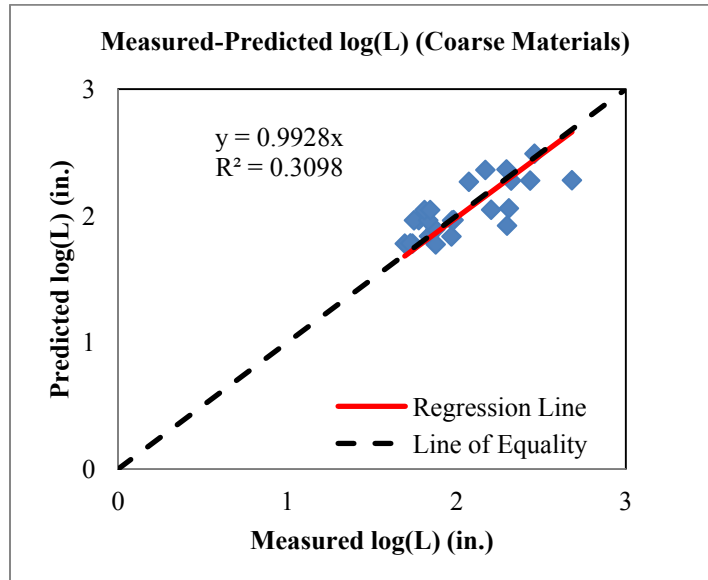


**Figure 7-2. Comparison of Predicted and Measured CSL Shrinkage Crack Spacing for Stabilized Coarse Materials**

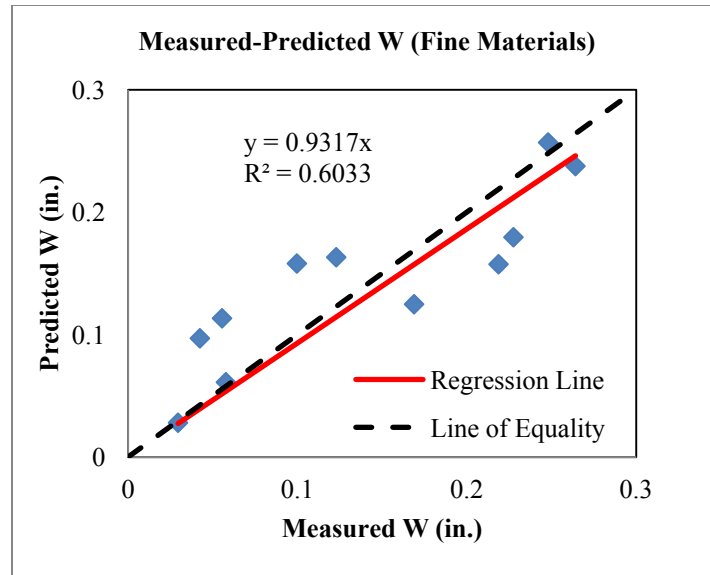


**Figure 7-3. Comparison of Predicted and Measured CSL Shrinkage Crack Widths for Stabilized Fine Materials**

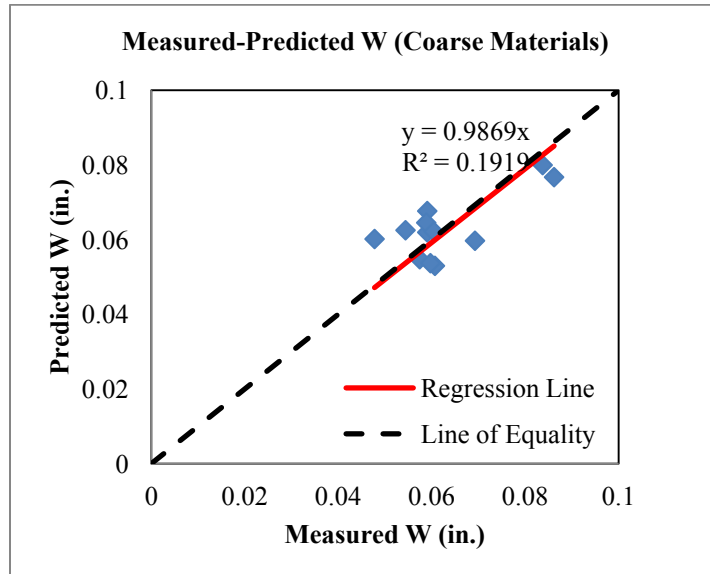


**Figure 7-4. Comparison of Predicted and Measured CSL Shrinkage Crack Widths for Stabilized Coarse Materials**

**Table 7-3. Field-Calibrated Parameters of CSL Shrinkage Crack Spacing Model for Fine and Coarse Host Materials**

Parameters	Fine Materials	Parameters	Coarse Materials
$l_1 (<0)$	-1.19E-01	$l_1 (<0)$	0
$l_2 (>0)$	5.98E-01	$l_2 (<0)$	-1.39E-01
$l_3 (<0)$	-7.78E-01	$l_3 (<0)$	-1.36E-04
$l_4 (<0)$	0	$l_4 (<0)$	0
$l_5 (>0)$	0	$l_5 (<0)$	-1.46E-01
$l_6 (>0)$	0	$l_6 (>0)$	2.11E+00
$l_7 (<0)$	-2.20E-03	$l_7 (<0)$	0
$l_8 (<0)$	-2.53E-01	$l_8 (<0)$	0
$l_9$	8.74E+00	$l_9$	3.85E+00

( ) contains the parameter constraints.

**Table 7-4. Field-Calibrated Parameters of CSL Shrinkage Crack Width Model for Fine and Coarse Host Materials**

Parameters	Fine Materials	Parameters	Coarse Materials
$w_1 (>0)$	7.81E-03	$w_1 (>0)$	0
$w_2 (<0)$	-1.20E+00	$w_2 (>0)$	0
$w_3 (>0)$	7.67E-01	$w_3 (>0)$	1.34E+00
$w_4 (>0)$	0	$w_4 (>0)$	1.76E-05
$w_5 (<0)$	0	$w_5 (>0)$	3.63E-02
$w_6 (<0)$	0	$w_6 (<0)$	0
$w_7 (>0)$	6.69E-01	$w_7 (>0)$	0
$w_8 (>0)$	4.71E-01	$w_8 (>0)$	5.36E-02
$w_9$	8.63E-04	$w_9$	1.78E-01

( ) contains the parameter constraints.

#### 7.4 APPRAISAL OF SHRINKAGE CRACKING MODELS

The shrinkage cracking models are appraised for three different materials (cement-clay, cement-silt and cement-gravel) and constant environmental conditions (68°F and 90% RH). The underlying layer under the CSL is clay with a coefficient of friction of 21.8 psi/in. Table 7-5 presents the material properties.

**Table 7-5. Input for Simulation of Shrinkage Cracking Model**

	Cement-Clay	Cement-Silt	Cement-Gravel
$\mu$ (psi/in.)	21.8	21.8	21.8
cement content (%)	12.0	8.0	3.0
c%	7.6	5.0	1.9
$\omega$ (lb/ft <sup>3</sup> )	18.6	13.3	8.7
$\gamma$ (pcf)	103.2	119.9	140.1
H (in.)	4.0	4.0	4.0
UCS <sub>28</sub>	607.3	905.4	823.9
Ave Temp (°F)	68.0	68.0	68.0
$\Delta T$ (°F)	1.0	1.0	1.0
RH (%)	90.0	90.0	90.0
COTE ( $\times 10^{-6}$ /°F)	12.6	9.3	8.5

Figures 7-5 and 7-6 present the appraisal results. The crack spacing and crack width are predicted for five years. The figures show that both crack spacing and crack width stabilize after two years. It is noted that in the field, reflective cracking could continue to develop in the asphalt layer after two years. The cement-silt has relatively large crack spacing compared to that of cement-clay and cement-gravel, as shown in Figure 7-5. Figure 7-6 shows that the crack widths of the stabilized fine material are larger than those of the stabilized coarse material. Overall, the characteristics of the host materials directly affect the shrinkage behavior of the CSL, and the fine material exhibits more severe shrinkage crack distress than the coarse material.

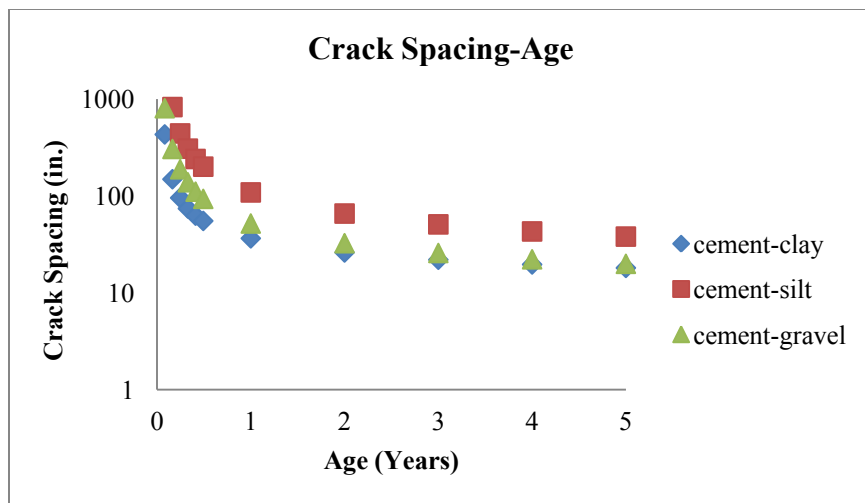


**Figure 7-5. Predicted Crack Spacing of Three Materials**

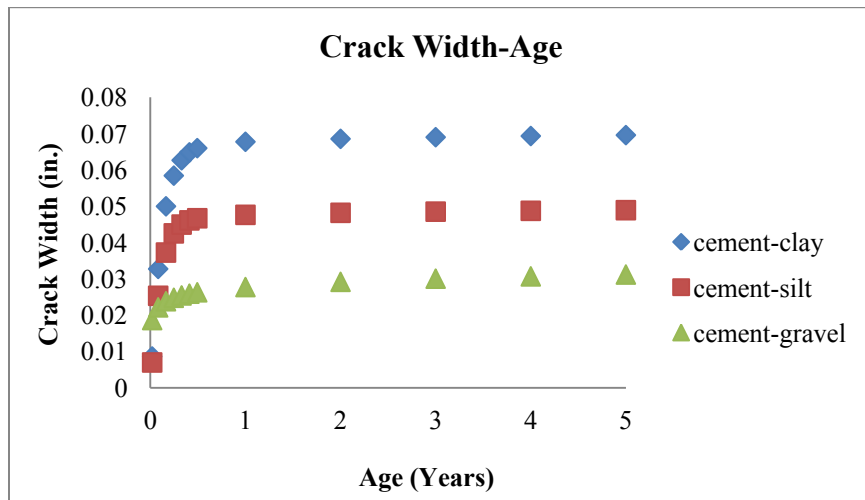


**Figure 7-6. Predicted Crack Widths of Three Materials**

## 7.5 SUMMARY

Field data, collected in the literature and/or from field experiments, include crack length, number of cracks, or crack map, age of CSL, density, water content, binder content, and CSL thickness, UCS of CSL, and daily climate information. The crack spacing and width are calculated or measured from crack length, number of cracks, or crack map. The tensile strength

and stiffness are predicted from the IDT strength and modulus growth models. The ultimate shrinkage strain and shrinkage strain on top of CSL are estimated from the material properties based on the developed shrinkage strain models, which are introduced in Section 6.2. The mechanical shrinkage cracking model developed was found not effective in predicting the field shrinkage cracking. Instead, a dimensional analysis was used to develop shrinkage cracking model, based on the field data. The development was carried out for fine host material and coarse host material, respectively. The developed shrinkage cracking models can predict both laboratory and field data very well. The shrinkage cracking models are appraised for three different materials (cement-clay, cement-silt and cement-gravel) and constant environmental conditions (68°F and 90% RH). The crack spacing and crack width are predicted for five years. Overall, the characteristics of the host materials directly affect the shrinkage behavior of the CSL, and the fine material exhibits more severe shrinkage crack distress than the coarse material.

# CHAPTER EIGHT

## CONCLUSIONS AND RECOMMENDATIONS

### 8.1 CONCLUSIONS

The objective of this research is to recommend shrinkage cracking-related procedures for characterizing CSL for use in pavement design and analysis and incorporation into the MEPDG. This research addresses material properties and related test methods that can be used to predict shrinkage cracking of CSL. This research is concerned with subgrade, subbase, and/or base materials that have been stabilized with hydraulic cement, fly ash, lime, or combinations thereof and used in pavements.

The overall contributions of this research are the evaluations and recommendations of several test procedures that can identify the CSM properties linked to shrinkage cracking, and the development of shrinkage cracking models to predict field cracking issues due to CSL shrinkage. The detailed conclusions of the study are as follows:

(1) Based on the literature review and state agency survey results, block cracking and transverse cracking are the most severe distresses for pavements with CSL which are due to the shrinkage cracking of CSL. When the tensile stress due to shrinkage is beyond the tensile strength, shrinkage cracking occurs. The properties of CSL that can influence shrinkage cracking include the shrinkage of CSL, strength and stiffness of CSL, and the bonding condition between CSL and sublayer. Only limited models are available for the CSL shrinkage and cracking.

(2) The test procedures for characterizing material properties related to shrinkage cracking were appraised in terms of their performance predictability, precision, accuracy, practicality, cost, and other pertinent factors. UCS, IDT strength and modulus tests are considered suitable for

strength and stiffness tests of CSM. A suite of shrinkage-related tests is evaluated. Free drying shrinkage, free autogenous shrinkage, and COTE tests are recommended to identify the shrinkage properties of CSM. Free gradient drying shrinkage test was designed and recommended to simulate the loss of moisture in field condition. Restrained beam specimen with sealed sides is recommended to induce shrinkage cracking for model development. By artificially creating a high level of bond, shrinkage cracking can be generated in a lab specimen for model development. The interface friction/bond can be measured by bond strength or direct shear test.

(3) Tests related to shrinkage cracking were developed, including COTE, ultimate drying shrinkage, gradient drying shrinkage, restrained shrinkage cracking, and coefficient of friction tests. These tests were conducted at various temperature and/or RH values. To simulate the field pavement conditions, the beams were side-sealed as in the gradient drying shrinkage strain test. These results are used to develop shrinkage cracking models.

(4) The newly developed strength growth model was developed to predict UCS and IDT strength based on 28-day strength. The IDT strength and modulus models were developed to predict the IDT strength and modulus at various temperature and RH values. The ultimate shrinkage model was developed to estimate shrinkage potential which is an important input for the gradient drying shrinkage strain model. The gradient drying shrinkage strain model can determine the shrinkage strain at different depths when only the top surface loses moisture. The shrinkage cracking model was developed in this study based on the strain gradient formulation. The new models can predict the shrinkage crack spacing and width in lab, though they have several limitations.

(5) No existing, modified, or new models were found to be able to predict shrinkage crack spacing and width with field collected data, which might be due to the big differences between lab and field conditions. Dimensional analysis was conducted to develop shrinkage cracking and width models based on field and laboratory data. The calibration was carried out for both fine and coarse host materials, respectively. The developed empirical shrinkage cracking models can predict both laboratory and field data reasonably well. The appraisal of the shrinkage cracking model indicates that the characteristics of the host materials directly affect the shrinkage behavior of the CSL, and the fine material exhibits more severe shrinkage crack distress than the coarse material.

### **8.1.1 Models Recommended for the MEPDG**

The shrinkage cracking models that are recommended for inclusion in the MEPDG are summarized in Table 8-1.

### **8.1.2 Material Inputs**

Table 8-2 presents the three levels of design input to the MEPDG; these inputs include:

1. Level 1: site- and/or material-specific inputs for the project obtained through direct testing or measurements.
2. Level 2: the use of correlations to establish or determine the required inputs.
3. Level 3: the use of national or regional default values to define the inputs. Laboratory UCS after 28-day curing at room temperature and 100% RH were collected from extensive literature review. The range and typical values of IDT strength and modulus were predicted from the UCS values based on the Level 2 correlations, as shown in Table 8-2.

**Table 8-1: Models Recommended for MEPDG**

Type	Model	Equation	Parameter	Fine	Coarse	Level 1 Material Property
Shrinkage Crack Spacing in CSL	$\log\left(\frac{L}{H}\right) = \left[ \left( \frac{\mu}{\rho \cdot H \cdot t^{-2}} \right)^{l_1} \cdot (c\%)^{l_2} \cdot \left( \frac{\omega}{\rho} \right)^{l_3} \cdot (\Delta T \cdot COTE)^{l_4} \right. \\ \cdot \left( \frac{UCS_{28}}{\rho \cdot H^2 \cdot t^{-2}} \right)^{l_5} \cdot (RH\%)^{l_6} \cdot \left( \frac{\varepsilon_{top}}{\varepsilon_{ult}} \right)^{l_7} \\ \cdot \left( \frac{\varepsilon_{top} \cdot E_t}{S_{DT}} \right)^{l_8} \left. \right] \cdot l_9$	$l_1$	-1.19E-01	0		
		$l_2$	5.98E-01	-1.39E-01		
		$l_3$	-7.78E-01	-1.36E-04		
		$l_4$	0	0		
		$l_5$	0	-1.46E-01		
		$l_6$	0	2.11E+00		
		$l_7$	-2.20E-03	0		• Calcium content
		$l_8$	-2.53E-01	0		• Water content
		$l_9$	8.74E+00	3.85E+00		• Maximum dry density
Shrinkage Crack	$W = \left[ \left( \frac{\mu}{\rho \cdot H \cdot t^{-2}} \right)^{w_1} \cdot (c\%)^{w_2} \cdot \left( \frac{\omega}{\rho} \right)^{w_3} \cdot (\Delta T \cdot COTE)^{w_4} \right. \\ \cdot \left( \frac{UCS_{28}}{\rho \cdot H^2 \cdot t^{-2}} \right)^{w_5} \cdot (RH\%)^{w_6} \cdot \left( \frac{\varepsilon_{top}}{\varepsilon_{ult}} \right)^{w_7} \\ \cdot \left( \frac{\varepsilon_{top} \cdot E_t}{S_{DT}} \right)^{w_8} \left. \right] \cdot w_9$	$w_1$	7.81E-03	0		• 28-day UCS
		$w_2$	-1.20E+00	0		• COTE
		$w_3$	7.67E-01	1.34E+00		
		$w_4$	0	1.76E-05		
		$w_5$	0	3.63E-02		
		$w_6$	0	0		
		$w_7$	6.69E-01	0		
		$w_8$	4.71E-01	5.36E-02		
		$w_9$	8.63E-04	1.78E-01		

**Table 8-2. Three Levels of Input for MEPDG**

	<b>Level 1</b>	<b>Level 2</b>	<b>Level 3 (28-day curing at 68°F and 100% RH)</b>	
<b>Material Properties</b>	<b>Recommended Test Procedure</b>	<b>Recommended Relationship</b>	<b>Range</b>	<b>Typical Value</b>
<b>UCS</b>	Test protocol depends on binder and host material type (see Note below*).	Same to Level 1 input.		Table 8-3
<b>IDT Strength</b>	Test protocol is recommended in this research.	$S_{IDT} = 0.11 \times UCS$ where $S_{IDT}$ = IDT strength, psi $UCS$ = unconfined compressive strength, psi.		Table 8-4
<b>IDT Modulus</b>	Test protocol is recommended in this research.	$E_t = 7980.1 \times S_{IDT}$ $E_t = 910.5 \times UCS$ where $E_t$ = IDT modulus, psi $S_{IDT}$ = IDT strength, psi $UCS$ = unconfined compressive strength, psi		Table 8-5
<b>Coefficient of Thermal Expansion</b>	Test protocol is recommended in this research.	Not available	2 to 50 ( $10^{-6}/^{\circ}\text{F}$ ) Clay 25.4 ( $10^{-6}/^{\circ}\text{F}$ ) Silt 9.4 ( $10^{-6}/^{\circ}\text{F}$ ) Gravel 8.5 ( $10^{-6}/^{\circ}\text{F}$ )	
<b>Coefficient of Friction</b>	Test protocol is recommended in this research.	$\mu = 156.48 \times S_{IDT}$ where $\mu$ = coefficient of friction, psi/in. $S_{IDT}$ = IDT strength, psi	22 to 14000 (psi/in.) Cement-stabilized, 13415 psi/in. Granular, 169 psi/in. Lime-treated clay, 146 psi/in. Clay, 22 psi/in.	Table 8-3

\*Note:

- (1) For cement-stabilized fine-grained materials (clay, silt and sand), UCS was tested in accordance with ASTM D1633, *Standard Test Methods for Compressive Strength of Molded Soil-Cement Cylinders*.
- (2) For cement-stabilized granular materials, UCS was tested in accordance with AASHTO T22, *Standard Method of Test for Compressive Strength of Cylindrical Concrete Specimens*.
- (3) For lime-stabilized clay, UCS was tested in accordance with ASTM D5102, *Standard Test Method for Unconfined Compressive Strength of Compacted Soil-Lime Mixtures*.
- (4) For fly ash-stabilized soils, UCS was tested in accordance with ASTM C593, *Standard Specification for Fly Ash and Other Pozzolans for Use with Lime for Soil Stabilization*.

**Table 8-3. Level 3 Input of UCS (psi)**

Binder	Values	Host Materials				
		Clay	Silt	Sand	Gravel	Recycled Materials
Cement	Range	40 ~ 1015	88 ~ 900	80 ~ 843	392 ~ 1296	30 ~ 1088
	Typical	263	363	350	763	653
Lime	Range	19 ~ 522	78 ~ 510	Not applicable	64 ~ 91	Not applicable
	Typical	150	158		78	
C fly ash	Range	19 ~ 668	39 ~ 268	31 ~ 693	59 ~ 305	Not applicable
	Typical	181	115	174	214	
Lime and F fly ash	Range	Not applicable	150 ~ 190	Not applicable	Not applicable	120 ~ 200
	Typical		170			190

**Table 8-4. Level 3 Input of IDT Strength (psi)**

Binder	Values	Host Materials				
		Clay	Silt	Sand	Gravel	Recycled Materials
Cement	Range	5 ~ 116	10 ~ 103	9 ~ 96	45 ~ 148	3 ~ 124
	Typical	30	41	40	87	74
Lime	Range	2 ~ 60	9 ~ 58	Not applicable	7 ~ 10	Not applicable
	Typical	17	18		9	
C fly ash	Range	2 ~ 76	4 ~ 31	4 ~ 79	7 ~ 35	Not applicable
	Typical	21	13	20	24	
Lime and F fly ash	Range	Not applicable	17 ~ 22	Not applicable	Not applicable	14 ~ 23
	Typical		19			22

**Table 8-5. Level 3 Input of IDT Modulus (ksi)**

Binder	Values	Host Materials				
		Clay	Silt	Sand	Gravel	Recycled Materials
Cement	Range	36 ~ 924	81 ~ 819	73 ~ 768	357 ~ 1180	27 ~ 990
	Typical	239	330	319	695	594
Lime	Range	17 ~ 475	71 ~ 464	Not applicable	58 ~ 83	Not applicable
	Typical	137	144		71	
C fly ash	Range	17 ~ 608	36 ~ 244	28 ~ 631	54 ~ 277	Not applicable
	Typical	165	104	158	195	
Lime and F fly ash	Range	Not applicable	137 ~ 173	Not applicable	Not applicable	109 ~ 182
	Typical		155			173

## **8.2 RECOMMENDATIONS**

### **8.2.1 Further Validation of Models**

The recommended models presented in Table 8-1 are calibrated based on limited data. It is necessary to validate these models using local field data.

### **8.2.2 Reflective Cracking Model**

This study developed shrinkage cracking and width models for CSL. However, a reflective cracking model is needed to determine the reflective cracking in the asphalt layer. The NCHRP 1-41 project has developed reflective cracking models for different scenarios, such as asphalt overlay on existing asphalt pavement and asphalt overlay on existing concrete pavement. However, the case of asphalt on CSL is not available. A reflective cracking model for asphalt layers on CSL with shrinkage cracking needs to be developed.

## REFERENCES

- Applied Research Associates, Inc. 2004. *Guide for Mechanistic-Empirical Design for New and Rehabilitated Pavement Structures*. NCHRP 1-37A Final Report, National Cooperative Highway Research Program, Transportation Research Board, National Research Council (March).
- ACI. *Guide for Modeling and Calculating Shrinkage and Creep in Hardened Concrete*. ACI 209.2R-08.
- Arora, S. and A. H. Aydilek. 2005. Class F Fly-Ash-Amended Soils as Highway Base Material. *Journal of Materials in Civil Engineering* 17 (6) (November): 640-649.
- Ashtiani, R. S., D. N. Little, E. Masad. 2007. Evaluation of the Impact of Fines on the Performance of Lightly Cement-Stabilized Aggregate Systems. *Journal of the Transportation Research Board* 2026: 81–88.
- Atkinson, D. J. 1990. *Evaluation of Rehabilitation Measures for Cracked Cement Treated Pavements*. Main Road Department 6, Queensland, Australia.
- Austroads. 2008. *Guide to Pavement Technology: Part 2: Pavement Structural Design*.
- Barstis, W. F. and A. B. Crawley. 2000. *The Use of Fly Ash in Highway Construction U.S. 84/98 Adams County*. Final Report No. 84-DP59-MS-05, Federal Highway Administration (May).
- Bhattacharja, S. and J. Bhatty. 2003. *Comparative Performance of Portland Cement and Lime in Stabilization of Moderate to High Plasticity Clay Soils*. RD125, Portland Cement Association, Skokie, Illinois, USA, 26 pages,.
- Bofinger, H. E., H. O. Hassan, and R. I. T. Williams. 1978. *The Shrinkage of Fine-Grained Soil-Cement*. TRRL Supplementary Report 398.
- Bonnot, J. 1991. *Semi-rigid Pavements*. Association Internationale Permanente des Congrès de la Route.
- Carteret, R. D., H. Chen, L. Comport, D. Firth, and A. Howard. 2009. *Cost-Effective Structural Treatments for Rural Highways--Cemented Materials*. Interim Report, Austroads Project No: TT1359 (June).
- Cauley, R. P. and T. W. Kennedy. 1972. *Improved Tensile Strength for Cement-Treated Bases and Subbases*. Research Report No. 98-11, The Texas Highway Department (August).

- Chakrabarti, S. and J. Kodikara. 2003. *Basaltic Crushed Rock Stabilized with Cementitious Additives-Compressive Strength and Stiffness, Drying Shrinkage, and Capillary Flow Characteristics*. Eighth International Conference on Low-Volume Roads: 18-26.
- Chakrabarti, S. and J. Kodikara. 2007. Direct Tensile Failure of Cementitiously Stabilized Crushed Rock Materials. *Can. Geotech. J.* 44: 231–240.
- Chen, D. 2007. Field and Lab Investigations of Prematurely Cracking Pavements. *Journal of Performance of Constructed Facilities* (July/August): 293-301.
- Corp of Engineers. 1994. *Soil Stabilization for Pavement*. Department of the Army, the Navy, and the Air force.
- Cusson, D. and T. J. Hoogeveen. 2006. *Measuring Early-Age Coefficient of Thermal Expansion in High-Performance Concrete*. International RILEM Conference on Volume Changes of Hardening Concrete: Testing and Mitigation, Lyngby, Denmark (August 20).
- De Beer, M. 1990. *Aspects of the Design and Behaviour of Road Structures Incorporating Lightly Cementitious Layers*. Ph.D. dissertation, Faculty of Engineering, University of Pretoria, Pretoria (February).
- Departments of the Army and the Air Force. 1994. *Pavement Design for Roads, Streets, and Open Storage Areas, Elastic Layered Method*. Army TM 5-822-13/Air Force AFJMAN 32-1018 (October).
- Foley, G. 2002. *Mix Design for Stabilised Pavement Materials (AP-T16)*. Austroads.
- Freeman, T. and D. Little. 2002. *Maintenance Strategies for Pavements with Chemically Stabilized Layers*. Research Report No. FHWA/TX-01/1722-6, Texas Department of Transportation (March).
- Gaspard, K. J. 2002. *In-Place Cement Stabilized Base Reconstruction Techniques--Interim Report: Construction and Two Year Evaluation*. LTRC Project No. 95-3GT, Louisiana Transportation Research Center (August).
- George, K. P. 1968a. Shrinkage Characteristics of Soil-Cement Mixtures. *Highway Research Record* 255: 42-58.
- George, K. P. 1968b. Cracking In Cement-Treated Bases and Means for Minimizing It. *Highway Research Record* 255: 59-71.
- George, K. P. 1990. Characterization and Structural Design of Cement-Treated Base. *Transportation Research Record* 1288: 78-87.
- George, K. P. 2001. *Soil Stabilization Field Trial--Interim Report*. Interim Report No.

FHWA/MS-DOT-RD-03-133, Mississippi Department of Transportation.

George, K. P. 2002. Minimizing Cracking in Cement-treated Materials for Improved Performance. *Portland Cement Association*.

Gnanendran, C. T. and J. Piratheepan. 2008. Characterisation of a Lightly Stabilised Granular Material by Indirect Diametrical Tensile Testing. *International Journal of Pavement Engineering* 9 (6): 445-456.

Grogan, W. P., C. A. Weiss, and R. S. Rollings. 1999. *Stabilized Base Courses for Advanced Pavement Design--Report 1--Literature Review and Field Performance Data*. Final Report to Project DOT/FAA/AR-97/65, Office of Aviation Research (September).

Guthrie, W. S., S. Sebesta, and T. Scullion. 2001. *Selecting Optimum Cement Contents For Stabilizing Aggregate Base Materials*. Report 7-4920-2, Project 7-4920, Project Title: Improving Long-Term Flexible Pavement Performance, Performed in Cooperation with the Texas Department of Transportation and the Federal Highway Administration, 64 pages (September).

Hall, K. and J. Crovetti. 2007. *Performance of Drained and Undrained Rigid Pavements in the LTPP SPS-2 Experiment*. TRB 2007 Annual Meeting CD-ROM.

Hudson, W. R. and T. W. Kennedy. 1968. *An Indirect Tensile Test for Stabilized Materials*. Research Report No. 98-1, The Texas Highway Department (January).

Iowa Department of Transportation. 2000. *Method of Test for Determining Shearing Strength of Bonded Concrete*. Iowa Test 406-C, Ames, IA.

Jameson, G. 2013. *Review of Definition of Modified Granular Materials and Bound Materials*. Report No. AP-R434-13 for Austroads (May): 21 pages.

Jayawickrama, P. W., W. K. Wray, R. C. Seal, and N. E. Wright. 1998. *Experimental Pavement Reconstruction Project to Determine Long-Term Effectiveness of Lime and Cement for Stabilization of Pavement Subgrade Soils*. Report No. TX-7-2967-F, Texas Department of Transportation (September).

Jung, Y., D. G. Zollinger, M. Won, and A. J. Wimsatt. 2009. *Subbase and Subgrade Performance Investigation for Concrete Pavement*. Technical Report (Texas Transportation Institute), 6037-1.

Kennedy, T. W. and W. R. Hudson. 1973. *Tensile Properties of Subbases for Use in Rigid Pavement Design*. Report No. CFHR 3-8-66-98-14F, Texas Highway Department (February).

Khoury, N. N. 2005. *Durability of Cementitious Stabilized Aggregate Bases for Pavement*

*Application.* Ph.D. dissertation, The University of Oklahoma.

- Kodikara, J. and S. Chakrabarti. 2001. Shrinkage Behaviour of Cemented Materials as Applicable to Insitu Pavement Stabilisation.
- Kota, P.B.V.S., T. Scullion, and D. N. Little. 1995. Investigation of Performance of Heavily Stabilized Bases in Houston, Texas, District. *Transportation Research Record* 1486: 68-76.
- Lim, S. and D. G. Zollinger. 2003. Estimation of the Compressive Strength and Modulus of Elasticity of Cement-Treated Aggregate Base Materials. *Transportation Research Record* 1837: 30-38.
- Little, D. N. 1999. *Evaluation of Structural Properties of Lime Stabilized Soils and Aggregates - Volume 1 Summary of Findings*. The National Lime Association (January 5).
- Little, D. N. and S. Nair. 2007. *Sensitivity of Selected Colorado Soils to Form Ettringite/Thaumasite when Treated with Calcium-Based Stabilizers and when Soluble Sulfates are Available*. Final Report to CDOT-2007-14, Texas Transportation Institute.
- Little, D. N., T. Scullion, P. B. V. S. Kota, and J. Bhuiyan. 1995. *Guidelines for Mixture Design and Thickness Design for Stabilised Bases and Subgrades*. Final Report to FHWA/TX-95/1287-3F, Texas Transportation Institute (October).
- Mallela, J., J. Hall, and K. Smith. 2007. Role of Stabilized and Drainable Bases in Early-Age Cracking on Concrete Airfield Pavements. *Journal of the Transportation Research Board* 2004: 150–162.
- Marais, C. P., E. Otte, and L. A. Bloy. 1973. The Effect of Grading on Lean-Mix Concrete. *Highway Research Record* 441: 86-96.
- Matthews, S. C. *Control of Reflective Cracking*. Cement & Concrete Association of Australia.
- Midgley, L. and R. Yeo. 2008. *The Development and Evaluation of Protocols for the Laboratory Characterisation of Cemented Materials*. Austroads Publication No. AP-T101/08, 89.
- Mokarem, D. W., R. M. Meyerson, and R. E. Weyers. 2003. *Development of Concrete Shrinkage Performance Specifications*. Virginia Transportation Research Council (August).
- Naik, T. R., Y. Chun, R. N. Kraus. 2006. *Investigation of Concrete Properties to Support Implementation of the new AASHTO Pavement Design Guide (Completed)*. Final Report to 0092-06-03, Wisconsin Department of Transportation (November).
- Nakayama, H. and R. L. Handy. 1965. Factors Influencing Shrinkage of Soil-Cement. *Highway*

*Research Record* 86: 15-27.

- National Lime Association. 2006. *Technical Brief: Mixture Design and Testing Procedures for Lime Stabilized Soil* (October).
- Neal, B. F. and J. H. Woodstrom. 1977. *Faulting of Portland Cement Concrete Pavements*. Report to FHWA-CA-TL-5167-77-20, California Department of Transportation (July).
- Norling, L. T. 1973. Minimizing Reflective Cracks in Soil-Cement Pavements: A Status Report of Laboratory Studies and Field Practices. *Highway Research Record* 442: 22-33.
- Nussbaum, P. J. and L. D. Childs. 1975. Repetitive Load Tests of Concrete Slabs on Cement-Treated Subbases. *Portland Cement Association*.
- Otte, E. 1978. *A Structural Design Procedure for Cement-Treated Layers In Pavements*. Ph.D. dissertation, Faculty of Engineering, University of Pretoria.
- Palmer, A. C. 2007. *Dimensional Analysis and Intelligent Experimentation*. World Scientific Publishing Co. Pte. Ltd.
- Portland Cement Association. 1992. *Soil-Cement Laboratory Handbook*.
- Pretorius, P. C., Bruinette, Kruger, Stoffberg, Hugo, and C. L. Monismith. 1972. Fatigue Crack Formation and Propagation in Pavements Containing Soil-cement Bases. *Highway Research Record* 407: 102-150.
- Pretorius, P.C., and C. L. Monismith. 1971. Prediction of Shrinkage Stresses in Pavements Containing Soil-Cement Bases. *Highway Research Record* 362: 63-86.
- Raad, L., C. L. Monismith, and J. K. Mitchell. 1977. Tensile Strength Determinations for Cement-Treated Materials. *Transportation Research Board* 641: 48-52.
- Ramme, B. and M. Tharaniyil. 2004. Coal Combustion Products Utilization Handbook.
- Ramsey, W. J. and O. L. Lund. 1959. *Experimental Lime Stabilization in Nebraska*. Bureau of Public Roads, Hpr-1/6/: 63-104.
- Romanoschi, S. A. and J. B. Metcalf. 2001. Effects of Interface Condition and Horizontal Wheel Loads on the Life of Flexible Pavement Structures. *Transportation Research Board* 1778: 123-131.
- Ruiz, J. M., R. O. Rasmussen, G. P. Chang, J. C. Dick, and P. K. Nelson. 2005. *Computer-Based Guidelines For Concrete Pavements Volume II—Design and Construction Guidelines and HIPERPAV II User's Manual*. Final Report No. FHWA-RD-04-121, Office of Infrastructure Research and Development, Federal Highway Administration (February).

- Scullion, T. 2002. *Field Investigation: Pre-Cracking of Soil-Cement Bases to Reduce Reflection Cracking*. TRB 2002 Annual Meeting CD-ROM.
- Scullion, T. and P. Harris. 1998. Forensic Evaluation of Three Failed Cement-Treated Base Pavements. *Transportation Research Board* 1611: 10-18.
- Scullion, T., S. J. Sebesta, P. Harris, and I. Syed. 2000. *A Balanced Approach to Selecting the Optimal Cement Content for Soil-Cement Bases*. Report 404611-1. Texas Transportation Institute, College Station, Tex.
- Scullion, T., S. Sebesta, J. P. Harris, and I. Syed. 2005. Evaluating the Performance of Soil-Cement and Cement-Modified Soil for Pavements: A Laboratory Investigation. *Portland Cement Association*.
- Sebesta, S. 2005a. Use of Microcracking to Reduce Shrinkage Cracking in Cement-Treated Bases. *Journal of the Transportation Research Board* 1936: 3-11.
- Sebesta, S. 2005b. *Continued Evaluation of Microcracking in Texas*. Report No. FHWA/TX-06/0-4502-2, Texas Department of Transportation (November).
- Sebesta, S. and T. Scullion. 2004. *Effectiveness of Minimizing Reflective Cracking in Cement-Treated Bases by Microcracking*. Technical Report No. FHWA/TX-05/0-4502-1, Texas Transportation Institute (October).
- Selezneva, O., J. Jiang, and S. D. Tayabji. 2000. *Preliminary Evaluation and Analysis of LTPP Faulting Data*. Final Report No. FHWA-RD-00-076 (September).
- Si, Z. 2008. Forensic Investigation of Pavement Premature Failure due to Soil Sulfate-Induced Heave. *Journal of Geotechnical and Geoenvironmental Engineering* (August): 1201-1204.
- Thogersen, F. and L. Bjulf. 2005. *Mechanistic Design of Semi-rigid Pavement: An Incremental Approach*. <http://www.vejdirektoratet.dk/publikationer/VIrap138/index.htm>
- Van Blerk, P. G. and T. Scullion. 1995. *Evaluation of Stabilized Base Durability Using a Modified South African Wheel Tracking Device*. Research Report to TX-96/29/2919-1, Texas Department of Transporation.
- Veisi, M., B. Chittoori, M. Celaya, S. Nazarian, A. J. Puppala, and C. Solis. 2010. *Accelerated Stabilization Design of Subgrade Soils*. Research Report No. TX FHWA/TX 06/0-5569-1 (February).
- Von Quintus, H. L., J. Mallela, and J. Jiang. 2005. *Expected Service Life and Performance Characteristics of HMA Pavements in LTPP*. Asphalt Pavement Alliance (February).
- Wang, M. and M. T. Huston. 1972. Direct-Tensile Stress and Strain of a Cement-Stabilized Soil.

*Highway Research Record* 379, Cement-stabilized Soil, Highway Research Board.

Weiss, W. J., W. Yang, and S. P. Shah. 1998. Shrinkage Cracking of Restrained Concrete Slabs. *Journal of Engineering Mechanics* 124 (7) (July): 765-774.

Wen, H. and R. Y. Kim. 2002. Simple Performance Test for Fatigue Cracking and Validation with WesTrack Mixtures. *Transportation Research Record* 1789: 66-72.

Wesovich, J., B. F. McCullough, and N. H. Burns. 1987. *Stabilized Subbase Friction Study for Concrete Pavements*. Research Report University of Texas at Austin. Center for Transportation Research, No. 459-1.

Westergaard, H. M. 1927. Analysis of Stresses in Concrete Pavements due to Variations of Temperature. *Highway Research Record* 6: 201-215.

White, D. J., D. Harrington, and Z. Thomas. 2005. *Fly Ash Soil Stabilization for Non-Uniform Subgrade Soils, Volume I-Engineering Properties and Construction Guidelines*. IHRB Project TR-461, FHWA Project 4, Iowa Department of Transportation (April).

Wimsatt, A. J., B. F. McCullough, and N. H. Burns. 1987. *Methods of Analyzing and Factors Influencing Frictional Effects of Subbases*. Research Report University of Texas at Austin. Center for Transportation Research, No. 459-2F.

Yeo, R., B. Vuong, and A. Alderson. 2002. *Towards National Test Methods for Stiffness and Fatigue Characterisation of Stabilised Materials*. Report RC2028- 002 for Austroads (July): 26 pages.

Yeo, Y. 2008. *Fatigue Performance of Cemented Materials under Accelerated Loading – Influence of Vertical Loading on the Performance of Unbound and Cemented Materials*. Austroads (August).

Yue, F. and C. Yang. 2004. Semi-Rigid Asphalt Pavement Thermal Reflective Crack in Finite Element Method. *Journal of Guilin Institute of Technology* 24 (1) (January): 52-54.

Zhang, J. and V. Li. 2001. Influence of Supporting Base Characteristics on Shrinkage-Induced Stresses in Concrete Pavements. *Journal of Transportation Engineering* 127 (6) (November/December).

Zube, E., C. G. Gates, E. C. Shirley, and H. A. Munday. 1969. Service Performance of Cement treated Base as Used in Composite Pavements. *Highway Research Record* 291: 57-69.

## **APPENDIX A. FINDINGS OF SURVEY AND REVIEW OF SPECIFICATIONS**

- 1. Survey Results**
- 2. Summary of State Agencies' Specifications**

## NCHRP Project 04-36

# Characterization of Cementitiously Stabilized Layers for Use in Pavement Design and Analysis

### **Results from Survey of State Highway Agencies**

The research team distributed questionnaires to collect information about cementitiously stabilized layers from state highway agencies. In total, the team received 40 responses from state DOTs. The goal of the survey was to collect feedback from state DOTs regarding the characterization of cementitiously stabilized layers in pavements. The survey covers specifications for types of cementitious additives, the extent of their use, engineering parameters, pavement performance, quality control methods, and construction practices.

#### Statistics of the Results from Questionnaire

The following 8 questions were listed in the questionnaire. The number of occurrences per answer relative to the total responses is shown in parentheses or in graphs.

1) Does your agency use cementitiously stabilized materials for subgrade, subbase or base of pavement construction?

[ **28 of 40**-out of 40 responses, 28 states use it ] Yes; if so, what is the extent of use?

Subgrade modification: (**10 of 28**) Little; (**6 of 28**) Moderate; (**7 of 28**) Extensive

Subbase modification: (**12 of 28**) Little; (**2 of 28**) Moderate; (**3 of 28**) Extensive

Base modification: (**9 of 28**) Little; (**9 of 28**) Moderate; (**5 of 28**) Extensive

[ 12 of 40 ] No; if so, please provide details for non-usage (please use additional page as needed and there is no need for providing input for the items below):

**Wyoming chooses “No” for Q1, but it still answers the other questions.**

---

Summary: Most of the agencies (28 of 40) use cementitiously stabilized materials. Little subgrade and subbase modifications are used, and most of stabilization focuses on base.

2) If Yes, what type of cementitious additives are used:

	Clay	Silt	Sand	Gravel	RAP	Expansive Soil
Cement	9/28	19/28	17/28	14/28	5/28	4/28
Lime	18/28	4/28		1/28	2/28	11/28
Class C fly ash	3/28	7/28	5/28	4/28	5/28	2/28
Lime+Class F fly ash	2/28	2/28	1/28	1/28	1/28	1/28
Lime+cement	3/28	1/28	1/28	1/28		2/28
Cement kiln dust	2/28	2/28	1/28	2/28	1/28	

Note:

---

Summary: Cement and lime are the two major additives. Cement is usually used to stabilize cohesionless soils, such as silt (19/28), sand (17/28), and gravel (14/28). Lime is applied to cohesive soils, such as clay and expansive soil. Other stabilizers include class C fly ash, a mixture of lime and class F fly ash, and cement kiln dust.

3) How are the cementitiously stabilized materials incorporated in your agency's pavement design?

[ 18/27 ] Layer Coefficient

[ 8/27 ] Modulus

[ 8/27 ] Others

---

Summary: Most of the agencies use a layer coefficient (18/27) to incorporate cementitious stabilized materials in pavement design, followed by the modulus (8/27). In addition, there are some other situations, a) Gravel Equivalent; b) when allowed; Mr ( $Mr < 3000\text{psi}$ ); c) no contribution; and d) soil support value or K value.

4) In your opinion, what are the important engineering parameters for cementitious stabilized materials that should be considered? Please place a rank order of importance with 1 being the most important.

[ ] Strength; Test Method: \_\_\_\_\_

[ ] Stiffness; Test Method: \_\_\_\_\_

[ ] Durability; Test Method: \_\_\_\_\_

[ ] Erodibility; Test Method: \_\_\_\_\_

[ ] Swelling; Test Method: \_\_\_\_\_

[ ] Shrinkage; Test Method: \_\_\_\_\_

[ ] Fatigue; Test Method: \_\_\_\_\_

[ ] Others: \_\_\_\_\_

Summary: 28 states responded to this question. Strength (17 of rank 1), durability (8 of rank 2; 7 of rank 3) and stiffness (8 of rank 2; 4 of rank 3) are the three most significant engineering parameters for cementitious stabilized materials. The agencies also consider erodibility, swelling, shrinkage, fatigue, and some other engineering parameters.

5) List the key performance issues for pavements with cementitiously stabilized layers based on your experience and knowledge? Please place a rank order of importance with 1 being the most important for each type of pavement.

**Asphalt Pavement:**

- [ ] Transverse Cracking; Reasons: \_\_\_\_\_
- [ ] Longitudinal Cracking in Wheelpatch; Reasons: \_\_\_\_\_
- [ ] Longitudinal Cracking Outside Wheel path; Reasons: \_\_\_\_\_
- [ ] Alligator Cracking; Reasons: \_\_\_\_\_
- [ ] Block Cracking; Reasons: \_\_\_\_\_
- [ ] Others; Reasons: \_\_\_\_\_

Summary: For asphalt pavement, 23 states responded to this question. Transverse cracking receives the most attention (13 of rank 1), followed by alligator cracking, longitudinal cracking in the wheel path, block cracking, and longitudinal cracking outside the wheel path.

**Concrete Pavement:**

- [ ] Transverse Cracking; Reasons: \_\_\_\_\_
- [ ] Others; Reasons: \_\_\_\_\_

Summary: For concrete pavements, 12 states answered this question. As for asphalt pavement, transverse cracking is also the most crucial pavement issue. In addition, there are some other issues reported: faulting due to CTB erosion, large-area block cracking, improvements needed in uniformity, freeze and thaw and load transfer, joint spalling, base failure, and longitudinal cracking.

6) What is the field quality control method adopted by your agency? Check all apply.

[ 27/27 ] Density; Method & Specifications: \_\_\_\_\_

[ 13/27 ] Moisture content; Method & Specifications: \_\_\_\_\_

[ 10/27 ] Uniformity of mixing; Method & Specifications: \_\_\_\_\_

[ 12/27 ] Strength; Method & Specifications: \_\_\_\_\_

[ 5/27 ] Others; Method & Specifications: \_\_\_\_\_

Summary: The results indicate the importance of a field quality control method from high to low density, moisture content, strength and uniformity of mixing. Other methods include uniform interval thickness, immediate bearing value, gradation, and deflection.

7) What are your agency's construction practices for cementitious stabilization?

Mixing: [ 27/27 ] In-situ Mixing [ 12/27 ] Plant Mixing

Curing Method: [ 18/24 ] Asphalt emulsion; [ 14/24 ] Moisture;

[ 4/24 ] others: wax; plastic sheeting; contractor's choice; cutback asphalt

Construction Cut-off Date/temperature: \_\_\_\_\_

Summary: For mixing, all agencies that responded to this question allow the use of *in situ* mixing (27/27), and almost half of them (12/27) specify plant mixing. In general *in situ* mixing is applicable to lime as a stabilizer, whereas plant mixing, which could provide higher quality, is used when cement is the stabilizer.

With regard to curing method, 24 agencies responded. 18 of 24 agencies specify curing with asphalt emulsion; 14 of 24 use a moisture curing method. Other curing methods are wax, plastic sheeting, cutback asphalt and contractor's choice.

8) Did your agency conduct any field study/experiment in connection with cementitious stabilization of pavement materials?

[ 14/27 ] Yes; [ 13/27 ] No;

If yes, please provide information for lab test results and field distress survey data, or provide contacts for these studies/experiments?

(Please see the “Survey Results”)

Summary: Out of 27 state DOTs, almost half of them (14/27) use field study/experiments; the others (13/27) do not. The information for lab tests or contacts are in the document “Survey Results.”

Complete Listing of Responses Received for the NCHRP 04-36 Survey

	<b>1</b>	<b>2</b>	<b>3</b>	<b>4</b>	<b>5</b>	<b>6</b>	<b>7</b>	<b>8</b>
	Extent of use	Stabilized materials	Pavement design	CSL Properties	Ranking of performance of pavement (1-most important)	Field quality control	Construction practices	Field study/experiment
State	Subgrade	Subbase	Base	additives-soil	Ranking (1-most important)	Flexible	Rigid	Method
Alabama	moderate	little	little	•cement-sand •lime-clay, expansive soil	1-strength (lime stabilization AASHTO T 208, soil-cement AASHTO T 22) 2-reduction in Plasticity Index (lime stabilization, AASHTO T 90)	1-transverse (reflective cracking and ride quality)	1-transverse (ride quality, water infiltration (potential pumping))	•density (AASHTO T 310) •moisture content (lime, AASHTO T 265, soil-cement, AASHTO T 134) •strength (lime, AASHTO T 208; soil-cement, AASHTO T 22)
Alaska	little	•cement-gravel modulus	1-shrinkage 2-durability 3-stiffness 4-fatigue	1-alligator cracking (shrinkage cracking) 2-block cracking (shrinkage cracking)	density	in-situ	•in-situ-lime •plant-soil-cement •asphalt •moisture •lime-not between Oct. 1 and Apr. 1 •soil-cement-air, 40F; soil, 50F	No.
Arizona	no cementitious bases due to cracking							

	<b>1</b>	<b>2</b>	<b>3</b>	<b>4</b>	<b>5</b>	<b>6</b>	<b>7</b>	<b>8</b>	
	<b>Extent of use</b>	<b>Stabilized materials</b>	<b>Pavement design</b>	<b>CSL Properties</b>	<b>Ranking of performance of pavement (1-most important)</b>	<b>Field quality control</b>	<b>Construction practices</b>	<b>Field study/experiment</b>	
<b>State</b>	<b>Subgrade</b>	<b>Subbase</b>	<b>Base</b>	<b>additives-soil</b>	<b>Ranking (1-most important)</b>	<b>Flexible</b>	<b>Rigid</b>	<b>Method</b>	
<b>Connecticut</b>	<b>Colorado</b>	<b>California</b>							
Soils provide excellent support.	little little	little little moderate	•cementsilt, sand, RAP, expansive soil •lime-RAP •class C fly ash RAP •lime+cemen t-expansive soil •cement kiln dust-RAP	Gravel Equivalent  layer coeff.	1-strength 2-stiffness 3-swelling 4-durability 5-shrinkage 6-fatigue 7-erodibility	*-transverse (reflective cracking) *longitudinal outside (reflective cracking) *block (shrinkage cracking in CTN)	•density(CT231,CT312) •moisture(CT226) •uniformity (CT338(ASTMM 92)) •strength(CT 312, CT 373 (ASTM C 977)) •others(CT 217(sand equivalent), CT 202 (ASHTOM 92))	Mixing  Curing  Cut-off Date / temp	Pulverized Asphalt Concrete and FDR-Foamed Asphalt data at: <a href="http://www.its.berkeley.edu/pavementresearch/">www.its.berkeley.edu/pavementresearch/</a> •Contact Dave Jones: <a href="mailto:djones@ucdavis.edu">djones@ucdavis.edu</a>

	<b>1</b>	<b>2</b>	<b>3</b>	<b>4</b>	<b>5</b>	<b>6</b>	<b>7</b>	<b>8</b>		
<b>State</b>	<b>Subgrade</b>	<b>Subbase</b>	<b>Extent of use</b>	<b>Stabilized materials</b>	<b>Pavement design</b>	<b>CSL Properties</b>	<b>Ranking of performance of pavement (1-most important)</b>	<b>Field quality control</b>	<b>Construction practices</b>	<b>Field study/experiment</b>
<b>Georgia</b>	little	little								
	little									
moderate	little	moderate	•cement-silt, sand	layer coeff.	1-strength 2-stiffness 3-durability 4-fatigue 5-erodibility 6-swelling 7-shrinkage	1-transverse (reflective cracking) 2-alligator 3-longitudinal in 4-block 5-longitudinal out	•density •moisture •strength	in-situ	asphalt	
•cement-clay •lime-clay	Layer coeff.	•layer coeff. •when allowed	*-strength (Florida Test Method FM 5-520)	*-transverse (reflective)	•density (In archived specification 270, Soil – Cement Base)	•in-situ •plant	•asphalt •moisture	7 days	Yes	
			1-strength (CBR, Density) 2-stiffness (CBR) 3-durability	1-transverse (reflective joint cracking of a composite pavement because of similar appearance) 2-block cracking (same to transverse)	*- Large area block cracking on a high truck volume facility had a detrimental effect with time.	•density (Theoretical density; % of theoretical) •strength (Core breaks; 300 psi) •in-situ •plant	Cutback asphalt	40F	Yes. Dwane Lewis 404-694-6685	

1	2	3	4	5	6	7	8	
Indiana	Illinois	State	Extent of use	Ranking of performance of pavement (1-most important)	Field quality control	Construction practices	Field study/experiment	
		Subgrade	Stabilized materials	CSI Properties	Pavement design			
extensive	extensive	Subbase	Stabilized materials	CSI Properties	Pavement design			
	little	Base	Stabilized materials	CSI Properties	Pavement design			
	little	additives-soil	Stabilized materials	CSI Properties	Pavement design			
•cement-silt, sand, gravel •lime-clay •modulus •Mr (Mr<3000psi)	•cement-silt, sand, gravel •lime-clay	Ranking (1-most important)	Flexible	Rigid	Method	Mixing	Curing	
•cement-silt, sand, expansive soil •lime-clay, silt, expansive soil •class C fly ash-silt, sand •lime+class F fly ash-clay, silt •CKD-clay,silt	•cement-silt, sand, modulus	*strength (AASHTO T 208) *stiffness (AASHTO T 208) *swelling (IL Modified AASHTO T 193)	(*others (12" modification or full-depth HMA and PCC))	same to asphalt	•density (AASHTO T 99) •moisture content (AASHTO T 99) •uniformity (IL DOT's Standard Specifications) •strength (AASHTO T 208) •IBV (IL Test Procedure 501)	•in-situ plant	45F	Riyad Wahab at 217-782-2704 or Greg Heckel at 217-782-6709
		1-strength 2-stiffness 3-swelling 4-durability 5-erodibility 6-shrinkage 7-fatigue *-leaching *-freeze & thaw *-drainage	1-transverse 2-longitudinal in 3-tongitudinal out		•asphalt •moisture •plastering •sheeting			
			in-situ					

	1	2	3	4	5	6	7	8				
State	Subgrade	Extent of use	Stabilized materials	Pavement design	CSI Properties	Ranking of performance of pavement (1-most important)	Field quality control	Construction practices	Field study/experiment			
Maine	Kentucky	Kansas			Ranking (1-most important)	Flexible	Rigid	Method	Mixing	Curing	Cut-off Date / temp	Information or contact
little	little				extensive							
little					extensive							
moderate	•cement-silt, sand, gravel, RAP, expansive soil layer coeff.	•cement-silt, sand •lime-clay layer coeff.			Layer coeff.	1-transverse (thermal cracking) 2-alligator (Poor bond between HMA layers, insufficient structure) 3-longitudinal in (poor bond between HMA layers, insufficient support, inadequate mixing of cementitious stabilized subgrades) (Construction joints)	1-joint spalling (inadequate air void system in concrete, also durability factors due to poor aggregates – “D”-cracking) 2-transverse (non-uniform subgrade or base material, gradation requirements on mixed material)	•density (Kansas Test Method KT-51, Nuclear Gauge) •moisture content (Gas Pressure Method, Kansas Test Method KT-11, or KT-51, Nuclear Gauge) •uniformity (Spec, test application rate of material, gradation requirements on mixed material)	•in-situ •plant	•asphalt •moisture	40°F or subgrade frozen	Yes. Contact Greg Schieber, at greggs@ksdot.org or 785-296-1198 and will send reports
1-stiffness 2-strength 3-fatigue 4-durability 5-shrinkage 6-swelling 7-erodibility	1-transverse (low temp) 2-longitudinal in (heavy truck) 3-longitudinal out(bond)	•density (Nuclear method–98% of test strip)	in-situ	asphalt	Oct/ 40F	attachment						

	<b>1</b>	<b>2</b>	<b>3</b>	<b>4</b>	<b>5</b>	<b>6</b>	<b>7</b>	<b>8</b>
<b>Extent of use</b>	<b>Subgrade</b>	<b>Subbase</b>	<b>Base</b>	<b>additives-soil</b>	<b>Ranking (1-most important)</b>	<b>Flexible</b>	<b>Rigid</b>	<b>Method</b>
<b>State</b>	<b>Subgrade</b>	<b>Subbase</b>	<b>Base</b>	<b>additives-soil</b>	<b>Ranking (1-most important)</b>	<b>Flexible</b>	<b>Rigid</b>	<b>Method</b>
<b>Maryland</b>	moderate				(For all ASTM or AASHTO) 1-strength 2-stiffness 3-durability 4-fatigue 5-shrinkage 6-swelling 7-erosibility			
<b>Minnesota</b>	little							
<b>Massachusetts</b>	little							
No use due to cracking	just HMA							

	1	2	3	4	5	6	7	8
Nebraska	Montana		State	Subgrade	Extent of use	Stabilized materials	Pavement design	CSI Properties
extensive				•cement-gravel, RAP •class C fly ash-gravel, RAP (typically use 3% portland cement and 2% class C fly ash, for total of 5% cementitious material.)	Layer Coefficient	0.20 in/in	Ranking (1-most important)	Ranking of performance of pavement (1-most important)
extensive				•cement-silt •lime-clay, expansive soil •class C fly ash-clay, silt, RAP •CKD-clay			Flexible	Field quality control
extensive				•density (nuclear density, 96% of standard Proctor) •moisture content (+/- optimum moisture from standard Proctor) •strength (unconfined compression of proctor sample, 400 psi minimum) •gradation			Rigid	Construction practices
extensive				•in-situ •plant			Method	
extensive				•asphalt			Mixing	
extensive				•35F(ground) •40F(air)			Curing	
extensive							Cut-off Date / temp	
extensive								Information or contact
extensive				•density (rolling) •moisture (mix design) •uniformity (specs)	in-situ			Field study/experiment
extensive				•asphalt •moisture	60F	Mick Syslo 402-479-4791 or mick.syslo@nebraska.gov		



	<b>1</b>	<b>2</b>	<b>3</b>	<b>4</b>	<b>5</b>	<b>6</b>	<b>7</b>	<b>8</b>	
	<b>State</b>	<b>Subgrade</b>	<b>Subbase</b>	<b>Base</b>	<b>additives-soil</b>	<b>Ranking (1-most important)</b>	<b>Field quality control</b>	<b>Construction practices</b>	<b>Field study/experiment</b>
	<b>New Mexico</b>	<b>CSL Properties</b>	<b>Pavement design</b>	<b>Stabilized materials</b>	<b>Extent of use</b>	<b>Ranking of performance of pavement (1-most important)</b>			
<b>North Dakota</b>	moderate	moderate	moderate	•cement-sand, gravel •lime-clay, silt	layer coeff. (based on compressive strength)	1-stiffness 2-strength 3-durability 4-swelling 5-shrinkage 6-erodibility			
<b>New York</b>	no use for cost	•cement-gravel •class C fly ash-expansive soil •lime-class F fly ash-expansive soil	layer coeff.				•density •moisture •uniformity	in-situ	Mixing
							moisture	Curing	Cut-off Date / temp
									Information or contact

1	2	3	4	5	6	7	8
Extent of use of stabilized materials	Subgrade	Subbase	Base	Ranking of performance of pavement (1-most important)	Field quality control	Construction practices	Field study/experiment
	Stabilized materials	CSL Properties	additives- soil		Pavement design		
Oklahoma	Ohio						
extensive	moderate						
little							
little							
•cementsilt, sand, gravel •lime-clay, expansive soil •class C fly ash-clay, sit, sand, gravel •lime+class F fly ash- clay •CKD-silt, sand, gravel	•cement- clay, silt •lime-clay •layer coeff. •modulus	in design no stiffness, but constructability has  * -strength * -stiffness * -durability * -credibility	no issues in Ohio	no issues in Ohio	•density •moisture in-situ	•asphalt •others 40F	<a href="http://www.dot.state.oh.us/Divisions/TransSysDev/Research/Reports/sandplassns/Reports/2004/Pavements/14746-FR.pdf">http://www.dot.state.oh.us/Divisions/TransSysDev/Research/Reports/sandplassns/Reports/2004/Pavements/14746-FR.pdf</a>

	<b>1</b>	<b>2</b>	<b>3</b>	<b>4</b>	<b>5</b>	<b>6</b>	<b>7</b>	<b>8</b>
	Subgrade	Subbase	Base	additives-soil	Ranking (1-most important)	Flexible	Rigid	Method
	Extent of use	Stabilized materials	Pavement design	CSL Properties	Ranking of performance of pavement (1-most important)	Field quality control	Construction practices	Field study/experiment
<b>Oregon</b>								
little	•cement-clay, silt, gravel	1-strength (Unconfined Compressive Strength) 2-durability(Freeze-thaw performance)	1-block(reflective) 2-transverse(reflective)	1-ODOT uses CRCP— longitudinal cracking has occurred in CRCP over CTB, likely due to a non-effective or non-existent bond breaker	•density-ODOT Spec 00344&00330 •moisture-ODOT Spec 00344&00330 •uniformity-ODOT Spec 00344 •deflection-ODOT TM 158	•density-ODOT Spec 00344&00330 •moisture-ODOT Spec 00344&00330 •in-situ contractor's choice	Limited Dynamic Cone Penetrometer (DCP) data collection on Subgrade (silt soil) in 2007 Contact is Rene' Renteria, 503-986-3122	Information or contact
little	•lime-clay, silt, expansive soil	3-longitudinal in (more in HMA failure) 4-longitudinal out(reflective) 5-alligator(more in HMA failure)						
non-structural for subgrade, a construction platform								
<b>Rhode Island</b>								
not using cement treated bases, but lean concrete base								
<b>Puerto Rico</b>	has very good aggregate that is used for subgrades							

	<b>1</b>	<b>2</b>	<b>3</b>	<b>4</b>	<b>5</b>	<b>6</b>	<b>7</b>	<b>8</b>			
State	Extent of use		Pavement design	Ranking of performance of pavement (1-most important)		Field quality control	Construction practices	Field study/experiment			
	Subgrade	Subbase									
	Base	additives-soil		Ranking (1-most important)	Method						
Tennessee	South Dakota	South Carolina									
little	little	moderate									
little		little									
moderate		moderate									
Cement-clay, silt, sand, gravel											
•layer coeff.											
1-strength (SC-T-38) 2-shrinkage (No test) 3-durability (No test)											
no cement treated material in design											
•class C fly ash-silt, expansive soil											
layer coeff.		1-strength (initial strength)									
•cement-clay, silt, sand •lime-clay •lime+cement+gravel											
		1-alligator (In compatibility of flexible pavement and stabilized material)									
		•density									
		•moisture									
		•in-situ plant									
		asphalt									

	<b>1</b>	<b>2</b>	<b>3</b>	<b>4</b>	<b>5</b>	<b>6</b>	<b>7</b>	<b>8</b>
<b>State</b>	<b>Subgrade</b>	<b>Subbase</b>	<b>Base</b>	<b>additives-soil</b>	<b>Ranking (1-most important)</b>	<b>Flexible</b>	<b>Rigid</b>	<b>Method</b>
<b>Extent of use</b>	<b>Stabilized materials</b>	<b>Pavement design</b>	<b>CSL Properties</b>		<b>Ranking of performance of pavement (1-most important)</b>	<b>Field quality control</b>	<b>Construction practices</b>	<b>Field study/experiment</b>
<b>Texas</b>								
extensive	•cementsilt, sand, gravel, RAP	1-durability (Tex120E, Tex121E)	1-transverse (shrinkage from excessive placement moisture)					
extensive	•lime-clay, gravel, expansive soil	2-strength(Tex120E, Tex121E & Tex117E, 3-stiffness(NA, FWD)	2-longitudinal (poor subgrade)					
extensive	•class C fly ash-silt, sand, gravel, RAP	4-Fatigue 5-shrinkage (Tex 107E) 6-erosibility 7-swelling(Tex124E)	3-alligator cracking (structure inadequate sawing)					
Utah	Specs. don't provide it, but have some application	•lime+cerement-clay •CKD-gravel	5-longitudinal out (moisture loss) 5-block (not due to stabilization or has been subject of environmental material shrinkage)	2-transverse sawing requirements)	•strength (rarely used) •density •moisture •in-situ •plant •asphalt •moisture	35F and rising or 40F	•Proj. 4182 •Proj 4502 •Proj 4920	Information or contact

	<b>1</b>	<b>2</b>	<b>3</b>	<b>4</b>	<b>5</b>	<b>6</b>	<b>7</b>	<b>8</b>
	Extent of use	Stabilized materials	Pavement design	CSL Properties	Ranking of performance of pavement (1-most important)	Field quality control	Construction practices	Field study/experiment
State	Subgrade	Subbase	Base	additives-soil	Ranking (1-most important)	Flexible	Rigid	Method
<b>Vermont</b>					1-strength 2-durability 3-stiffness 4-swelling 5-fatigue 6-shrinkage 7-erodibility	1-transverse (freeze-thaw, thermal contraction)		
<b>Virginia</b>	extensive	little	moderate	•cement-silt, sand, gravel	1-strength 2-erodibility 3-durability 4-fatigue			•density •moisture •strength
<b>Washington</b>	extensive	moderate	extensive	•cementsilt, sand, gravel •lime-clay, expansive soil	1-in-situ layer coeff.	1-transverse (reflective)	in-situ asphalt	Oct.15 Jennifer Fitch Research Engineer 802-828-2553
	In the past we have used cement modified base. When we used it we were prone to reflective cracking of the HMA layer. So we discontinued use.					•density •moisture •in-situ •plant	40F •asphalt •moisture	

	<b>1</b>	<b>2</b>	<b>3</b>	<b>4</b>	<b>5</b>	<b>6</b>	<b>7</b>	<b>8</b>	
	Extent of use	Subgrade	Subbase	Base	additives-soil	Ranking (1-most important)	Field quality control	Construction practices	Field study/experiment
	Wisconsin								
<b>Wyoming</b>	little little little	•cement-clay •lime-clay •class C fly ash-clay	soil support value or K value	1-strength (Mr or plate bearing) 2-durability 3-stiffness 4-erodibility	Stabilization is not used very often	Stabilization is not used very often	•density (AASHTO T-99) •moisture	in-situ •35F(ground) •50F(air)	See whrp.org for study reports
	don't use cement treated base now	•cement-gravel •class C fly ash-gravel	layer coeff.	1-transverse 2-longitudinal out 3-block	plant	•density (AASHTO T 99 and AASHTO T19) •moisture •uniformity (pug mill)	40F	Several of our LTPP-GPS sites have cement treated base. Rick Harvey – State Materials Engineer- 307-777-4476 rick.harvey@dot.state.wy.us	

Characterization of Cementitious Stabilized Layers for Use in Pavement Design and  
Analysis

## **Results from Standard Specifications of State DOTs**

The research team reviewed the standard specifications for construction posted on the 50 agencies' websites to complement the information about cementitious stabilized layers. In total, 32 state agencies have pertinent specifications. From the standard specifications, the team obtained information about cementitious stabilized materials, including the type of stabilizers and soils, the *in situ*/pugmil mixing process, temperature during the time of construction, and compaction density and moisture.

### Statistics of the Results from Standard Specifications

#### *1) Type of cementitious additives*

Out of the 32 states, lime (22/32) and cement (27/32) are the two most important kinds of cementitious stabilized materials; the mixture of lime and fly ash (5/32) also occupies a certain proportion. Other stabilizers include borrowed materials, pozzolan, soil binder, chloride, mixture of lime and fly ash and cement, mixture of fly ash and cement, and mixture of fly ash and cement and cement kiln dust.

#### *2) What types of cementitious additives are used to stabilize different layers?*

Lime is often used to stabilize subgrade (7/29); cement is usually applied to the base (14/29). Other additives are fly ash/cement, lime/fly ash, etc.

### *3) Mixing location*

For lime, most of the mixing locations are *in situ* (11/18), followed by plants (6/18) and yard (1/18). For cement, the order from high to low is plants (19/36), *in situ* (14/36), transit (2/36), and yard (1/36). (The total number of 36 is greater than 32, as some state agencies have specifications for several mixing locations.)

### *4) Additive placement*

More than half of the states (20/37) require lime in slurry condition; the others (17/20) use dry lime. More states prefer dry application of cement (8/10) than cement slurry (2/10). For lime and fly ash, slurry placement (4/6) is preferred over dry placement (2/6).

### *5) Mix design*

Only a few state agencies have specifications for mix design. For example, California specifies California Test 338 as the mix design method; Illinois's mix design is based on "the Department's Geotechnical Manual Procedure;" Oklahoma's mix design is "OHD L 50/51." Texas has different mix design methods: for lime the mix design is TX-121-E; for cement it is TX-120-E; and for the mixture of fly ash and lime it is TX-127-E.

### *6) Cut-off date/temperature*

All the agencies have specifications about cut-off date/temperature. The typical cut-off temperature is around 40°F and cut-off date between April 1st and the end of October. The temperature has to be above the freezing point during construction.

### *7) Placement after slurry*

When additive is applied for the slurry condition, it is specified to be mixed with the natural soil within a time window since the production of slurry. Illinois and Mississippi require that the placement of lime slurry is less than 6 hours after the production of slurry. Virginia also requires that the placement of mixture of lime and fly ash should be less than 6 hours. The placement of cement slurry should be less than 30 minutes in Nevada and Virginia, and less than 2 hours in Texas.

#### *8) Mixing delay*

The time of mixing delay after placement of an additive is different depending on the additive. Lime has a longer time (4-6 hours) than cement (less than 1 hour).

#### *9) Moisture tolerance during mixing*

Because density can reach the maximum value under the optimum moisture content, the moisture during mixing should be around the optimum value. For soil-lime, the moisture content is specified above the optimum value to account for the evaporation during the longer mixing delay. For cement, the moisture content is specified to be in the range of -2% to +2% of the optimum value.

#### *10) Mellowing time*

Mellowing time is needed when lime is used as the stabilizer. From the standard specifications, mellowing for more than two days is typical.

#### *11) Compaction delay*

For soil-lime, the compaction is allowed to finish within 6-24 hours; 2 hours is typical for cement-stabilized materials, and 4 hours for fly ash-stabilized materials.

*12) Compaction moisture*

The results are similar to 8) Moisture tolerance during mixing.

*13) Density target*

Most of the standard specifications require that the minimum value is 95% of the maximum dry density based on either standard or modified proctor.

*14) Time between compaction and curing*

After compaction, the layer should be cured under some special conditions. The time between compaction and curing is specified to be less than 24 hours (8/11).

*15) Curing method*

Asphalt curing is the most common curing method for any stabilized material. However, when cement is the stabilizer, there are some other choices in several states. Kansas allows the use of a wax-based liquid membrane-forming compound, Pennsylvania the use of a white membrane forming curing compound, Tennessee the use of transparent or white polyethylene sheeting, and West Virginia the use of white polyethylene sheeting.

*16) Minimum curing time*

Different states have different requirements; seven-day curing is the most common for various cementitiously stabilized materials.

*17) Curing temperature*

The temperature-specified curing process is the same as for the cut-off temperature. The temperature is specified to be above the freezing point during curing. The typical minimum curing temperature is 40°F.

**Complete Listing of Standard Specifications for the NCHRP 04-36 Survey**

Arizona	Alabama				State	
					Additive	
					Layer	
			Mixing location		Mixing location	
			Additive placement		Additive placement	
			Mix design		Mix design	
			Cut off temp (°F)		Cut off temp (°F)	
			Placement after slurry production		Placement after slurry production	
			Mixing delay		Mixing delay	
			Moisture tolerance during mixing		Moisture tolerance during mixing	
Lime			Mellowing time		Mellowing time	
			Compaction delay		Compaction delay	
			Compaction moisture		Compaction moisture	
			Density target		Density target	
			Time between compaction and curing		Time between compaction and curing	
			Curing method		Curing method	
			Minimum curing time		Minimum curing time	
			Minimum curing temp (F)		Minimum curing temp (F)	
In situ	plant	yard	In situ	plant	In situ	
dry						
Lime subgrade						

State		Additive		Layer		Mixing location		Additive placement		Mix design		Cut off temp (°F)		Placement after slurry production		Mixing delay		Moisture tolerance during mixing		Mellowing time		Compaction delay		Compaction moisture		Density target		Time between compaction and curing		Curing method		Minimum curing time		Minimum curing temp (F)	
<b>California</b>		cement	subgrade	In situ	In situ	40F	±2% optimum	2.5 hr	100% of maximum density	Bituminous	3 d																								
<b>Arkansas</b>		cement	base	plant	slurry	40F	±2% optimum	2.5 hr	100% of maximum density	Bituminous	3 d																								
		lime	subgrade	In situ	•dry •slurry	50F / Apr1 to Oct31	±2% optimum	3 d	»95% maximum density																										
		cement	base	plant	dry	40F	60 min	±5% optimum	2 hr	»95% maximum density	asphalt																								
		cement	crushed stone base	plant	dry	40F	±1% optimum																												
		In situ	In situ	California Test 338		35F	7 d	above optimum	«24 hr																										
		cement				35F	»99%	optimum	«48 hr	asphalt	3 d	40F																							

State		Additive		Layer		Mixing location		Additive placement		Mix design		Cut off temp (°F)		Placement after slurry production		Mixing delay		Moisture tolerance during mixing		Mellowing time		Compaction delay		Compaction moisture		Density target		Time between compaction and curing		Curing method		Minimum curing time		Minimum curing temp (F)															
Georgia	Florida	Delaware	Colorado	Lime	In situ	plant	California Test 338	35F	»99% optimum	2.5 hr	optimum	asphalt	35F	35F	slurry	» optimum	» 48 hr	2 ± 1% percent above the optimum	»95% maximum density	asphalt	»7d	35F	permeable base	plant	•dry •slurry	slurry	•dry •slurry	40	±2% optimum	»100% maximum density	No requirements	3~4 d	lime	•45F •April to Oct15	±5% optimum	3 ~14 d	100~102% optimum	«24hr	bituminous	7d	cement	40F	45 min	100~120 % optimum	2h	100~120 % optimum	»98% maximum density		

<b>Indiana</b>	<b>Illinois</b>				<b>State</b>
					<b>Additive</b>
					<b>Layer</b>
				plant	<b>Mixing location</b>
Hydrated Lime and Quicklime	dry	dry	•dry •slurry		<b>Additive placement</b>
		Department's Geotechnical Manual procedure	40F	45 min	<b>Mix design</b>
		40F	45F	6hr	<b>Cut off temp (°F)</b>
		80~ 110% optimum	100~ 103% optimum	48 hr	<b>Placement after slurry production</b>
		2hr	100% standard dry density (AASHTO T 134)		<b>Mixing delay</b>
•cement- 3hr •fly ash- 4hr •lime-24hr		slightly » optimum			<b>Moisture tolerance during mixing</b>
	40F	90 min optimum			<b>Mellowing time</b>
					<b>Compaction delay</b>
					<b>Compaction moisture</b>
					<b>Density target</b>
					<b>Time between compaction and curing</b>
					<b>Curing method</b>
					<b>Minimum curing time</b>
					<b>Minimum curing temp (F)</b>
fly ash/lime/cement		lime fly ash,14hr; cement fly ash,12hr	asphalt	72hr	

		State		Additive		Layer			
		Kansas		Mixing location		Additive placement		Mix design	
		lime subgrade		In situ		slurry		Cut off temp (°F)	
		cement/fly ash subgrade		plant		40F		»108% optimum	
		cement base		plant		40F		»108% optimum	
		lime roadway		dry		30 min		»24hr	
		cement roadway		dry		30 min		asphalt	
		In situ		•dry •slurry		slurry		7d	
<b>Louisiana</b>		<b>Kentucky</b>						Placement after slurry production	
								Mixing delay	
								Moisture tolerance during mixing	
								Mellowing time	
								Compaction delay	
								Compaction moisture	
								Density target	
								Time between compaction and curing	
								Curing method	
								Minimum curing time	
								Minimum curing temp (F)	

State		Additive		Layer			
		Mixing location	Additive placement				
Mississippi	lime	In situ	plant	•dry •slurry	slurry	Cut off temp (°F)	Mix design
Mississippi	cement	In situ	plant	40F	6hr	»48hr	Placement after slurry production
Missouri	lime/fly ash	In situ	plant	40F	3 hr	5~20d	Mixing delay
Montana	cement	In situ	•dry •slurry	40F	60 min	»95% maximum density	Moisture tolerance during mixing
Montana	cement	In situ		40F	«102% optimum	»95% standard density	Mellowing time
Montana	cement	In situ		40F	4hr	»98% standard density	Compaction delay
Montana	cement	In situ		No		«24hr asphalt	Compaction moisture
Montana	cement	In situ		40F	±2% optimum	7d	Density target
Montana	cement	In situ		2hr	» optimum	» freezing	Time between compaction and curing
Montana	cement	In situ		7d	»96% maximum dry density	» freezing	Curing method
Montana	cement	In situ		48 hr	bituminous	48 hr	Minimum curing time
Montana	cement	In situ			7d		Minimum curing temp (F)

State		Additive		Layer			
New York		Nebraska		Nevada			
soil binder							
cement		In situ		In situ		Mixing location	
base		35F min		<30 min		Additive placement	
plant		35F min		<30 min		Mix design	
lime		40F •dry •slurry		103~105% optimum		Cut off temp (°F)	
cement		40F 100~105% optimum		24 hr 4hr		Placement after slurry production	
In situ		In situ •dry •slurry		100% maximum density		Mixing delay	
lime		40F 100~102% optimum		asphalt		Moisture tolerance during mixing	
cement		40F 100~102% optimum		2d 48hr		Mellowing time	
				asphalt		Compaction delay	
				3d 3d		Compaction moisture	
						Density target	
						Time between compaction and curing	
						Curing method	
						Minimum curing time	
						Minimum curing temp (F)	

North Dakota		North Carolina		State	
lime	plant	lime	plant	Additive	Layer
•dry •slurry	•dry •slurry	In situ	plant	Mixing location	Additive placement
base	cement	40F	45F	Cut off temp (°F)	Mix design
plant	base	30 min	30 hr	Placement after slurry production	Cut off temp (°F)
•dry •slurry	•dry •slurry	100~102% optimum	100~103% optimum	optimum	Moisture tolerance during mixing
40F	40F	1~4d	4d	»95% maximum density	Mellowing time
100~101.5% optimum	100~101.5% optimum	3hr	100~102% optimum	48hr	Compaction delay
» optimum	« optimum	3hr	100~101.5% optimum	bituminous	Compaction moisture
40F	40F	»97% maximum density	»97% maximum density	asphalt	Density target
lime subgrade	lime subgrade	asphalt	asphalt	7d	Time between compaction and curing
Lime / fly ash subgrade	40F	7d	7d	5d •freezing- 7d	Curing method
cement base	»optimum	bituminous	bituminous	48 hr	Minimum curing time
cement base	optimum	bituminous	bituminous		Minimum curing temp (F)

State													
		Additive											
			Layer										
			Mixing location			Additive placement							
						Mix design							
				Cut off temp (°F)		Placement after slurry production							
				Mixing delay		Moisture tolerance during mixing							
				Mellowing time		Compaction moisture							
				Density target		Compaction delay							
				Time between compaction and curing		Curing method							
						Minimum curing time							
				Minimum curing temp (F)									
<b>Oregon</b>		<b>Oklahoma</b>	<b>Ohio</b>										
				lime									
				lime									
				cement									
				cement/flyash/CKD									
				lime									
				lime									
				lime									
				lime									
				lime									
				lime									
				lime									
				lime									
				lime									
				lime									
				lime									
				lime									
				lime									
				lime									
				lime									
				lime									
				lime									
				lime									
				lime									
				lime									
				lime									
				lime									
				lime									
				lime									
				lime									
				lime									
				lime									
				lime									
				lime									
				lime									
				lime									
				lime									
				lime									
				lime									
				lime									
				lime									
				lime									
				lime									
				lime									
				lime									
				lime									
				lime									
				lime									
				lime									
				lime									
				lime									
				lime									
				lime									
				lime									
				lime									
				lime									
				lime									
				lime									
				lime									
				lime									
				lime									
				lime									
				lime									
				lime									
				lime									
				lime									
				lime									
				lime									
				lime									
				lime									
				lime									
				lime									

State		Additive		Layer		Mixing location		Additive placement		Mix design		Cut off temp (°F)		Placement after slurry production		Mixing delay		Moisture tolerance during mixing		Mellowing time		Compaction delay		Compaction moisture		Density target		Time between compaction and curing		Curing method		Minimum curing time		Minimum curing temp (F)	
<b>South Carolina</b>		<b>Pennsylvania</b>		chloride	subgrade	optimum	12hr	96~102% optimum	»95% maximum density																										
cement	subgrade	optimum	12hr	96~102% optimum	»95% maximum density																														
cement	base	•plant •truck	40F				1hr																												
modified cement subbase	In situ	dry	40F	3 hr	«optimum	2hr	±2% optimum	»95% maximum density	asphalt	3d																									
modified recycled cement base	In situ		40F	«optimum	2hr																														
stabilized earth base	In situ	40F	±2% optimum	2hr	±2% optimum	»95% maximum density	«12hr	asphalt	7d																										
plant		40F	60 min	«102% optimum	2hr	±2% optimum	»95% maximum density	«12hr	asphalt	7d																									

Tennessee				State
				Additive
				Layer
				<b>Mixing location</b>
				<b>Additive placement</b>
				<b>Mix design</b>
				<b>Cut off temp (°F)</b>
				<b>Placement after slurry production</b>
				<b>Mixing delay</b>
				<b>Moisture tolerance during mixing</b>
				<b>Mellowing time</b>
				<b>Compaction delay</b>
				<b>Compaction moisture</b>
				<b>Density target</b>
				<b>Time between compaction and curing</b>
				<b>Curing method</b>
				<b>Minimum curing time</b>
				<b>Minimum curing temp (F)</b>
cement lime/ fly ash base	In situ plant	In situ	In situ	stabilized aggregate base
cement permeable base		hydrated Lime	hydrated Lime	•dry •slurry
				40F
				102~108% optimum
				2~7d
				±3% optimum
				»95% maximum density
				bituminous
		40F		
				±2% optimum
				8hr
				99~103% optimum
				»100% maximum density
				«24hr bituminous
				7d
		±2% optimum	8hr	»100% maximum density
				«24hr bituminous
				7d
				transparent or white polyethylene sheeting
				7d

Texas							State
Lime							Additive
							Layer
Plant	In situ	Plant	In situ		<b>Mixing location</b>		
cement slurry	cement slurry	Lime slurry	Lime slurry		<b>Additive placement</b>		
Tex-120-E	Tex-120-E	TX-121-E	TX-121-E		<b>Mix design</b>		
35F↑ or 40F	35F↑ or 40F	35F↑ or 40F	35F↑ or 40F		<b>Cut off temp (°F)</b>		
«2hr	«2hr	«2hr	6 hr		<b>Placement after slurry production</b>		
±2% optimum	±2% optimum	±2% optimum	•1-4 Days •2-4 Days (Pebble Quicklime)		<b>Mixing delay</b>		
asphalt	asphalt	asphalt	95%		<b>Moisture tolerance during mixing</b>		
6 hr	6 hr	6 hr	•1-4 Days •2-4 Days (Pebble Quicklime)		<b>Mellowing time</b>		
asphalt	asphalt	asphalt	95%		<b>Compaction delay</b>		
asphalt	asphalt	asphalt	95%		<b>Compaction moisture</b>		
asphalt	asphalt	asphalt	95%		<b>Density target</b>		
asphalt	asphalt	asphalt	95%		<b>Time between compaction and curing</b>		
asphalt	asphalt	asphalt	asphalt		<b>Curing method</b>		
»3d	»3d	»3d	7d		<b>Minimum curing time</b>		
asphalt	asphalt	asphalt	•PI<35,2d •PI>35,5d		<b>Minimum curing temp (F)</b>		

Virginia				State
Fly Ash/ Lime				Additive
				Layer
plant	In situ	•In situ •plant	In situ	Mixing location
		•dry •slurry	Lime slurry	Additive placement
			Tex-127-E	Mix design
			40F	Cut off temp (°F)
			6 hr	Placement after slurry production
		≤6hr		Mixing delay
				Moisture tolerance during mixing
			•1-4 Days •2-4 Days (Pebble Quicklime)	Mellowing time
			6hr	Compaction delay
				Compaction moisture
				Density target
				Time between compaction and curing
				Curing method
			•LFA:7d-14d •FA:24hr	Minimum curing time
				Minimum curing temp (F)

<b>Wyoming</b>	<b>West Virginia</b>	<b>State</b>
lime	cement open graded free draining base	<b>Additive</b>
plant	plant	<b>Layer</b>
•dry •slurry		<b>Mixing location</b>
		<b>Additive placement</b>
		<b>Mix design</b>
45F	40F	<b>Cut off temp (°F)</b>
		<b>Placement after slurry production</b>
48 hr	45 min	<b>Mixing delay</b>
		<b>Moisture tolerance during mixing</b>
		<b>Mellowing time</b>
		<b>Compaction delay</b>
		<b>Compaction moisture</b>
		<b>Density target</b>
		<b>Time between compaction and curing</b>
	white polyethylene sheeting	<b>Curing method</b>
24 hr		<b>Minimum curing time</b>
		<b>Minimum curing temp (F)</b>

## APPENDIX B. MATLAB PROGRAM FOR IDT MODULUS PARAMETERS

The center strain at horizontal direction ( $\varepsilon$ ), Poisson's ratio ( $v$ ), and creep compliance [ $D(t)$ ] are calculated with following equations (Wen and Kim 2002):

$$\varepsilon = U(t) \frac{\gamma_1 + \gamma_2 v}{\gamma_3 + \gamma_4 v} \quad \text{Eq. (B-1)}$$

$$v = -\frac{a_{11}U(t) + b_{11}V(t)}{a_{22}U(t) + b_{22}V(t)} \quad \text{Eq. (B-2)}$$

$$D(t) = -\frac{d}{P} [c \cdot U(t) + e \cdot V(t)] \quad \text{Eq. (B-3)}$$

where,

$U(t)$  = horizontal displacement, m, 1 m = 0.0254 in.

$\varepsilon$  = cyclic horizontal tensile strain

$v$  = Poisson's ratio, assuming 0.2 for CSM

$D(t)$  = creep compliance, 1/psi

$P$  = maximum applied load, lb

$d$  = diameter of the specimen, in.

$a_{11}, a_{22}, b_{11}, b_{22}, c, e, \gamma_1, \gamma_2, \gamma_3, \gamma_4$  = constants.

This research assumes the Poisson's ratio ( $v$ ) of CSM is 0.2, and the vertical displacement was not measured, so only Eq. (B-1) is used in this study. The constant values from Eqs. (B-1) through (B-3) can be calculated from the MATLAB program below.

### B-1. Script File:

```
% Script file: IDTmodulusparameters.m
```

```
%
```

% Purpose:

% This program calculates the parameters which are used to determine

% Poisson's ratio and center strain for different specimen dimension and

% gauge length.

%

% Reference:

% Kim, Daniel, and Wen (2002) FATIGUE PERFORMANCE EVALUATION OF

WESTRACK

% Wen and Kim (2002) Simple Performance Test for Fatigue Cracking and Validation with

WesTrack Mixtures

%

% Record of revisions:

% Date      Programmer      Description of change

% =====      ======      ======

% Apr-24-2012 Jingan Wang      Original code

%

% Define variables:

% b      --loading strip width,m

% R      --specimen radius,m

% D      --specimen diameter,m

% a      --radial angle

% L      --gauge length,m

%

```

clear all;
clc;

%Input load strip width, diameter of specimen, and gauge length
b=0.01905;
D=0.1524;
L=0.1016;

%Calculate the radial angle
R=D/2;
a=asin((b/2)/R);

%Integrate intermediate variables: fx, gx, my, ny
ff2=quad(@(x)fx(x,R,a),-L/2,L/2);
gg2=quad(@(x)gx(x,R,a),-L/2,L/2);
mm2=quad(@(y)my(y,R,a),-L/2,L/2);
nn2=quad(@(y)ny(y,R,a),-L/2,L/2);

%Calculate the fx and gx when x=0
f0=fx(0,R,a);
g0=gx(0,R,a);
m0=my(0,R,a);
n0=ny(0,R,a);

%Calculate the parameters in the equation of Poisson's Ratio v
a1=mm2+nn2;
a2=mm2-nn2;
b1=ff2-gg2;

```

```

b2=ff2+gg2;

%All the parameters in the equation of Poisson's Ratio are divided by b1

a11=a1/b1;

a22=a2/b1;

b11=b1/b1;

b22=b2/b1;

%Calculate the parameters in the equation of center strain epsilon(t)

r1=(f0-g0)*100;

r2=(f0+g0)*100;

r3=(ff2-gg2)*100;

r4=(ff2+gg2)*100;

%Calculate the parameters in the equation of creep compliance D(t)

c=pi()*b/4*(a2/(nn2*ff2+mm2*gg2));

e=pi()*b/4*(b2/(nn2*ff2+mm2*gg2));

%Print results

disp('The parameters in the equation of Poissons ratio are:');

fprintf('a1 = %6.4f, a11=%6.4f\n',a1,a11);

fprintf('a2 = %6.4f, a22=%6.4f\n',a2,a22);

fprintf('b1 = %6.4f, b11=%6.4f\n',b1,b11);

fprintf('b2 = %6.4f, b22=%6.4f\n',b2,b22);

fprintf('c = %6.4f\n',c);

fprintf('e = %6.4f\n',e);

fprintf('r1 = %6.4f\n',r1);

```

```

fprintf('r2 = %6.4f\n',r2);
fprintf('r3 = %6.4f\n',r3);
fprintf('r4 = %6.4f\n',r4);

```

### **B-2. Function File**

```

function f=fx(x,R,a)
f=(1-x.^2/R^2)*sin(2*a)./(1+2*x.^2/R^2*cos(2*a)+x.^4/R^4);
end

```

```

function g=gx(x,R,a)
g=atan((1-x.^2/R^2)*tan(a)./(1+x.^2/R^2));
end

```

```

function m=my(y,R,a)
m=(1-y.^2/R^2)*sin(2*a)./(1-2*y.^2/R^2*cos(2*a)+y.^4/R^4);
end

```

```

function n=ny(y,R,a)
n=atan((1+y.^2/R^2)*tan(a)./(1-y.^2/R^2));
end

```

## APPENDIX C. MATLAB PROGRAM FOR SHRINKAGE CRACKING MODEL

Appendix C contains MATLAB programs to calculate IDT strength and modulus, gradient drying shrinkage strain, gradient force [ $\int_{-\frac{H}{2}}^{\frac{H}{2}} \varepsilon(y) dy$ ], and gradient moment [ $\int_{-\frac{H}{2}}^{\frac{H}{2}} \varepsilon(y) y dy$ ] parts in shrinkage cracking models, based on daily temperature and RH values.

### C-1. Function File of IDT Strength

```
function St = IDT_strength(UCS28,t,temp,RHai)

% This function calculates the IDT strength.

% IDT strength is calcualted step by step based on daily temperature and relative
% humidity.

% Only strength more than 2 days can be calculated,due to the model
% limitation.

% Record of revisions:

% Date    Programmer    Description of change
%
% ======  ======  ======
%
% 02/25/13 Jingan Wang    Original code

%% Parameters

p=[1.59026230967436,1.61304088199228,-1.49913460379867,23.4109261019315,0.1141];

%%
St1=zeros(length(t)-(2-t(1)),1); %strength of i day (psi)
St2=zeros(length(t)-(3-t(1)),1); %strength of (i-1) day (psi)
```

```

St=zeros(length(t)-(2-t(1)),1); %final IDT strength (psi)

for ii=(3-t(1)):length(t)
    St1(ii-(2-t(1)))=p(5)*UCS28*(p(1)^(1-1/((1+(t(ii)/30.5-
28/30.5)/p(2))*((1+RHai(ii)/100)/2)^p(3)*(((temp(ii)-32)/1.8+273.15)/293.15)^p(4)));
end

for ii=(4-t(1)):length(t)
    St2(ii-(3-t(1)))=p(5)*UCS28*(p(1)^(1-1/((1+((t(ii-1)/30.5-
28/30.5)/p(2))*((1+RHai(ii)/100)/2)^p(3)*(((temp(ii)-32)/1.8+273.15)/293.15)^p(4)));
end

delta_St=St1(2:end)-St2;
St(1)=St1(1);

for ii=2:length(t)-(2-t(1))
    St(ii)=St(ii-1)+delta_St(ii-1);
end
end

```

## **C-2. Function File of IDT Modulus**

```

function Mt = IDT_modulus(UCS28,t,temp,RHai)
% This function calculates the IDT strength.

% IDT strength is calcualted step by step based on daily temperature and relative
% humidity.

% Only modulus more than 2 days can be calculated,due to the model

```

% limitation.

% Record of revisions:

% Date	Programmer	Description of change
% =====	=====	=====

% 02/25/13 Jingan Wang Original code

%% Parameters

p=[1.59026230967436,1.61304088199228,-0.216318847798923,0,1223.92843869232];

%%

Mt1=zeros(length(t)-(2-t(1)),1); %modulus of i day (psi)

Mt2=zeros(length(t)-(3-t(1)),1); %modulus of (i-1) day (psi)

Mt=zeros(length(t)-(2-t(1)),1); %final IDT modulus (psi)

for ii=(3-t(1)):length(t)

Mt1(ii-(2-t(1)))=p(5)\*UCS28\*(p(1)^(1-1/((1+(t(ii)/30.5-  
28/30.5)/p(2))\*((1+RHai(ii)/100)/2)^p(3)\*(((temp(ii)-32)/1.8+273.15)/293.15)^p(4))));

end

for ii=(4-t(1)):length(t)

Mt2(ii-(3-t(1)))=p(5)\*UCS28\*(p(1)^(1-1/((1+((t(ii-1))/30.5-  
28/30.5)/p(2))\*((1+RHai(ii)/100)/2)^p(3)\*(((temp(ii)-32)/1.8+273.15)/293.15)^p(4))));

end

delta\_Mt=Mt1(2:end)-Mt2;

Mt(1)=Mt1(1);

for ii=2:length(t)-(2-t(1))

Mt(ii)=Mt(ii-1)+delta\_Mt(ii-1);

```
end  
end
```

### **C-3. Function File of Gradient Drying Shrinkage Strain**

```
function e_g=shrinkage_gradient(e_ul,RHaij,H,tj,w_c,y)  
% This function calcualtes shrinkage gradient step by step based on daily temperature and  
relative humidity.  
  
% Date    Programmer    Description of change  
% =====  ======  ======  
% 02/26/13 Jingan Wang  Original code  
  
% e_ul  ultimate shrinkage  
  
% RHaij air relative humidity from 0 to target day  
  
% H    thickness of the slab (in)  
  
% tj   target day (days)  
  
% w_c  water calcium ratio in mass (%)  
  
% y    distance from center of the slab (in)  
  
%% Parameters  
  
p=[1289202.01208494,0.0851880320476007,0.936834622824857,1.24377246958372,10209.32  
01202928,4.5134737760515];  
  
%%  
  
e_g1=zeros(tj,1); %gradient shrinkage of i day  
  
e_g2=zeros(tj,1); %gradient shrinkage of (i-1) day
```

```

e_g=zeros(tj+1,1); %final gradient shrinkage

for ii=1:tj

t=ii;

e_g1(ii)=e_ul*(1-(((RHaij(ii)+(100-RHaij(ii))*(1/(1+t/(p(1)*(H/2-
y)/12+p(2))^p(3)*w_c^p(4))))^p(5))/100)^p(6));

e_g2(ii)=e_ul*(1-(((RHaij(ii)+(100-RHaij(ii))*(1/(1+(t-1)/(p(1)*(H/2-
y)/12+p(2))^p(3)*w_c^p(4))))^p(5))/100)^p(6));

end

delta_e_g=e_g1-e_g2;

for ii=1:tj

e_g(ii+1)=e_g(ii)+delta_e_g(ii);

end

end

```

**C-4. Function File of Gradient Force  $[\int_{-\frac{H}{2}}^{\frac{H}{2}} \varepsilon(y) dy]$**

```

function N=force(e_ul,RHaij,H,tj,w_c)

% This function calcualtes the normal force due to strain gradient

% Date    Programmer    Description of change

% =====  =====  =====
% 02/26/13 Jingan Wang    Original code

%% Parameters

```

```
p=[1289202.01208494,0.0851880320476007,0.936834622824857,1.24377246958372,10209.32
01202928,4.5134737760515];
```

```
function e_g=shrinkage_gradient(y)

% shrinkage gradient is calcualted step by step based on daily temperature and relative
humidity.

e_g1=zeros(tj,1); %gradient shrinkage of i day

e_g2=zeros(tj,1); %gradient shrinkage of (i-1) day

e_g=zeros(tj+1,1); %final gradient shrinkage

for ii=1:tj

t=ii;

e_g1(ii)=e_ul*(1-(((RHaij(ii)+(100-RHaij(ii))*(1/(1+t/(p(1)*((H/2-
y)/12+p(2))^p(3)*w_c^p(4))))^p(5)))/100)^p(6));

e_g2(ii)=e_ul*(1-(((RHaij(ii)+(100-RHaij(ii))*(1/(1+(t-1)/(p(1)*((H/2-
y)/12+p(2))^p(3)*w_c^p(4))))^p(5)))/100)^p(6));

end

delta_e_g=e_g1-e_g2;

for ii=1:tj

e_g(ii+1)=e_g(ii)+delta_e_g(ii);

end

end

N=quadv(@shrinkage_gradient,-H/2,H/2);
```

**C-5. Function File of Gradient Moment [ $\int_{-\frac{H}{2}}^{\frac{H}{2}} \varepsilon(y) y dy$ ]**

```

function M=moment(e_ul,RHaij,H,tj,w_c)

% This function calcualtes the normal force due to strain gradient

% Date    Programmer    Description of change

% =====  ======  =====

% 02/26/13 Jingan Wang  Original code

%% Parameters

p=[1289202.01208494,0.0851880320476007,0.936834622824857,1.24377246958372,10209.32
01202928,4.5134737760515];

function e_g=shrinkage_gradient(y)

    % shrinkage gradient is calcualted step by step based on daily temperature and relative
    humidity.

    e_g1=zeros(tj,1); %gradient shrinkage of i day
    e_g2=zeros(tj,1); %gradient shrinkage of (i-1) day
    e_g=zeros(tj+1,1); %final gradient shrinkage

    for ii=1:tj

        t=ii;
        e_g1(ii)=e_ul*(1-(((RHaij(ii)+(100-RHaij(ii))*(1/(1+t/(p(1)*((H/2-
y)/12+p(2))^p(3)*w_c^p(4))))^p(5))/100)^p(6));
        e_g2(ii)=e_ul*(1-(((RHaij(ii)+(100-RHaij(ii))*(1/(1+(t-1)/(p(1)*((H/2-
y)/12+p(2))^p(3)*w_c^p(4))))^p(5))/100)^p(6));
    end
end

```

```

end

delta_e_g=e_g1-e_g2;

for ii=1:tj

e_g(ii+1)=e_g(ii)+delta_e_g(ii);

end

end

function e_g_M=y_strain(y)

e_g_M=shrinkage_gradient(y)*y;

end

M=quadv(@y_strain,-H/2,H/2);

end

```

## **APPENDIX D. DRAFT OF TEST PROTOCOLS**

- 1. Indirect Tensile Strength for Cementitious Stabilized Materials**
- 2. Indirect Tensile Modulus for Cementitious Stabilized Materials**
- 3. Coefficient of Thermal Expansion Test of Cementitiously Stabilized Soils**

# **Indirect Tensile Strength for Cementitious Stabilized Materials**

---

## **1. SCOPE**

- 1.1. This test method covers the determination of indirect tensile (IDT) strength of cementitiously stabilized materials.
  - 1.2. The values stated in SI units are to be regarded as the standard.
  - 1.3. *This standard does not purport to address all of the safety concerns, if any, associated with its use. It is the responsibility of the user of this standard to establish appropriate safety and health practices and determine the applicability of regulatory limitations prior to use.*
- 

## **2. REFERENCED DOCUMENTS**

### **2.1. AASHTO Standards:**

- T 22, Standard Method of Test for Compressive Strength of Cylindrical Concrete Specimens
- T 99, Standard Method of Test for Moisture-Density Relations of Soils Using a 2.5 kg Rammer and a 305 mm drop
- T 180, Standard Method of Test for Moisture-Density Relations of Soils Using a 4.54 kg Rammer and a 457 mm drop
- T 198, Standard Method of Test for Splitting Tensile Strength of Cylindrical Concrete Specimens

### **2.2. ASTM Standards:**

- C 496, Standard Test Method for Splitting Tensile Strength of Cylindrical Concrete Specimens
- D 6931, Standard Test Method for Indirect Tensile (IDT) Strength of Bituminous Mixtures
- D 558, Standard Test Methods for Moisture-Density (Unit Weight) Relations of Soil-Cement Mixtures
- D 653, Standard Terminology Relating to Soil, Rock, and Contained Fluids
- D 1632, Standard Practice for Making and Curing Soil-Cement Compression and Flexure Test Specimens in the Laboratory

## **3. SUMMARY OF TEST METHOD**

---

- 3.1. This test method consists of applying a diametral compressive force along the length of a cylindrical specimen at a rate that is within a prescribed range until failure occurs. This loading induces tensile stresses on the plane containing the applied load

and relatively high compressive stresses in the area immediately around the applied load. Tensile failure occurs rather than compressive failure.

- 3.2. Aluminum bearing blocks are used to distribute the load applied along the length of the cylinder.
- 3.3. The maximum load sustained by the specimen is divided by appropriate geometrical factors to obtain the splitting tensile strength.

---

#### 4. SIGNIFICANCE AND USE

- 4.1. This test method is used to determine the IDT strength of cementitious stabilized materials. IDT strength is a key parameter in the analysis of shrinkage cracking of cementitious stabilized layers.

---

#### 5. APPARATUS

- 5.1. *Testing Machine* — The testing machine shall conform to the requirements of T 22, and be of a type with sufficient capacity that will provide the rate of loading prescribed in Section 7.4.
- 5.2. *Plano-Cylindrical-Concave Bearing Blocks* — Two bearing blocks, free of imperfections, of a length equal to, or slightly longer than that of the specimen shall be provided for each specimen. The loading surface on the bearing blocks shall be flat, and the surface in contact with the specimen shall be concave. The distance between the curved and flat surfaces shall not be less than 18 mm at the thinnest section. Table 1 shows the width of the bearing blocks as measured from tip to tip of the concave face, and the radius of the curvature.

**Table 1**—Width and Radius of Curvature of Bearing Blocks (mm)

Nominal diameter of specimen	Width of bearing blocks	Radius of curvature of the concave face
152.4	19.05±2.0	75±2.0

- 5.3. *Dial Comparator* — Dial comparator, or other suitable device, for measuring the physical dimensions of the specimen to the nearest 0.1 mm.

**Note 1** — Vernier calipers are not recommended for soft specimens, which will deform as the calipers are set on the specimen.

---

#### 6. TEST SPECIMENS

- 6.1. *Specimen Preparation* — Cylindrical specimens are prepared in cylinder molds. The moisture content of soil is measured and then the soil is blended with the required percentage by weight of binders until the mixture has uniform color throughout. The soil stabilized (with cement or lime or fly ash) mixture is moistened with water to the

reach the desired optimum moisture content and blended until uniform; the mixtures are compacted immediately. The specimens are then compacted in one layer in the mold to achieve the maximum dry unit weight. The gravel stabilized specimens are compacted with modified compaction effort (AASHTO T-180); whereas, the sand, silt and clay stabilized specimens are compacted with standard compaction effort (AASHTO T-99). Appropriate amount of the test material for the specimen is compacted to achieve the target dry unit weight based on the applicable compaction test. Specimens shall have smooth, uniform parallel surfaces.

- 6.2. *Core Specimens* — Core undisturbed specimens from large undisturbed samples or from field. Handle specimens carefully to prevent disturbance, changes in cross section, or loss of water content. No moisture curing will be used for core specimens.
- 6.3. *Curing* — Cure the specimens for a total 28 days at 100% relative humidity and  $21\pm 2^\circ\text{C}$ .
- 6.4. *Test specimens* — The nominal dimensions of the cylindrical samples should be 152.4-mm diameter by 60 to 85-mm height.

---

## 7. PROCEDURE

- 7.1. *Marking* — Draw diametral lines on each end of the specimen using a suitable device that will ensure that they are in the same axial plane.
- 7.2. *Measurements* — Determine the diameter of the test specimen to the nearest 0.1 mm by averaging three diameters measured near the ends and the middle of the specimen and lying in the plane containing the lines marked on the two ends. Determine the length of the specimen to the nearest 0.1 mm by averaging at least two length measurements taken in the plane containing the lines marked on the two ends.
- 7.3. *Positioning Using Marked Diametral Lines* — Place the specimen on the lower bearing block and align so that the lines marked on the ends of the specimen are vertical and horizontal, and centered over the bearing block. Place a second bearing block lengthwise on the cylinder, centered on the lines marked on the ends of the cylinder.
- 7.4. *Rate of Loading* — Apply the load continuously and without shock, at a constant rate of  $100 \pm 5 \text{ kPa/min}$  splitting tensile stress or at a constant rate of displacement corresponding to this splitting tensile stress, until failure of the specimen (Note 2). Record the maximum applied load indicated by the testing machine at failure. Note the type of failure and the appearance of the specimen.

**Note 2** — The relationship between splitting tensile stress and applied load is shown in Section 8.

7.5. Three replicates are recommended.

---

## 8. CALCULATION

8.1. Calculate the splitting strength of the specimen as follows:

$$S_t = \frac{2P}{\pi l d} \quad (I)$$

where:

$S_t$  = IDT strength, Pa

$P$  = maximum applied load indicated by the testing machine, N

$l$  = height of the specimen, m

$d$  = diameter of the specimen, m

---

## 9. REPORT

9.1. Report the following information:

- 9.1.1. Specimen identification number;
- 9.1.2. Average diameter and length of the specimen, m;
- 9.1.3. Maximum failure load, N;
- 9.1.4. IDT strength calculated from Equation (I), Pa;
- 9.1.5. Age of specimen and curing conditions;
- 9.1.6. Curing history;
- 9.1.7. Defects in specimen;
- 9.1.8. Types of fracture; and
- 9.1.9. Types of specimen.

---

## 10. PRECISION AND BIAS

- 10.1. *Precision* — The precision of this test method has not been established by an interlaboratory test program. However, based on test data that are available, the following may serve as a guide to the variability of IDT strength test results.

- 10.1.1. Laboratory tests were performed on clay, silt, sand and gravel stabilized (with cement, fly ash and lime) specimens.
  - 10.1.2. The gravel was classified as GM, the sand as SP, the silt as ML, and the clay as CL. The clay had a liquid limit (LL) of 39 and a plastic limit (PL) of 23. The remaining materials were non-plastic (NP), although the silt had a LL of 17.
  - 10.1.3. The series of tests consisted of 9 different mixtures. Three replicates were prepared for each mixture. The cement binder used was in the range of 3-12%, class C fly ash 13% and lime 4-6%. It was noted that the average coefficient of variance was 7.3%.
- 10.2. *Bias* — There is no accepted reference value for this test method, therefore, bias cannot be determined.

---

## 11. KEYWORDS

- 11.1 Indirect tensile (IDT) strength; splitting tension; cementitiously stabilized materials; soil stabilization.

---

## 12. REFERENCES

- 12.1. Midgley, L. and R. Yeo. 2008. *The Development and Evaluation of Protocols for the Laboratory Characterisation of Cemented Materials*. Austroads Publication No. AP-T101/08, 89.

# **Indirect Tensile Modulus for Cementitious Stabilized Materials**

---

## **1. SCOPE**

- 1.1. This test method covers the determination of indirect tensile (IDT) modulus of cementitiously stabilized materials.
  - 1.2. The values stated in SI units are to be regarded as the standard.
  - 1.3. *This standard does not purport to address all of the safety concerns, if any, associated with its use. It is the responsibility of the user of this standard to establish appropriate safety and health practices and determine the applicability of regulatory limitations prior to use.*
- 

## **2. REFERENCED DOCUMENTS**

- 2.1. *AASHTO Standards:*
    - T 99, Standard Method of Test for Moisture-Density Relations of Soils Using a 2.5 kg Rammer and a 305 mm drop
    - T 180, Standard Method of Test for Moisture-Density Relations of Soils Using a 4.54 kg Rammer and a 457 mm drop
    - T307, Standard Method of Test for Determining the Resilient Modulus of Soils and Aggregate Materials
  - 2.2. *ASTM Standards:*
    - C 496, Standard Test Method for Splitting Tensile Strength of Cylindrical Concrete Specimens
    - D 6931, Standard Test Method for Indirect Tensile (IDT) Strength of Bituminous Mixtures
    - D 558, Standard Test Methods for Moisture-Density (Unit Weight) Relations of Soil-Cement Mixtures
    - D 653, Standard Terminology Relating to Soil, Rock, and Contained Fluids
    - D 1632, Standard Practice for Making and Curing Soil-Cement Compression and Flexure Test Specimens in the Laboratory
- 

## **3. SUMMARY OF TEST METHOD**

- 3.1. This test method consists of laboratory determination of the resilient modulus of cementitiously stabilized materials using cyclic load in indirect tensile test mode. The IDT modulus is the ratio of the amplitude of the repeated tensile stress to the amplitude of the resultant resilient horizontal strain on the plane containing the applied load.

- 3.2. Aluminum bearing blocks are used to distribute the load applied along the length of the cylinder.
  - 3.3. Resilient horizontal strain is defined as the difference between the peak horizontal strain associated with a load pulse and the horizontal strain at the end of the rest time of the load pulse.
- 

#### **4. SIGNIFICANCE AND USE**

- 4.1. This test method is used to determine the IDT modulus of cementitious stabilized materials. IDT modulus is a key parameter in the analysis of shrinkage cracking of cementitious stabilized layers.
- 

#### **5. APPARATUS**

- 5.1. *Loading Device* — The loading device shall be closed loop, electrohydraulic or electropneumatic testing machine with a function generator that is capable of applying repeated cycles of haversine-shaped load pulse.
- 5.2. *Load-Measuring Device* — The axial load-measuring device should be an electronic load cell located between the actuator and the bearing block, and have capacity equal to or greater than the maximum capacity of the loading ram.
- 5.3. *Displacement-Measuring Device* — Displacement-measuring device for all materials shall consist of 2 linear variable differential transformers (LVDTs) fixed to opposite sides of specimen. LVDT with a range of at least 5 mm and linearity error smaller than  $\pm 0.25\%$  is recommended, for measurement of horizontal displacement for each pulse and capable of being in contact with the specimen during the complete test.
- 5.4. *Plano-Cylindrical-Concave Bearing Blocks* — Two bearing blocks, free of imperfections, of a length equal to, or slightly longer than that of the specimen shall be provided for each specimen. The loading surface on the bearing blocks shall be flat, and the surface in contact with the specimen shall be concave. The distance between the curved and flat surfaces shall not be less than 18 mm at the thinnest section. Table 1 shows the width of the bearing blocks as measured from tip to tip of the concave face, and the radius of the curvature.

**Table 1—Width and Radius of Curvature of Bearing Blocks (mm)**

Nominal diameter of specimen	Width of bearing blocks	Radius of curvature of the concave face
152.4	19.0 $\pm$ 2.0	75 $\pm$ 2.0

- 5.5. *Dial Comparator* — Dial comparator, or other suitable device, for measuring the physical dimensions of the specimen to the nearest 0.1 mm.

**Note 1** — Vernier calipers are not recommended for soft specimens, which will deform as the calipers are set on the specimen.

---

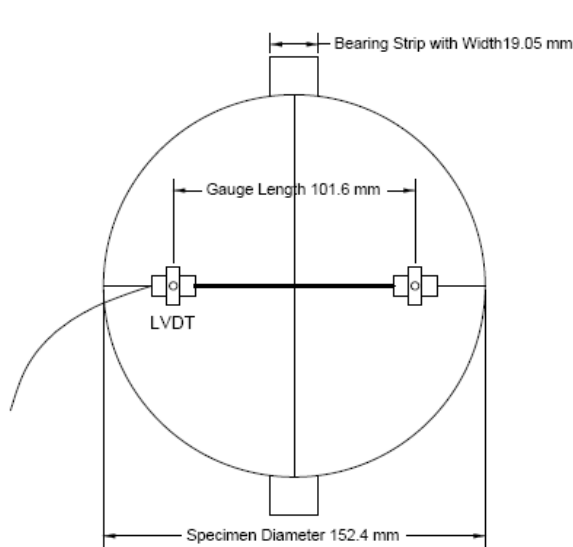
## 6. TEST SPECIMENS

- 6.1. *Specimen Preparation* — Cylindrical specimens are prepared in cylinder molds. The moisture content of soil is measured and then the soil is blended with the required percentage by weight of binders until the mixture has uniform color throughout. The soil stabilized (with cement or lime or fly ash) mixture is moistened with water to the reach the desired optimum moisture content and blended until uniform; the mixtures are compacted immediately. The specimens are then compacted in one layer in the mold to achieve the maximum dry unit weight. The gravel stabilized specimens are compacted with modified compaction effort (AASHTO T-180); whereas, the sand, silt and clay stabilized specimens are compacted with standard compaction effort (AASHTO T-99). Appropriate amount of the test material for the specimen is compacted to achieve the target dry unit weight based on the applicable compaction test. Specimens shall have smooth, uniform parallel surfaces.
- 6.2. *Core Specimens* — Core undisturbed specimens from large undisturbed samples or from field. Handle specimens carefully to prevent disturbance, changes in cross section, or loss of water content. No moisture curing will be used for core specimens.
- 6.3. *Curing* — Cure the specimens for a total 28 days at 100% relative humidity and  $21\pm 2^\circ\text{C}$ .
- 6.4. *Test Specimens* — The nominal dimensions of the cylindrical samples should be 152.4-mm diameter by 60 to 85-mm height.

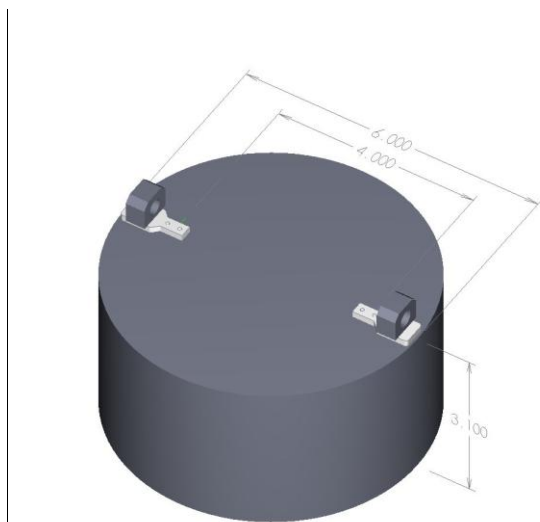
---

## 7. PROCEDURE

- 7.1. *Marking* — Draw diametral lines on each end of the specimen using a suitable device that will ensure that they are in the same axial plane.
- 7.2. *Measurements* — Determine the diameter of the test specimen to the nearest 0.1 mm by averaging three diameters measured near the ends and the middle of the specimen and lying in the plane containing the lines marked on the two ends. Determine the length of the specimen to the nearest 0.1 mm by averaging at least two length measurements taken in the plane containing the lines marked on the two ends.
- 7.3. *Positioning the LVDTs* — place LVDTs on the specimen along the horizontal diametric marking to measure the horizontal deformation. The gauge length should be 101.6 mm for 152.4-mm diameter specimen, as shown in Figure 1.



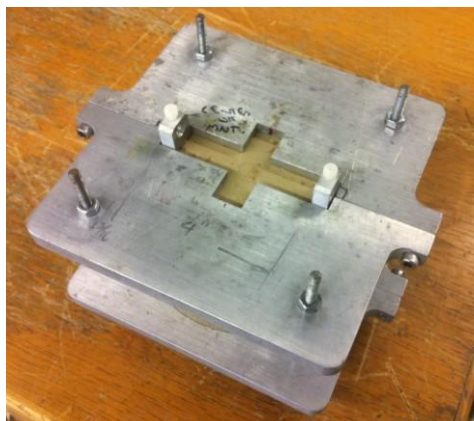
2D Schematic View



3D Schematic View

**Figure 1—IDT Modulus Test Setup**

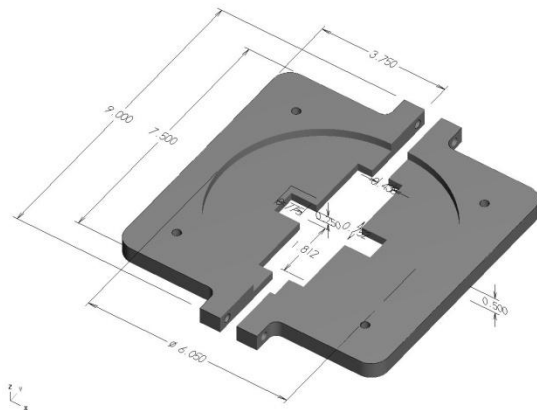
7.3.1. For granular material, position the specimen using a suitable device that will ensure that they are stable, such as that shown in Figure 2. Glue the LVDT mounts with quick-setting epoxy on one side first. After the epoxy is set, flip over the specimen, and glue LVDT mounts on the other side.



Outside of the Aligning Jig



Inside of the Aligning Jig



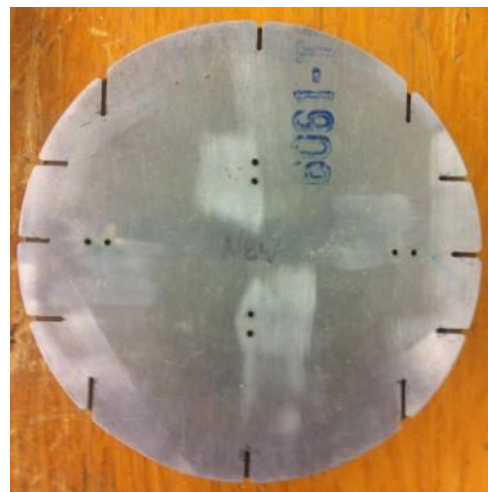
Schematic View the Aligning Jig

**Figure 2**—Aligning Jig for Gluing LVDT Mounts on the Specimen

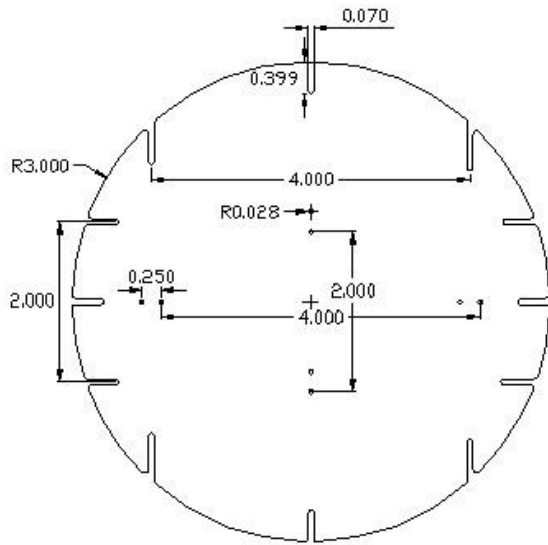
- 7.3.2. For fine materials, drill holes on both sides of the specimen with diameter equal to or smaller than the diameter of screws (Pan Head Phillips Screw for Sheet Metal 18-8 Stainless Steel, No. 2 Size, 3/8" Length). Fasten each LVDT mount with two holes along the marked diametral lines. Use aligning jig, as shown in Figure 3, to make sure all the four holes are aligned along the diametral line. After drilling all the holes on both sides, fasten the LVDT mounts with No. 2 screws.



Drill Press and Specimen



Top View of the Aligning Jig.



Schematic View of the Aligning Jig

**Figure 3—Drill Press and Aligning Jig for Fastening LVDT Mounts with Screws**

- 7.4. *Positioning Using Marked Diametral Lines* — Place the specimen on the lower bearing block and align so that the lines marked on the ends of the specimen are vertical and horizontal, and centered over the bearing block. Place a second bearing block lengthwise on the cylinder, centered on the lines marked on the ends of the cylinder.
- 7.5. *Indirect Tensile Strength* — Prior to the commencement of the modulus test the indirect tensile strength shall be determined on a separate set of specimens using the draft Standard Method of Test for Indirect Tensile Strength for Cementitious Stabilized Materials.
- 7.6. *Indirect Tensile Modulus* — To determine the specimen IDT modulus, apply peak load such that the material remains with its elastic range. 30% of IDT strength is recommended as a typical load level. Apply a contact load, which is about 44 N, to the specimen before the test. Apply 100 repetitions of the corresponding cyclic axial stress using a haversine-shaped load pulse with a 0.1 sec duration followed by a rest period of 0.9-sec duration.
- 7.7. Three replicates are recommended.

---

## 8. CALCULATION

- 8.1. The first 90 cycles are considered as pre-conditioning. The data from the last 10 cycles are used to calculate the IDT modulus of the specimen.
- 8.2. *Calculate the IDT resilient modulus as follows:*

$$\sigma = \frac{2P}{\pi l d} \quad (1)$$

$$\varepsilon = U \frac{\gamma_1 + \gamma_2 v}{\gamma_3 + \gamma_4 v} \quad (2)$$

$$E_{IDT} = \frac{\sigma}{\varepsilon} \quad (3)$$

where:

$\sigma$  = tensile stress, Pa

$P$  = maximum applied load indicated by the testing machine, N

$l$  = height of the specimen, m

$d$  = diameter of the specimen, m

$U$  = horizontal displacement, m

$v$  = Poisson's ratio, 0.2 for cementitious stabilized material

$E_{IDT}$  = indirect tensile modulus, Pa

$\gamma_1, \gamma_2, \gamma_3, \gamma_4$  = parameters dependent on diameter of specimen, gauge length, and bearing block width, which can be found in Tables 2 and 3 for bearing block width of 19.05 and 12.7 mm, respectively. The details on derivation and calculation of the parameters may be found elsewhere (Hondros 1959; and Kim et al 2001).

**Table 2** — Parameters when Bearing Block Width is 19.05 mm

Diameter (mm)	Gauge Length (mm)	$\gamma_1$	$\gamma_2$	$\gamma_3$	$\gamma_4$
101.6	25.4	17.97	55.70	0.4226	1.3431
	50.8	17.97	55.70	0.6873	2.3294
	76.2	17.97	55.70	0.7829	2.8494
152.4	25.4	12.27	37.34	0.3007	0.9259
	50.8	12.27	37.34	0.5434	1.7290
	76.2	12.27	37.34	0.7000	2.3342
	101.6	12.27	37.34	0.7781	2.7269
	127	12.27	37.34	0.8043	2.9328

**Table 3** — Parameters when Bearing Block Width is 12.7 mm

Diameter (mm)	Gauge Length (mm)	$\gamma_1$	$\gamma_2$	$\gamma_3$	$\gamma_4$
101.6	25.4	12.27	37.34	0.2880	0.8993
	50.8	12.27	37.34	0.4667	1.5561
	76.2	12.27	37.34	0.5305	1.9005

	25.4	8.27	24.95	0.2025	0.6186
	50.8	8.27	24.95	0.3655	1.1545
	76.2	8.27	24.95	0.4704	1.5575
	101.6	8.27	24.95	0.5225	1.8186
	127	8.27	24.95	0.5399	1.9554

## 9. REPORT

- 9.1. *Report the following information:*
- 9.1.1. Specimen identification number;
  - 9.1.2. Average diameter and length, m;
  - 9.1.3. Load level in IDT modulus test;
  - 9.1.4. IDT Modulus calculated from Equations (1) to (3), Pa;
  - 9.1.5. Age of specimen and curing conditions;
  - 9.1.6. Curing history;
  - 9.1.7. Defects in specimen;
  - 9.1.8. Types of fracture; and
  - 9.1.9. Types of specimen;

## 10. PRECISION AND BIAS

- 10.1. *Precision* —The precision of this test method has not been established by an interlaboratory test program. However, based on test data that are available, the following may serve as a guide to the variability of IDT strength test results.
- 10.1.1. Laboratory tests were performed on clay, silt, sand and gravel stabilized (with cement, fly ash and lime) specimens.
  - 10.1.2. The gravel was classified as GM, the sand as SP, the silt as ML, and the clay as CL. The clay had a liquid limit (LL) of 39 and a plastic limit (PL) of 23. The remaining materials were non-plastic (NP), although the silt had a LL of 17.
  - 10.1.3. The series of tests consisted of 5 different mixtures, including cement-clay, cement-silt, cement-gravel, lime-clay, and C fly ash-silt. Three replicates were prepared for each mixture. The cement binder used was in the range of 3-12%, class C fly ash 13% and lime 4%. It was noted that the average coefficient of variance was 11.3%.

- 10.2. *Bias* — There is no accepted reference value for this test method, therefore, bias cannot be determined.

---

## 11. KEYWORDS

- 11.1 Indirect tensile (IDT) modulus, cementitious stabilized materials, soil stabilization

---

## 12. REFERENCES

- 12.1. Midgley, L. and R. Yeo. 2008. *The Development and Evaluation of Protocols for the Laboratory Characterisation of Cemented Materials*. Austroads Publication No. AP-T101/08, 89.
- 12.2. Hondros G. 1959. *Evaluation of Poisson's Ratio and Modulus of Materials of a Low Tensile Resistance by Brazilian (Indirect Tensile) Test with Particular Reference to Concrete*. Australian Journal of Applied Science, 10(3): 243-268.
- 12.3. Kim, Y. R., J. S. Daniel, and H. Wen. 2001. *Fatigue Performance Evaluation of WesTrack Mixtures Using Direct Tension and Indirect Tension Tests*. Final Report submitted to North Carolina Department of Transportation and FHWA.

# Coefficient of Thermal Expansion Test of Cementitiously Stabilized Soils

---

## 1. SCOPE

- 1.1. This test method covers determination of the coefficient of thermal expansion (COTE) of cementitiously stabilized soil at early age due to temperature variation other than externally applied forces.
  - 1.2. The values stated in SI units are to be regarded as the standard. The English unit equivalents shown in parentheses may be appropriate, except with regard to sieve sizes and aggregate size as determined by the use of testing sieves, in which case the standard SI designation shown is the standard as required by AASHTO Specification M92.
  - 1.3. *This standard may involve hazardous materials, operations, and equipment. This standard does not purport to address all of the safety problems associated with its use. It is the responsibility of the user of this standard to establish appropriate safety and health practices and determine the applicability of regulatory limitations prior to use.*
- 

## 2. REFERENCED DOCUMENTS

- 2.1. *AASHTO Standards:*
    - M 92, Wire-Cloth Sieves for Testing Purposes
    - M 210, Use of Apparatus for the Determination of Length Change of Hardened Cement Paste, Mortar, and Concrete
    - T 180, Moisture-Density Relations of Soils Using a 4.54-kg (10-lb) Rammer and a 457-mm (18-in) Drop
  - 2.2. *ASTM Standards:*
    - D 698, Standard Test Methods for Laboratory Compaction Characteristics of Soil Using Standard Effort
- 

## 3. SUMMARY OF TEST METHOD

- 3.1. This test method consists of applying temperature cycles at a constant relative humidity condition on cementitiously stabilized prism specimen, and measuring the deformation due to temperature cycling.
- 3.2. The amplitude of strain cycles during the temperature cycles of the specimen is divided by the amplitude of temperature cycle to determine the COTE value.

---

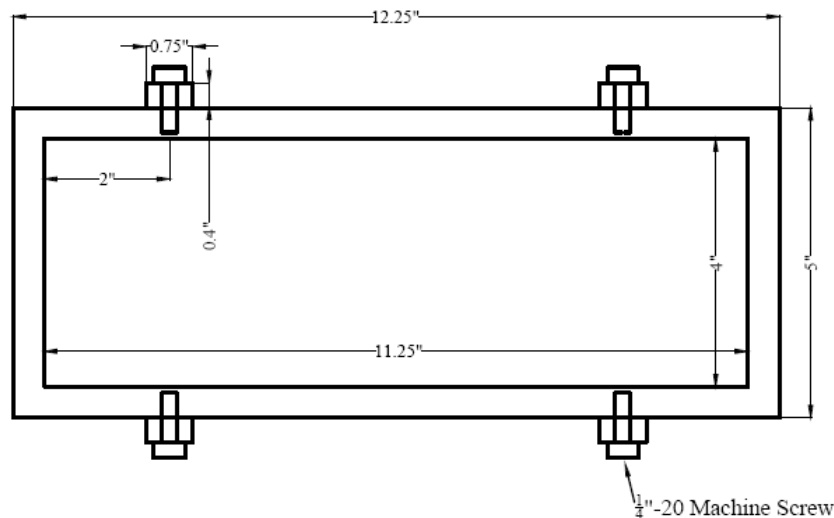
#### 4. SIGNIFICANCE AND USE

- 4.1. This test method is used to determine the COTE value of cementitously stabilized materials. COTE is critical for thermal shrinkage strain, and is a key parameter in the analysis of shrinkage cracking of cementitously stabilized layers.

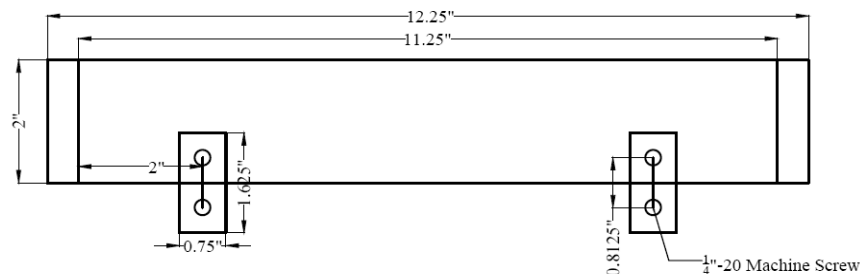
---

#### 5. APPARATUS

- 5.1. *Molds* — The molds for casting test specimens shall conform to the requirements of M 210 with internal dimension 101.6 mm × 101.6 mm × 285.75 mm (4 in. × 4 in. × 11.25 in.). A 50.8-mm (2-in.) tall extension collar should be fixed on the mold with screws. The extension collar shall be constructed as shown in Figure 1.



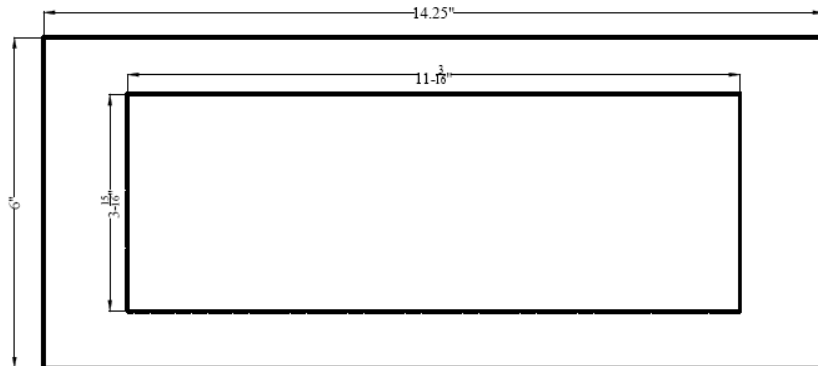
(a) Top View



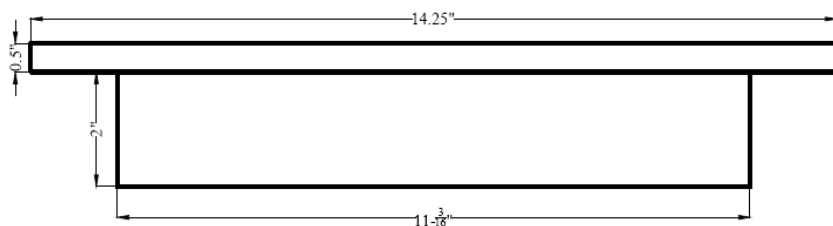
(b) Side View

**Figure 1**—Extension Collar

- 5.2. *Top Plate* — A 50.8-mm (2-in.) tall steel plate with a cap should fit in the extension collar and have a flat bottom surface. The top plate shall be constructed as shown in Figure 2.



(a) Top View



(b) Side View

**Figure 2—Top Plate**

- 5.3. *Gauge* — A linear variable differential transformer (LVDT) gauge head with excitation source and digital readout, with a minimum resolution of 0.00025 mm (0.00001 in.), and a range suitable for the test (for ease in setting up the apparatus, a range of  $\pm 2.5$  mm (0.1 in.) has been found practical). (Note 1).

**Note 1** — LVDT with the appropriate associated electronic actuating and indicating apparatus appears to give the best results with respect to stability, sensitivity, and reliability. Multichannel recording of outputs has been found to be practical and efficient. As an alternate, a data logger can be used to excite the LVDT and record the LVDT and both temperature and time outputs. The data can be stored directly in a personal computer for graphing of test results.

- 5.4. *Temperature Measuring Devices* — Two temperature measuring devices with a resolution of  $0.1^{\circ}\text{C}$  ( $0.2^{\circ}\text{F}$ ) and accurate to  $0.2^{\circ}\text{C}$  ( $0.4^{\circ}\text{F}$ ). T-Type thermal couple has been found to be suitable for this measurement.
- 5.5. *Dial Gauge Mount* — Dial gauge mount shall support the LVDT, and be glued on specimen directly.
- 5.6. *Balance* — A scale or balance have a capacity of 10 kg (22 lb), and accurate to 0.1 percent over its range.

- 5.7. *Mixing Tools* — Miscellaneous tools such as mixing pan, spoon, trowel, spatula, etc., or a suitable mechanical device for thoroughly mixing the sample of soil with increments of water.
- 5.8. *Containers* — Suitable containers made of material resistant to corrosion and not subject to change in mass or disintegration on repeated using.
- 5.9. *Compactor* — A compactor with enough power to obtain target density of specimen.
- 5.10. *Stainless Steel or Aluminum Plates* — Two stainless steel or aluminum plates should have smooth surface with dimension large enough to hold the specimen (101.6 mm × 285.75 mm or 4 in. × 11.25 in.).
- 5.11. *Environmental Chamber* — An environmental chamber shall be capable of applying variable temperature and humidity cycles without shock, and these cycles shall meet the specific test condition. Specimens shall be stored horizontally with suitable racks. The racks shall allow that the air circulation is not disturbed or restricted in the intervening space.

---

## 6. TEST SPECIMENS

- 6.1. Determine the optimum moisture content and maximum dry density of the material in accordance with the the ASTM D 698; except when the 152.4-mm (6-in.) mold is used, the hammer shall weigh 4.54 kg (10 lbs) and drops through a vertical distance of 457 mm (18 in.).
- 6.2. Calculate the total mass of mixture needed based on the maximum dry density, and add soil and required additive and water in the container.
- 6.3. Add to the soil the required amount of cementitious additive in the container. Mix the soil and additive thoroughly until color of the mixture is uniform.
- 6.4. Add potable water to reach the optimum moisture content and mix thoroughly.
- 6.5. Tape a thin layer of plastic, no more than 0.0254 mm (0.001 in.) thickness, inside the mold, in order to prevent the bonding between specimen and steel mold during compaction.
- 6.6. After imbedding the tip of thermal couple at center of the mold, transfer the calculated mass of mixture into the mold. If the mold is not big enough to hold the loose material, push the mixture with the top plate, until all the material is moved into the mold. Make sure the uncompacted mixture have uniform height.
- 6.7. Compact the specimen with the air hammer carefully. Check the height of specimen during compaction until it is close to the target height. Then put the top plate (Figure

- 2) on the mold and continue compaction till the top plate touches the mold.
- 6.8. Demold the specimen. Take apart the extension collar and 4 sides of the mold first. Then put a steel plate on the side of specimen, hold the bottom plate of mold and the steel plate, and flip the specimen 90°. Now the specimen is held by the steel plate. Replace the bottom plate of mold with another steel plate, and flip the specimen 90° in opposite direction. After that, the specimen is transferred from the mold to the steel plate.
- 6.9. Glue gauge mount with quick-setting epoxy on specimen, and make sure LVDT measure the longitudinal axis of specimen.
- 6.10. Move the specimen to the environmental chamber. Adjust the position of LVDT tip to the midpoint of entire range.
- 6.11. Place another thermal couple to collect chamber temperature during test. Connect the imbedded thermal couple and the ambient-temperature thermal couple to a data acquisition device.

## **7. PROCEDURE**

- 7.1. Place the specimen in the environmental chamber at an initial ambient temperature of 25°C until the temperature inside the specimen is uniform. The chamber shall start to cycle the temperature between 25°C and 30°C using a saw-tooth pattern with constant relative humidity. After the target temperature in the chamber is reached, which takes about 20 minutes, the temperature shall be kept constant for 4 hours, resulting in three full cycles (or six steps) per day. The constant temperature period is long enough to ensure a stable and uniformly distributed temperature in the prism specimen. The amplitude of the temperature cycle (5°C) is selected to be small enough to maximize the number of cycles per day and obtain more COTE values at early ages, and can minimize the temperature effect on the change in COTE over time.

## **8. CALCULATION**

- 8.1. Calculate the strain at any ages as follow:

$$\varepsilon = \left( \frac{L_x - L_i}{L} \right) \times 100 \quad (I)$$

where:

$\varepsilon$  = strain in length at  $x$  age, percent;

$L$  = initial specimen length, mm (in);

$L_x$  = LVDT reading at  $x$  age, mm (in); and

$L_i$  = initial LVDT reading, mm (in);

- 8.2. Calculate the coefficient of thermal expansion as follow (Note 3):

$$COTE = \frac{(\Delta\varepsilon_{max} - \Delta\varepsilon_{min})}{\Delta T} + \alpha' \quad (2)$$

where:

$\Delta\varepsilon_{max}$  = maximum strain in each step;

$\Delta\varepsilon_{min}$  = minimum strain in each step;

$\Delta T$  = the incremental change in temperature, 5°C in this case; and

$\alpha'$  = the COTE of LVDT, obtained from LVDT specifications.

**Note 2** – When plotting the development of COTE with time, the COTE shall be the average COTE in each cycle, including both temperature increase and decrease steps. It is suggested to calculate the COTE starting with the temperatures from imbedded and air-temperature thermal couples are close.

- 8.3. Calculate strain values for each specimen to the nearest  $10^{-6}$  and report averages to the nearest  $10^{-5}$ , and COTE to the nearest  $10^{-6}$ .

---

## 9. REPORT

- 9.1. *Report the following information:*

- 9.1.1. Identification as types of host material and additive, number of specimens for each condition, and date & place molded;
- 9.1.2. Source and identification of each material employed;
- 9.1.3. Type, maximum size, moisture condition, and grading of the soil;
- 9.1.4. Size of specimens;
- 9.1.5. Mixture proportions, including additive content, optimum moisture content, and maximum dry density;
- 9.1.6. Description of environmental condition, including temperature and humidity collected during the test;

- 9.1.7. Total elapsed time while recording readings;
  - 9.1.8. Length change data, reported as strain, either increase or decrease in linear dimension, to the nearest  $10^{-6}$  of the length based on the initial measurement at the time of placing LVDT on the specimen;
  - 9.1.9. Technician conducting test; and
  - 9.1.10. Any other pertinent information.
- 

## **10. PRECISION AND BIAS**

- 10.1. *Precision* — The precision of this test method has not been established by an inter laboratory test program. However, based on test data that are available, the following may serve as a guide to the variability of COTE test results.
  - 10.1.1 Laboratory tests were performed on clay, silt, and gravel stabilized (with cement and lime) specimens.
  - 10.1.2 The gravel was classified as GM, the silt as ML, and the clay as CL. The clay had a liquid limit (LL) of 39 and a plastic limit (PL) of 23. The remaining materials were non-plastic (NP), although the silt had a LL of 17.
  - 10.1.3 The series of tests consisted of 4 different mixtures, including cement-clay, cement-silt, cement-gravel, and lime-clay. Three replicates were prepared for each mixture. The cement binder used was in the range of 3-12% and lime 4%. It was noted that the average coefficient of variance was 8.3%.
- 10.2. Bias — No bias can be established because no reference material is available for this test.

---

## **11. KEYWORDS**

- 11.1 Coefficient of Thermal Expansion (COTE); cementitious stabilized materials; soil stabilization.
- 

## **12. REFERENCES**

- 12.1. Cusson, D. and T. J. Hoogeveen. 2006. *Measuring Early-Age Coefficient of Thermal Expansion in High-Performance Concrete*. International RILEM Conference on Volume Changes of Hardening Concrete: Testing and Mitigation, Lyngby, Denmark, August 20.